The lipid bilayer membrane

and its interactions with additives

Lucas A. Meijer

The lipid bilayer membrane

and its interactions with additives

Proefschrift

ter verkrijging van de graad van doctor

in de landbouw- en milieuwetenschappen

op gezag van de rector magnificus,

dr. C. M. Karssen,

in het openbaar te verdedigen

op maandag 19 december 1994

des namiddags te vier uur in de Aula

van de Landbouwuniversiteit te Wageningen.

cover: Matthijs J. Meijer

Stellingen

-1-

Bij hoge zoutconcentratie hebben de kopgroepen van dimyristoylfosfatidyl-
choline twee afzonderlijke conformaties. Eén met de cholinegroep dichtbij
de waterfase en één met de cholinegroep dichtbij de apolaire staarten.

Dit proefschrift, hoofdstuk 1.

-2-

De preferente adsorptie van meerwaardige kationen aan de kopgroepen van
dimyristoylfosfatidylcholine kan verklaard worden zonder specifieke
interacties.

Dit proefschrift, hoofdstuk 2.

-3-

Netto ongeladen lipide membranen kunnen elkaar elektrostatisch afstoten.

Dit proefschrift, hoofdstuk 3.

-4-

Het leven is per definitie uit evenwicht.
Dit maakt het streven naar een natuurlijk evenwicht bedenkelijk.

-5-

The principle "publish or perish" will make science perish in publications.

vgl. P.A. Barneveld, proefschrift LUW 1991, stelling x

-6-

Ook bij het gebruik van een rooster, in combinatie met een zelfconsistent-veldtheorie, moet men het hokjes denken voorkomen.

-7-

Financiering van onderwijs op basis van het aantal geslaagden leidt tot een verlaging van het niveau.

-8-

Het onderling afstemmen van de nummering van steden in bijvoorbeeld postcodes, netnummers en station nummers zou het gebruik ervan vergemakkelijken.

-9-

Blessures bij rugby zijn meer te wijten aan een poging van de speler in kwestie om een tekort aan techniek met een overdaad aan inzet te compenseren dan aan de aard van het spel.

-10-

Wetenschappelijk onderzoek convergeert niet.
Dit heeft geen positieve invloed op de werkgelegenheid.

Stellingen behorende bij het proefschrift:
"The lipid bilayer membrane and its interaction with additives."
L.A. Meijer
Wageningen, 19 december 1994.

Contents

Chapter 3

Modelling the Interactions Between Phospholipid Bilayer Membranes

Chapter 4

Self-Consistent-Field Modelling of Complex Molecules with Atomic Detail in

Chapter 0

Introduction

The fundamental organisation form of life is a cell. A thin semi-permeable sheet formed by two monolayers of short amphiphiles (lipids), each just more than a nanometer thick, envelopes every cell. The semi-permeable properties of these sheets, often called bilayer membranes, make it possible to create differences in chemical composition between the inside and the outside of the cell. These differences are essential for the performance of the cellular machinery. Membranes are thus the interfaces that support life. These important interfaces form the subject of this thesis. I have spent four years in contributing to the formulation of a better model to predict the equilibrium properties of these intriguing layers.

Membrane-forming molecules are amphiphilic; they are held together by the same forces that cause the demixing of oil and water. Amphiphiles combine both properties that can be described as oil-like and water-like and self-associate into structures with at least one length scale in the nanometer range. The geometry of these multi-molecular assemblies is not always flat, the interfaces may be curved to form spherical or cylindrical shapes, or even into more complicated bicontinuous labyrinths. Locally flat membranes can compartmentalise space. To enclose and partly separate a certain volume of a solution with its solutes from the environment is the primary biological function of a membrane. Communication between both sides of these interfaces is obviously needed. The semi-permeability of membranes and possibility of (energy-driven) selective transport of molecules is their second most important biological task. In higher organisms, such as man, the organisation of the many cells is very complex and lipid layers play important roles. Their barrier function is encountered in *e.g.* the skin, lungs and digestive systems. Membranes are key structural elements in the kidneys and the nervous system.

On the cell level a number of other membrane-related processes can be mentioned. Aggressive lythic enzymes are usually not produced in the cytoplasm of the cell but in small spheres, separated from the rest of the cell by membranes (vesicles) before they are secreted. Specific transport proteins, also part of the

membranes, transfer the building bricks for the enzymes into these vesicles. The energy production of a cell, in the form of ATP, depends on a concentration gradient of protons over the inner membrane of small cell organelles with a double membrane, called mitochondria. This gradient is created by the respiratory chain of reactions catalysed by enzymes located at and in the mitochondrial membrane. These are only a few examples of the chemistry of life that flourishes in many complex pathways on or near these biological interfaces.

Another type of chemistry becomes more and more essential for everyday life. To stay alive one needs to feed oneself and stay free from diseases. The crops that provide the nourishment are nowadays grown in such vast monocultures that they become proner to pests and plagues. Pathogens become resistant to existing chemicals and the chemical industry is constantly working on new crop protection agents (formerly known as pesticides, herbicides and fungicides) and drugs to combat life-threatening diseases.

In the development of these drugs and crop protection agents there are a lot of hurdles to be cleared. For instance, the drug has to be malignant only to pathogens and be harmless not only for the crop or person that it is protecting, but also for non-pathogenic organisms. Neither the production nor the waste of these agents should pollute the environment.

One of the strategies in the application is to limit the dose. This limits the amount in the body in general and reduces possible side effects and waste. For this purpose drug delivery systems are developed to release the drug gradually over a period of time instead of administering high initial doses that slowly decrease as the body breaks the molecules down or secretes them. So-called "stealth liposomes" are an example of these systems. They consist of a vesicle bordered by a membrane containing special lipids with polymer tails attached that prevent the normal break down by body-defence proteins. The drug that is encapsulated in the vesicle leaks out gradually. Incorporation in the membrane of other substances, that can have specific interactions with the target, can cause the drug to be released only in the part of the body where it is needed, say in a specific organ or in specific malignant cancer cells. This line of research is promising but still requires a lot of work.

The actual working mechanism of a drug often involves the interaction with biological structures such as DNA, proteins, ribosomes or membranes. Often the active site that the drug acts on resides inside a cell. The molecules then have to pass one or more membranes to reach their targets. Sometimes the target is located inside the membrane. In those cases also the local orientation of the molecules

inside the membranes may be of crucial importance.

In any of these cases it is obvious that a good understanding of the structure of membranes in general and, more specifically, the interaction of the drug molecules with these is of utmost importance. So we are back at the starting point of this introduction and the subject of this thesis: the membrane and its interactions with other (foreign) molecules. Understanding the forces that act on the molecules constituting a membrane can give leads in optimising the development of drug molecules and in this way reduce the time and the costs needed in their development.

A general measure of the passive transport efficiency of molecules through a membrane is the partition coefficient. This is the ratio between the concentration within the membrane and that in the water phase. The measurement of this quantity is not an easy task so other possibilities are considered. Since the membrane interior is often believed to be fluid, alkane-like, the octanol/water partition coefficient is sometimes used as measure of the uptake capability of membranes. There are, however, several problems with this ansatz. Membranes are, as told, extremely thin, so thin that the interfacial aspects dominate. Being anchored to the water/hydrocarbon surface by their head groups, the chains have a relatively high degree of order. In the octanol/water system, on the other hand, the measured partition coefficient depends on the interactions of the substance in both isotropic phases. It is therefore not surprising that some molecules partition very differently in bulk octanol and in the smectic membrane phase. This difference can be very large especially for relatively rigid molecules, as most drug are.[1-3] This can be due to the fact that these molecules cannot easily adapt their conformations to local gradients in hydrophobicity or electrostatic potential (see chapter 4). Development of a theory for the behaviour of such molecules near lipid membranes would therefore be of great help.

At the Agricultural University of Wageningen, interfacial chemistry is a field of attention and in this discipline there is a research group with a strong interest in the modelling of interfacial phenomena. Over the years a theory for the adsorption of long chain polymers was developed[4] and modified to describe self-assembling systems.[5-9] This theory will be used and further expanded in this thesis. Before giving an outline of this theory we below turn our attention to the nature of membranes and the state of the art of some research in the field. We conclude this introduction by outlining the scope of this thesis.
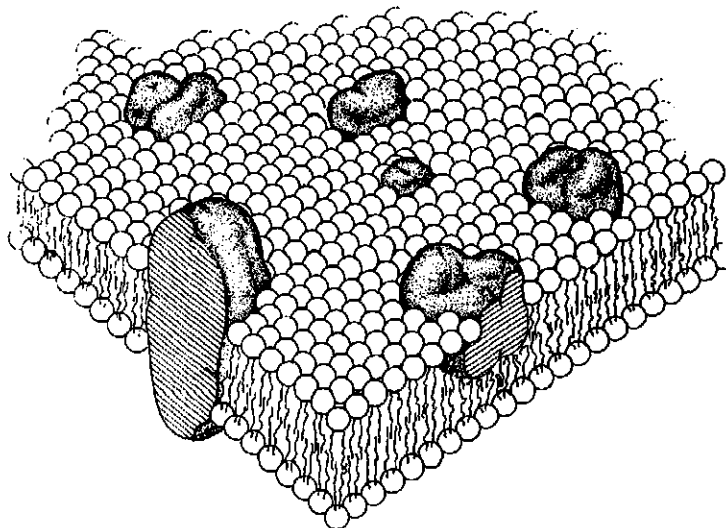
Figure 1. The membrane as it is pictured by Singer and Nicholson.[10]

The Nature of Bilayer Membranes

A typical biological membrane consists of a large number of amphiphiles: proteins, a host of lipids with various head groups, number of chains, chain lengths and degrees of unsaturation, and many other molecules such as steroids (*e.g.*, cholesterol). These molecules are organised in such a way that the apolar, oil-like, parts (tails) escape the water phase clustering together, while the polar, water-like, parts (head groups) reside on the interface with the water. Singer and Nicholson[10] proposed that the lipids form the membrane matrix like a two-dimensional sea (see figure 1). We now know that other geometries also exist in biological membranes, but the general picture has been shown to be essentially correct. In most membranes an order to disorder phase transition exists (they can freeze). Generally however most membranes are, although close to the phase transition, in the liquid-crystalline phase. Then the lateral mobility of the molecules is high and fluid-like while their movements perpendicular to the membranes surface (flip-flop and exchange with the water phase) is highly restricted. In this "sea" membrane-proteins are floating about. Sometimes they are demobilised by adsorption on structures outside the membrane, *e.g.* the cyto-skeleton, like buoys anchored to the bottom, sometimes they cluster together like bubbles on a cup of tea and often they fully penetrate the bilayer in a trans membrane structure like springs in a mattress. The

interaction of the lipid matrix with the proteins is generally believed to be of key importance for the biological (enzyme) function of these macro molecules.

The experiments to investigate the behaviour of foreign molecules in membranes can be done *in vivo, in vitro* and *'in computero'*. That is, they can be carried out experimentally with living cells, without living material and, as we will show, also theoretically. Below a few examples of the first two approaches will be discussed after which more details on the *in computero* state of the art is presented.

Experimental Examples

The forces that play in concert in a membrane are of various natures and membrane-research is the interface between several scientific disciplines. All these disciplines have their own way of approaching the membrane system. In experiments virtually no method is left unused to unravel the structural and functional properties of membranes. It is therefore impossible to fully review all these aspects. We limit ourselves by giving a few examples which are selected because of the links that exist between these experimental observables and the quantities that can be modelled.

The permeability of ions through membranes of living cells can be investigated through the change in the potential that exists *e.g.* over chloroplast membranes.[11,12] This potential can be measured by micro-electrodes that are brought into the chloroplast or by the potential gradient-dependent absorption of the pigment complexes that reside in these membranes. The change in potential upon illumination of the cells under various conditions is a parameter that is used to elucidate the membrane-bound photosynthesis.

The molecular order can be measured by magnetic resonance techniques (NMR[13,14] or EPR). An obvious drawback of NMR is that this technique is rather insensitive and therefore a considerable amount of additive in the membrane is needed to be able to perform these measurements. The high loading can influence the structure of the membrane which severely limits the applicability of the results. EPR requires, like other techniques (*e.g.* based on fluorescence[15]) specific probes that are sensitive to the wave length of the electromagnetic radiation used. These probes also potentially influence the membrane properties under investigation. The theory explained in this thesis can help interpreting some of the results by predicting the behaviour of the probe molecule in the membrane.

In biological systems the interaction between bilayers is an other often recurring event. Examples of interacting membrane systems are the double membranes of

mitochondria and chloroplasts and the myelin sheets (Schwann cells) around dendrites of nerve cells. This inherent importance has triggered many research activities regarding interacting membranes. Model membranes are examined by the surface force apparatus. In such experiments, two curved mica sheets, covered by a lipid bilayer are brought together up to molecular distances and the force between these sheets is measured mechanically.[16-18] An alternative method is developed by Rand and Parsegian who use an osmotic force to vary the membrane spacing which is measured with X-ray diffraction.[19,20]

These examples illustrate where well-controlled experiments on lipid bilayer systems contributed to the large knowledge of membrane systems. In many cases less attention has been paid to the molecular interpretations. A method to obtain a deeper insight into (model) membranes is the theoretical modelling, which nowadays is possible with the help of fast computers. The modelling efforts are discussed next.

Theoretical Overview

The theory of self-assembly of lipids, proteins etc. into membranes is surprisingly poorly developed. Clearly the complexity of biological membranes is yet beyond full comprehension. Even the lipid matrix on its own, without the proteins, is of a complexity that is yet out of reach. The existing theories deal mainly with simplified molecules and simplified conformations.

Molecular dynamics (MD) is the technique that has the most appeal, because at first glance, it is rather exact. According to this technique a certain number of particles are put into a box and then, knowing all the masses, velocities and forces between the particles, Newton's law ($F = m \cdot a$) is applied and the time evolution of the system is followed. There are however a few (hidden) flaws. First, the fundamental forces between all particles are not exactly known. So some approximations have to be made. Second, since only a large number of particles can make up a large supra-molecular structure like a membrane, long computation times are needed to follow a system even for a few nanoseconds simulated time. And, third, determining thermodynamic quantities is extremely difficult because these are defined for the limit of many particles and long times both leaning heavily on the computer power.

Nevertheless some interesting results have been obtained. For DMPC bilayers Berendsen *et al.* found that the order in the tail area is relatively low for membranes in the high temperature liquid state and that the DMPC head groups lie more or less

flat on the membrane surface.[21-24] They could not follow the membrane long enough to see *e.g.* any water molecules pass through the membrane. To obtain some insight into the permeability of additives, they invented a scheme to determine the forces that these molecules are exposed to in different parts of the membrane. They also managed to simulate a protein molecule close to the membrane surface.[25]

Another theoretical approach which is, in principle, exact is the Monte Carlo (MC) technique. The name is not chosen by accident since it involves some guessing. With this technique one tries to calculate the partition function by generating a representative set of all possible configurations of a system. The first reason for the guessing is to get a possible, non forbidden, independent configuration and the second reason to random guessing is to be sure that the set that is generated is representative for the system and not a biased artefact. There are clever tricks (*e.g.* the Metropolis algorithm) to generate a new configuration from the previous one, which ensures that the equilibrium properties of the system are reached in the limit of many simulation steps.

The application of MC to membranes is unfortunately limited. This can be attributed to the tail region being densely packed with chains, making it difficult to find (randomly) non-forbidden configurations of all the molecules. Therefore only MC studies on part of the problem are available *e.g.* some work is done on phosphatidyl head groups attached to a flat surface mimicking the apolar phase.[26,27] From these studies it became clear that the head groups have freedom to assume several conformations and that they lie, on average, flat on the surface. This is in line with MD results. With the superposition of carefully chosen local structural rearrangements Levine *et al.* perform MC *dynamics* for hydrocarbon tails attached to a surface mimicking the head-group area.[28-30] A combination of MC and a ten state Pink model has been used by Mouritsen *et al.* who approached a bilayer membrane as a two-dimensional plane composed of sites representing the lipid molecules. These sites can have several states. With state-dependent interactions they concentrated on the phase transition and the lateral phase behaviour.[31-33] Their results are quite unique especially where it comes to the lateral phase behaviour of the membrane. There is however the difficulty to *a priori* determine the various states and corresponding interactions for a molecule on the basis of its molecular structure.

Self-Consistent-Field Theory

The theory to be elaborated in this thesis differs from the ones mentioned above. Its principles are known under the term self-consistent-field (SCF) methods. SCF theories do not share the disadvantages of the former MD and MC simulations, in that they do not heavily depend on supercomputer power. The SCF method is based on the reduction of the many-molecule problem to the problem of one molecule in the (external) field of mean force of all the others. In general the external field is defined depending on the ensemble of all conformations of all molecules and their interactions. The potential field on its turn determines the statistical weight of the conformations that make up the complete system. The fixed point solution to this problem is referred to as the self-consistent-field solution which typically depends on boundary conditions and space filling constraints.

Several investigators have made various contributions along these lines to describe association of molecules into aggregates. Most of them use a lattice to discretise space and make use of the given symmetry of the aggregates. They consider the aliphatic chains to be attached to the surface of the aggregate but do not allow solvent (water) to penetrate into the aggregate. The external field is mostly a pressure field that ensures the core of the aggregate to have a density comparable to that of liquid alkane.[34-38] Sometimes an order-dependent field is used.[39,40] Marčelja showed that the gel-to-liquid phase transition could be modelled in this way. Additives in bilayers are either modelled as structureless isotropic monomers that mostly have no specific contact interaction with the lipid tails, or small chain molecules of the same origin as the tails. The results are, despite these approximations, promising and give some insight into the importance of the included field components.

The theory to be discussed in this thesis will not only include volume interactions and an anisotropic field (of a different origin than used by Marcelja or Gruen), but also cover electrostatic interactions and contact interactions between segments in a Bragg-Williams approximation, parametrised in terms of Flory-Huggins χ-parameters. These interactions are employed to allow the lipids to self-assemble in a presumed geometry. Apart from the assumption of a lattice geometry no restrictions are imposed on the segment positions.[6,41]

Simplified model membranes were investigated with this theory several years ago.[5,42,43] Although the molecular representation was, at that time, rather crude, the main features of the tail region, i. e. the large degree of disorder and the fact that the
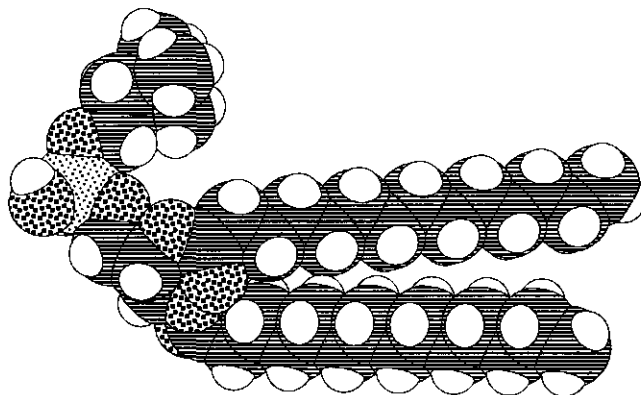
Figure 2. A model drawing of the molecule of the lipid dimyristoyl-
phosphatidylcholine.

segments closest to the hydrophobic-hydrophilic "interface" in the lipid molecules have the most narrow distribution were reproduced, in line with MD predictions. Phase transitions in these membranes were also reproduced and the interaction of membranes both in the liquid crystalline and in the gel phase were probed. The influence of simple model surfactants on the bending of membranes in vesicles has been a point of interest as well.

In this thesis we will consider, in addition to the volume-filling potential, the contact energies as described by the Flory-Huggins χ-parameter and the anisotropic field as was used in previous work, and an electrostatic contribution to the potential of mean force that the segments feel. In comparison to earlier work we describe the lipid molecules in more detail so that the segments now represent more realistic atoms or groups of atoms. In most of our work we have chosen to simulate dimyristoylphosphatidylcholine (DMPC, see figure 2). DMPC is a lipid with a zwitterionic head group at neutral pH; it is a key component in most animal cells. For comparison we have also modelled membranes composed of a frequently occurring anionic phospholipid: dimyristoylphosphatidylserine (DMPS).

Short Contents of the Thesis

First we will consider the bare membrane in chapter 1. Much attention will be paid to the head group conformations of (modified) DMPC and DMPS membranes.[44] The PC head group appears to have, on average, a conformation parallel to the membrane surface. In line with experimental data[45] it will be shown that, at high salt concentrations, the choline group distribution splits into two

orientations, one closer to the hydrocarbon phase and one closer to the water phase. To make a link with the "stealth" liposomes, mentioned above, calculations will be done with a hydrophilic chain attached to the DMPC head group.

In the second chapter calculation will be done on a lipid monolayer adsorbed on a flat apolar surface, comparable to half a bilayer on a mercury electrode as studied by Nelson.[46,47] It will be shown that the zwitterionic nature of DMPC gives rise to a profile in the electrostatic potential which in turn causes cations to associate with the phosphate group. The association is clearly stronger the higher the valence of the ions is. These results were of interest in interpreting experimental data and used to conjecture that the concentration of ions in the head group area is a factor determining the permeability of ions through ion channels.

Apart from the fact that equilibrium membranes have a vanishing surface tension, free-standing lipid bilayers only occur when they do not attract each other. Therefore, membrane-membrane interactions will be calculated for various conditions in chapter 3. Not only bare membranes are considered but also membranes doped with non-ionic, anionic and cationic surfactants as a prelude to the final chapter. Results on the free standing membranes and the interaction curves will be reported.

In chapter 4, an extension to the theory is made to account for the incorporation of arbitrary shaped rigid structures composed of equally sized segments. The partition coefficients of several groups of linear and branched alcohols and para-substituted phenols will be computed and compared to the experimental results. To illustrate the kind of information that can be retrieved, three groups of the same zwitterionic isomers ($C_{22}N^+S^-$ with a benzene like structure) will be systematically calculated and their change in partition coefficient can be related to structural changes in the molecular architecture. The orientation of a naphthalene ring system will be investigated by adding four hydroxyl groups as substituents in various ways.

The thesis is concluded by a general chapter containing a discussion on some remaining imperfections of the theory and an outlook for further improvements.

Although we hope that the chapters in this thesis form a logical series, they are written such that they can be read independently: each chapter has its own abstract, introduction and conclusions.

Literature

1. Davis, S.S., M.J. James and N.H. Anderson, Faraday Discuss. Chem. Soc., 1986 **81** p. 1-15.

2. Anderson, N.H., S.S. Davis, M. James and I. Kojima, J. Pharm. Sci., 1983 72(4) p. 443-448.
3. De Young, L.R. and K.A. Dill, J. Phys. Chem., 1990 94 p. 801-809.
4. Scheutjens, J.M.H.M. and G.J. Fleer, J. Phys. Chem., 1979 83 p. 1619-1635.
5. Leermakers, F.A.M. and J.M.H.M. Scheutjens, J. Chem. Phys., 1988 89 p. 3264-3274.
6. Barneveld, P.A., D.E. Hesselink, F.A.M. Leermakers, J. Lyklema and J.M.H.M. Scheutjens, Langmuir, 1994 10 p. 1084-92.
7. Böhmer, M.R., O.A. Evers and J.M.H.M. Scheutjens, Macromolecules, 1990 23 p. 2288-2301.
8. Evers, O.A., J.M.H.M. Scheutjens and G.J. Fleer, J. Phys. Chem., 1979 83 p. 1619-1635.
9. Van Lent, B., R. Israels, J.M.H.M. Scheutjens and G.J. Fleer, J. Colloid. Interface Sci., 1990 137(2) p. 380-393.
10. Singer, J.S. and G.L. Nicholson, Science, 1972 175 p. 720-731.
11. Mansfield, R.W., H.Y. Nakatani, J. Barber, S. Mauro and R.Lannoye, FEBS Letters, 1982 137(1) p. 133-136.
12. Van Kooten, O., J. Snel F.H. and W.J. Vredenberg, Photosnthesis Research, 1986 9 p. 211-227.
13. Marassi, F.M. and P.M. MacDonald, Biochemistry, 1992 31 p. 10031-10036.
14. Seelig, J., P.M. MacDonald and P.G. Scherer, Biochemistry, 1987 26(24) p. 7535-7541.
15. Van Ginkel, G., L.J. Korstanje, H. Van Langen and L.Y. K., Faraday Discuss. Chem. Soc., 1986 81 p. 49-61.
16. Israelachvili, J.N. and H. Wennerström, Langmuir, 1990 6 p. 873-876.
17. Israelachvili, J.N. and H. Wennerström, J. Phys. Chem., 1992 96 p. 320-351.
18. Israelachvili, J.N., Langmuir, 1992 8 p. 1501.
19. Rand, R.P. and V.A. Parsegian, in The Structure of Biological Membranes, Yeagle, P., Editor. 1992, CRC Press: Boca Raton p. 251-306.
20. Parsegian, V.A. and R.P. Rand, Langmuir, 1992 8 p. 1502.
21. Berendsen, H.J.C., W.F. van Gunsteren, E. Egberts and J.d. Vlieg, in Supercomputer Research. 1987, American Chemical Society:
22. Egberts, E. and H.J.C. Berendsen, J. Chem. Phys., 1988 89(6) p. 3718-3732.
23. Van der Ploeg, P. and H.J.C. Berendsen, J. Chem. Phys., 1982 76(6) p. 3271-3276.
24. Van der Ploeg, P. and H.J.C. Berendsen, Molecular Physics, 1983 49(1) p.

233-248.

25.   Berendsen, H.J.C., B. Egberts, S.-J. Marrink and P. Ahlström, in *Membrane Proteins: Structures, Interactions and Models,* Pullman, A., Editor. 1992, Kluwer Academic Publishers: Dordrecht p. 457-470.

26.   Granfeldt, M.K. and S.J. Miklavic, J. Phys. Chem., 1991 **95** p. 6351-6360.

27.   Granfeldt, M.K. and B. Jöhnsson, Mol. Phys., 1988 **64** p. 129-142.

28.   Van der Sijs, D.A. and Y.K. Levine, J. Chem. Phys., 1994 **100**(9) p. 6783-6790.

29.   Levine, Y.K., Mol. Phys., 1993 **78**(3) p. 619-628.

30.   Levine, Y.K., J. Chem. Phys., 1993 **98**(9) p. 7581-7587.

31.   Ipsen, J.H., K. Jorgensen and O.G. Mouritsen, Biophys. J., 1990 **58** p. 1099-1107.

32.   Mouritsen, O.G. and M. Bloom, Biophys. J, 1984 **46** p. 141-153.

33.   Sperotto, M.M. and O.G. Mouritsen, Eur. Biophys. J., 1990 pre-print.

34.   Marqusee, J.A. and K.A. Dill, J. Chem. Phys., 1986 **85**(1) p. 434-444.

35.   Gruen, D.W.R., J. Phys. Chem., 1985 **89** p. 146.

36.   Gruen, D.W.R. and E.H.B. de Lacey, in *Surfactants in Solution,* Mittal, K.L. and Lindman, B., Editor. 1984, Plenum: New York p. 279-306.

37.   Szleifer, I., A. Ben-Shaul and W.M. Gelbart, J. Chem. Phys., 1985 **83**(7) p. 3612-3620.

38.   Ben-Shaul, A., I. Szleifer and W.M. Gelbart, J. Chem. Phys., 1985 **83**(7) p. 3597-3611.

39.   Gruen, D.W.R. and D.A. Haydon, Pure & Appl. Chem., 1980 **52** p. 1229-1240.

40.   Marcelja, S., Biochim. Biophys. Acta, 1974 **367** p. 165-176.

41.   Barneveld, P.A., J.M.H.M. Scheutjens and J. Lyklema, Langmuir, 1992 **8** p. 3122-3130.

42.   Leermakers, F.A.M. and J.M.H.M. Scheutjens, J. Chem. Phys., 1989 **93** p. 7417-7426.

43.   Leermakers, F.A.M. and J.M.H.M. Scheutjens, J. Chem. Phys., 1988 **89** p. 6912-6924.

44.   Meijer, L.A., F.A.M. Leermakers and J. Lyklema, Recl. Trav. Chim. Pays-Bas, 1994 **113** p. 167-175.

45.   Hauser, H., I. Pasher, R.H. Pearson and Sundell, Biochim. Biophys. Acta, 1981 **650** p. 21-51.

46.   Nelson, A., J. Chem Soc. Faraday Trans., 1993 **89** p. 2799-2805.

47.   Nelson, A., J. Chem. Soc., Faraday Trans., 1993 **89** p. 3081-3090.

Chapter 1

Head-Group Conformations
in Lipid Bilayer Membranes·

Abstract

The self-assembly of lipid molecules into lamellar liquid-crystalline bilayer membranes was studied using a statistical thermodynamic method elaborating a Scheutjens-Fleer-like approach. In the modelling much attention was paid to the two-tail character and the complex head-group structure of the lipids that comprise the bilayer.

Zwitterionic head groups like phosphatidylcholine (PC) are, on average, oriented nearly flat onto the interface. At not too low ionic strengths, we find that the PC head group has two preferred conformations. Ionic head groups like phosphatidylserine (PS) are tilted towards the solution. These two predictions are consistent with experimental data.

Both co- and counter-ions penetrate the head-group region, compensating for part of the head group charges. Usually the counter-ions adsorb preferentially. However, at high salt concentrations, no positive adsorption of ions is found in dimyristoylphosphatidylserine (DMPS) bilayers. Due to the lateral pressure in the head-group area, all ions are depleted. Since negative ions are more depleted than positive ones, charge compensation is still achieved.

In order to investigate how the membrane structure can be modulated we modified the lipids by adding a hydrophilic chain onto the end of the PC head group. There are two effects. First, the increase of the bulkiness of the head group reduces the number of lipids per unit area in the membrane so that the size of the hydrophobic core diminishes. Second we predict that the orientation of the PC part of the head group is altered non-monotonically. Increasing the electrostatic screening promotes the out-of-plane tilting of the head groups toward entropically more favourable positions.

Introduction

The principle of self-assembly is one of the most essential physical ingredients that makes life possible as we know it today. Bilayer membranes are prominent manifestations of this phenomenon. It is well recognised that membrane structures belong to the more general class of association colloids. Association colloids consist of amphiphilic molecules, *i.e.* molecules with an apolar unit, often called the tail, and a polar unit generally referred to as the head group. Usually this class of molecules is known as surfactants. Apolar tails of the surfactant molecules escape the water phase by clustering together, forcing in this process the polar head groups to the outside of the aggregate. The built-up of a head group rich region creates an opposing force that, at a given stage in the self-assembling process, inhibits further growth. The aggregates formed are called micelles. Self-association only occurs above a threshold surfactant concentration that is known as the critical micelle concentration (CMC). At the CMC especially, micelles are spherical; then the number of surfactant molecules in each micelle, its aggregation number, is low (of order 50). When the concentration is increased, the aggregation number increases often to a much larger value depending on the surfactant architecture. The shape of the new aggregate may be cylindrical or lamellar-like, where at leats one dimension is related to the length scale of the size of the molecules.

In this paper we discuss lamellar aggregates, especially free, unsupported bilayer membranes. Surfactants forming membranes well, are abundant in nature. They have a glycerol backbone on which on the sn_1 and sn_2 position apolar tails are esterified and on the sn_3 position a hydrophilic head group is present. The surfactants are called phospholipids when the head group contains a phosphate group. Most natural lipids are of this type.

Lipid membranes are of interest to (molecular) biologists, because membranes are essential in many processes in the living cell. Membranes are semi-permeable barriers used to compartmentalise cells. Most biochemical reaction pathways are membrane-bound (protein molecules are embedded in the lipid matrix) or membrane-mediated (transport of molecules across membranes occurs). In most cases the membranes are expected to be inert to the processes studied and no specific changes of the membrane that might be relevant for the process studied are considered.

Lipid membranes are further of interest to physicists, because they can be envisioned as two-dimensional liquids. It turns out that the lipid molecules, especially when they are in the liquid-crystalline state, move rapidly parallel to the surface, but that flip-flop is restricted. A further rather unique property of bilayer sheets is that they have an extremely low surface tension. The

consequence of the lack of surface tension is that the membranes do not remain flat but easily change their shape. Out-of-plane thermal excursions of the membrane are known as undulations. Typically in this field molecular aspects of the bilayer are not considered. Instead, the mechanical parameters of the bilayer membrane, such as the bending elasticity, are input parameters.[1-3]

Lipid membranes are also of interest to chemists and the introduction of this paper is written from a typical chemist's point of view. A central issue for the chemist is the relation between the molecular building blocks, the association structure and its performance. For several decades qualitative insight into membrane self-assembly has been available. The amphiphilic nature of lipids is well appreciated. An important part of our understanding has come from analysing the phase diagrams of various surfactants, a time-consuming and specialised job. A theory that predicts the phase behaviour in terms of molecular structure and interactions would obviously be of great use. Some success has been obtained with a model based on a dimensionless packing parameter, $p = v/(a_0 l_c)$ (where v is the hydrocarbon volume, a_0 is the head group area, and l_c is the critical hydrocarbon chain length of the surfactant).[4,5] Four conditions can be distinguished: at $p < \frac{1}{3}$, spherical micelles; in the region $\frac{1}{3} < p < \frac{1}{2}$, cylindrical; at $p > 1$, inverted micelles are expected; at $\frac{1}{2} < p < 1$ vesicles (closed bilayers) or flexible bilayers are the preferred geometries. Of course, p gives only a first estimate for the molecular shape and obviously there is a need for a molecular interpretation. Such a model of surfactant membranes has only become possible recently with the advent of fast computers. In this paper we will show results of a statistical thermodynamic treatment of the bilayer membrane. The method used is based on a self-consistent field approximation first introduced by Scheutjens and Fleer (SF) in the context of the modelling of polymers at interfaces.[6]

Before going into details of the theory, we should mention that there are alternative techniques that are in use to study self-assembly theoretically. The MD (Molecular Dynamics) simulations of the Groningen group are probably the most detailed.[7-9] They take a large number of lipids in a lamellar geometry with water and ions in a periodic system. In an MD simulation, dynamic information of the multi-particle system is obtained in a nanoseconds time-scale. The problem, however, is that membranes do not reach equilibrium in such a short time, and up til now no convincing 'run' has been made which shows how far their structures are from equilibrium. A second problem of MD is that a single run takes many days, even on a fast computer, and that the analysis of the results is time-consuming. Nevertheless, many valuable results have been obtained so far from these simulations.

Presently it is impractical to sample a large range of parameters with MD and thus MD cannot be used for the study of the effects of lipid structure variations on self-assembling phenomena. In this paper we will present results of a study based on an SF approach for membrane formation where the conditions (*e.g.* ionic strength, surfactant structure) are systematically modified. We focus on overall membrane properties, like membrane thickness and thermodynamic stability, and on the head-group conformations of the lipids in the membrane. There are several techniques for measuring the conformation of head groups and hence it is possible to check the predictions of the theory.

The principles of the theory will be outlined to appreciate the results. For a more detailed discussion and further mathematics we refer to earlier work.[10-12]

Theory

In a first approximation, short chain surfactants are small rods and the conformational degrees of freedom of the tails are of minor importance. Indeed, when a surfactant is modelled as a dimer with a polar and an apolar part, one can reproduce the basic property of surfactants, *i.e.* their tendency to self-associate. This has been shown by MD simulations[13] and is confirmed by the present theory. Obviously, this trivial result is of limited use. We therefore consider chain molecules with given flexibilities so that they can assume many different conformations. In MD simulations, this type of complexity can also be handled but at the expense of keeping the number of molecules in the simulation box low and of uncertainty about reaching equilibrium. In our approach these restrictions are relaxed, but some model assumptions have to be made, of which the validity can be verified.

A common simplification is the use of a lattice that serves as a system of coordinates to which segments of chain molecules, solvent molecules and ions are restricted. We define flat layers of L lattice sites, each with a characteristic length ℓ and number them $z = 1,...,$ M. Between layers $z = 0$ and 1 and $z = M$ and M+1, reflecting boundary conditions are chosen such that an infinitely large (periodic) system is simulated. Near one of the boundary layers (often layer 1) we position the membrane such that the centre of the membrane coincides with the reflecting boundary. Thus there is only half a bilayer within layers 1 to M. As all our membranes are exactly symmetrical we typically present only information on half the bilayer. Note that it is permissible for the surfactants to cross the bilayer mid plane.

In this lattice we generate the full set of conformations that a chain molecule can assume. This is a time-consuming step when it is done exactly, *i.e.* when the chains are completely self-avoiding. Therefore a second simplification is carried

through in the process of chain-conformation generation. For the chains on the lattice we only correct for intramolecular correlations up to four consecutive segments. We use a tetrahedral lattice on which, in a RIS (Rotational Isomeric State) scheme, all chains are only locally self-avoiding. The local stiffness of the chain is controlled by the difference in energy between *gauche* and *trans* conformers, with *trans* being the lower in energy.

Next we determine the statistical weight of a chain in a given conformation. Once this is known we perform an ensemble averaging to determine the equilibrium properties of the system. In doing this a third simplification is used, generally referred to as the SCF (self-consistent field) approximation. The central idea behind this approach is the assumption that we can replace the extremely complicated many-chain problem by a test-chain problem in an external (potential) field (which is felt by the segments of the chain). A conformation c of a molecule is specified by the z coordinates of the segments with ranking numbers $s = 1, \cdots, N$ denoted by $\{(z,s)\}_c$. The statistical weight of this conformation, G_c is found by the Boltzmann equation $G_c = \omega_c \exp(-u_c/k_B T)$ where u_c is the potential energy felt by the conformation c, k_B is Boltzmann's constant, T is the absolute temperature and ω_c is the degeneracy of the conformation. The overall potential energy u_c is given by the sum of the individual segment contributions $u_c = \sum_s u_c(z,s)$. Let the type of segment s be given by the variable x, then $u_c(z,s) = u_x(z)$. The potential energy field $u_x(z)$ that this segment feels at position z, also referred to as the segment potential, mimics the other molecules surrounding the test chain; in fact the external field is assumed to be caused by the molecules themselves (see eqn [1]). The ensemble averaged properties of the test-chain can be found by an extremely efficient recursive method[14] that results in the overall density distributions. These distributions are used to update the potential field and the cycle is closed. A self-consistent field solution is the fixed point in this implicit set of equations (under the constraint that the lattice is completely filled). Through the potential field, intermolecular correlations can be accounted for. Inherent in the SCF approximations is the use of volume fractions $\varphi_x(z) = n_x(z)/L$, where $n_x(z)$ is the number of segments of type x in layer z. In this way the positional information of segments in the layer is neglected. We refer to this as a local-mean-field approximation. The step from segment densities (volume fractions) to external potential fields is of course crucial in the performance of an SCF theory. For this it is necessary to define energy parameters for the various segmental contacts in the system. We must take two types of interactions into account.

(i) Short-range nearest-neighbour interactions in terms of well-known Flory-

Huggins χ_{xy} interaction parameters (which are only non-zero between unlike segments; when there are q segment types, q(q–1)/2 different parameters are present).

(ii) Long-range electrostatic interactions, accounted for in a multi-Stern layer approximation. Ions and charged groups can only be positioned on lattice sites so that the evaluation of the electrostatic potential is easy once the positions of the charges are known.

We will assume the charged groups to be strong. For calculating the potential field from the charges, one needs to know the local dielectric constants.[12,15] As a first approximation we assume that the local permittivity is given by the density average over the permittivities of the various components: $\epsilon(z) = \epsilon_o \sum_x \epsilon_{rx} \varphi_x(z)$, where ϵ_o is the dielectric permittivity of vacuum and ϵ_{rx} the relative dielectric constant of a pure phase of segments of type x. The result is that inside the bilayer the dielectric constant is much lower than in the water phase. The expression used for the segmental potential is:

$$\frac{u_x(z)}{k_B T} = \frac{u'(z)}{k_B T} + \sum_y \chi_{xy}\left(\varphi_y(z) - \varphi_y^b + \frac{1}{3}\ell^2\frac{\partial^2 \varphi_y(z)}{\partial z^2}\right) + \frac{v_x e \psi(z)}{k_B T} \qquad [1]$$

The superscript b indicates the value in the bulk; $u'(z)$ is a segment-type-independent potential that is coupled to the volume constraint $\sum_x \varphi_x(z) = 1$; $\psi(z)$ is the electrostatic potential; v_x is the charge of segment x and e is the elementary charge. As both $u'(z)$ and $\psi(z)$ are chosen to be zero in the bulk, eqn [1] is normalised such as to render the bulk value: $u_x^b = 0$. We see that the short-range interactions are proportional to the local volume fraction $\varphi_y(z)$. This is typical for the Bragg-Williams approximation. It is further noteworthy that we also include the second derivative of the density profile in the short-range interaction term. This term, which is only non-zero when the segment density profile is non-linear, is essential for those systems that have sharp interfaces (as is the case in membrane systems).

It turns out that an SCF theory, which only accounts for excluded volume correlations of the type given above, is able to capture many aspects of self-assembling systems. However, the gel-liquid phase transition of lipid bilayer membranes, in which the bilayer goes from a high-temperature liquid-crystalline state, where the apolar tails are allowed to form *gauche* conformers, to a low-temperature crystalline state (characterised by the fact that the tails are in the all-*trans* configuration) is not recovered. To find this first-order phase transition one needs to also include correlations between the orientations of the bonds in the system. The theory that includes this type of nematic interactions is referred to as

the SCAF (self-consist nt anisotropic field) theory.[10,11] The result is that by keeping track of the bonds in the system one can better predict the statistical weight of a test chain. If a conformation of the test-chain has a bond in the same direction as many other bonds (also of other chains), the statistical weight of the conformation is increased, whereas when many bonds go in other directions, its contribution to the ensemble is almost unaffected. These corrections can be included without any additional parameters. Obviously, also for these nematic interactions we have to find a self-consistency criterion: the number of bonds in a given direction should match the direction-dependent nematic fields. It can be shown that the SCAF extension of the SCF theory predicts a cooperative phase transition as described above. In this paper we will use the SCAF approach but we will not discuss the low-temperature phase (gel-state) and remain in the experimentally most interesting fluid phase (liquid-crystalline state).

In the above we discussed three types of approximations: (1) the use of a lattice; (2) RIS (Markov statistics); (3) SCF approximations (including SCAF). On all three aspects of the theory one can make systematic improvements: (1) We can reduce the lattice sizes and gradually go towards continuum space.[16] (2) For short chains one can go towards completely self-avoiding chains. (3) One can include higher order correlations by using the so-called quasi-chemical instead of the Bragg-Williams approximation.[17-19] This last type of improvement will undoubtedly improve our description of water, that is presently modelled as a simple (non-associative) monomer. Work on these extensions is presently in progress.

Thus far we have discussed the (semi) one-dimensional theory. We allowed for density gradients in the z direction and applied a mean field approximation in the remaining ones (x and y). In this case lateral inhomogeneities, *e.g.* in membranes, cannot be studied, however the approach can be extended to a (semi) two-dimensional analysis at the cost of computing time. This might then be compared to the work of Mouritsen[20] who studies exclusively the x and y directions based on the ten-state model of Pink *et al.*[21]

In the introduction we have discussed association colloids with other than flat geometries. These systems can be modelled by choosing an appropriate lattice geometry (way of defining the lattice layers). Note that spherical and cylindrical geometries can still be modelled (semi) one-dimensionally. Typically, for a given association one should study various geometries (flat, spherical, etc.) and check which of the geometries has the lowest Gibbs energy. This type of micelle shape is then the preferred one. However, before we can do this we should know the thermodynamic criteria for equilibrium in a given geometry.

The thermodynamics of small systems pioneered by Hill[22] and applied to
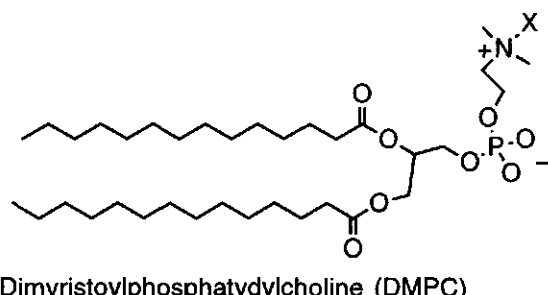
Dimyristoylphosphatydylcholine (DMPC)
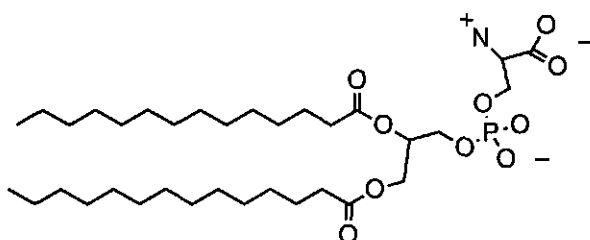
Dimyristoylphosphatydylserine (DMPS)

Figure 1. The phospholipids used in the calculations. In DMPC, X denotes CH_3 or $(EO)_n$. With n between 1 and 128, $(EO)_n$ is a hydrophilic tail (comparable to polyethylene oxide). In DMPS, the hydrogen atoms around the N are not indicated because it is treated in the same way as the N in DMPC. In the actual computations the charges on the phosphate and carbonyl groups are evened out over all oxygens and the central P and C segments, respectively.

micelle formation by Hall and Pethica[23], can be applied to the present calculations. Restricting ourselves to membranes of infinite surface area, which are not allowed to undulate, we arrive at the condition that the surface tension γ of the membrane vanishes and that $\partial\gamma / \partial d_m < 0$, where d_m is the thickness of the membrane[23,24] (see also Chapter 3). This result can be understood by considering what happens when the membrane surface tension has a finite value.

(1) A positive surface tension. This means that there is an (unfavourable) excess Gibbs energy per unit membrane area. This excess Gibbs energy is reduced when the membrane thickness, d_m, increases. This can be realised by reducing the membrane surface area, a process that will continue until the surface tension becomes negligible.

(2) A negative surface tension. In this non-equilibrium case it is favourable for the system to increase the area of the membrane. However, as the total number

Table I. The properties of the various monomer types used in this study

		H₂O	C	O	EO	PO	COO	N	Na	Cl
ε_r		80	2	80	80	80	80	80	80	80
ν		0.0	0.0	0.0	0.0	−0.2	−0.33	+1.0	+1.0	−1.0
χ	H₂O	0.0	1.6	0.0	0.0	−1.0	−1.0	−1.0	−1.0	−1.0
	C	1.6	0.0	1.6	1.6	2.6	2.6	2.6	2.6	2.6
	O	0.0	1.6	0.0	0.0	0.0	0.0	0.0	0.0	0.0
	EO	0.0	1.6	0.0	0.0	0.0	0.0	0.0	0.0	0.0
	PO	−1.0	2.6	0.0	0.0	0.0	0.0	0.0	0.0	0.0
	N	−1.0	2.6	0.0	0.0	0.0	0.0	0.0	0.0	0.0
	Na	−1.0	2.6	0.0	0.0	0.0	0.0	0.0	0.0	0.0
	Cl	−1.0	2.6	0.0	0.0	0.0	0.0	0.0	0.0	0.0

of lipids in the membrane is virtually constant this implies that the membrane thickness diminishes. Again, the expansion of the membrane will continue until the tension is gone.

In the SCAF approach we can compute the excess Gibbs energy per unit area of the membrane from the equilibrium segment distributions.[11] The computation of the equilibrium membrane thickness is therefore a double iterative process consisting of (1) an inner iteration: at a fixed overall composition of the system, SCAF solution and equilibrium segment density profiles are obtained and (2) an outer iteration: the composition is altered until the membrane surface tension is zero. When both iterations converge one has the equilibrium membrane structure, given the constraints that (a) the membranes are 2M layers apart, and (b) that the aggregation structure is lamellar. To prove that one has thus obtained the appropriate membrane structure both these aspects should be confirmed. Regarding point (a) the Gibbs energy of interaction of two bilayers should be computed. Free floating membranes are only stable if membranes are mutually repulsive. If an attractive part in the two-membrane interaction curve is found, a condensed multi-lamellar phase is preferred, *i.e.* the Kraft point has been passed. Regarding point (b) by checking whether other aggregate shapes would have a lower Gibbs energy (at a given overall composition of the system). In the following we will discuss thermodynamically stable (regarding points 1 and 2, and, unless otherwise stated, regarding points a and b) free-floating liquid-crystalline membrane systems.

Procedure

The theory outlined above is implemented in a computer program called

GOLIATH. The systems discussed in this paper consist of: (modified) DMPC or DMPS as shown in figure 1, water, modelled as monomers, and salt ions referred to as Na^+ and Cl^-. The lattice size was large enough to prevent bilayer interaction (usually M = 40 layers) with reflecting boundary conditions between layers 0 and 1 and layers M and M+1. The lattice spacing, ℓ, was set to 0.3 nm. The water was regarded as the solvent and the salt was normalised with a given bulk volume fraction. The energy between a *gauche* and a *trans* state was set at 1 k_BT, irrespective of the segment types involved. Further segment properties were chosen as given in table I. The relative dielectric constants of all components apart from the hydrocarbon C were taken as $\varepsilon_r = 80$. The relative dielectric constant of hydrocarbon was set to $\varepsilon_r = 2$, corresponding to the value found in bulk hydrocarbon fluids.

Referring to table I the contact energy between hydrocarbon and water reflected in χ_{C,H_2O}, is the most important parameter for membrane formation as it is the driving force for self-assembly. The value was chosen to be $\chi_{C,H_2O} = 1.6$, similar to the value taken in earlier studies[10,11,14] and consistent with the estimates found in the literature.[25] The value $\chi_{C,H_2O} = 1.6$ is also consistent with the dependencies of the CMC on the surfactant tail length.[26] The uncharged polar segments (O and EO) are set to be energetically equal to water with respect to their interaction with hydrocarbon. Charged components (N, Na, Cl, P and the O from the phosphate group) have a favourable χ of −1 with water to mimic solvation in water and an unfavourable one with the hydrocarbons of +2.6 for the lack of solvation in hydrocarbon. Other interactions are kept to zero for the sake of simplicity.

Since the phosphate group has a low intrinsic pK_a value of < 2.25 [27,28] it has a net negative charge of −1 at neutral pH. This charge is assumed to be distributed over all five segments. Thus, effectively we put a charge of −0.2 on each of these segments. The same approach was followed for the carbonate of PS, leading to a charge of −0.33 on each of the COO segments. The nitrogens in the choline and the serine group have a valence of +1.

Results

In the following a detailed discussion will be presented on DMPC and DMPS membranes, emphasising the changes induced by modifying the PC head group in several ways: by changing the phosphate group, the choline group and the salt strength and by grafting a long EO tail onto the nitrogen.
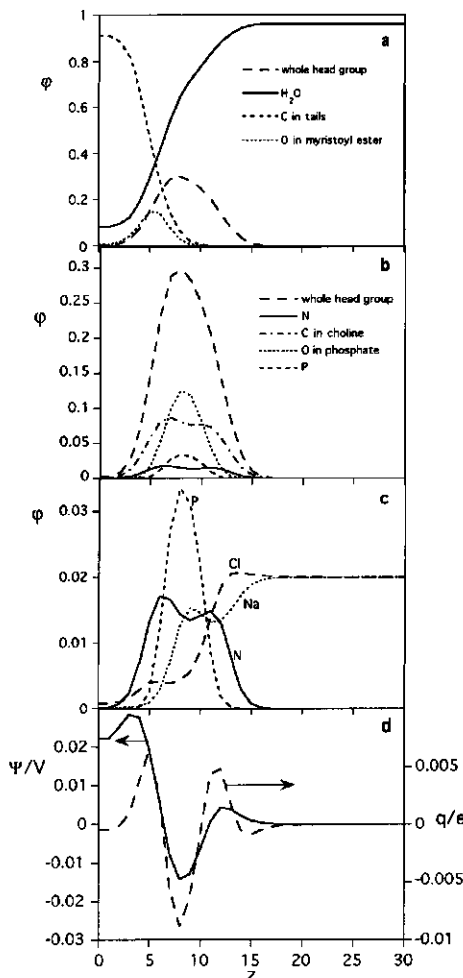
Figure 2. Segment-density profiles though a cross-section of a DMPC membrane. The bulk volume fraction of NaCl ($\varphi^b_{NaCl} = 0.04$) and ε_r and χ parameters are as in table I. The centre of the membrane is between $z = 0$ and $z = 1$. Figure (a) shows the overall distribution of the main components: the water, the hydrocarbon and the head-group segments as well as the oxygen from the myristoyl (tetradecanoyl) ester. Figure (b) shows detailed distributions of the head group area. In figure (c) the main charged segments are shown and in figure (d) the total charge [$q(z) = \sum_A v_A \varphi_A(z)$] and the potential profile across the membrane are presented.

We first present a liquid-crystalline DMPC membrane in water at a NaCl bulk volume fraction of 0.04 (figure 2a). The core of the membrane consists almost entirely of hydrocarbon units originating from the tails (short dashes). Although the head groups are positioned in between the hydrocarbon tails and the water solution, they do not fill all available space (long dashes). In fact, the volume fraction of the head groups never exceeds the value of 0.4. This implies many unfavourable hydrocarbon-water contacts. In spite of this, the membrane is stable and has no net surface tension. This is consistent with earlier work.[14,29] In previous SCAF modelling of lipid bilayers much attention was given to the tail region.[11] The two tails appear to behave slightly differently. The one in the sn_1 position is buried a few tenths of nms deeper in the membrane than the sn_2 tail. It was also found that the segments in the sn_1 tail have a slightly wider distribution than the corresponding segments in the sn_2 tail. The segment order parameter has also been previously analysed. Characteristically, the order parameter remains relatively constant for the segments in the middle of the chain, whereas it falls off to zero at the tail ends.[11] This is consistent with measurements.[30]

In figure 2b all segment types of the head group are shown individually. Clearly the phosphorus (short dashes) and the surrounding oxygen segments (dotted curve) make a rather sharp peak, while the nitrogen (solid curve) and the carbon segments (dash-dot) have a much broader distribution. There even appears to be a dip in the middle of the nitrogen distribution. We interpret this as being caused by the occurrence of two conformations of the head group that will be further investigated below.

One of the ways to characterise the head group conformation is to define a tilting angle. When we assume that the P–O–C–C–N sequence is in the all-*trans* configuration we can compute the average angle α that the head group makes with the plane of the membrane by:

$$\sin(\alpha) = \frac{\bar{z}_N - \bar{z}_P}{4} \qquad [2]$$

Where 4 is the number of bonds between the nitrogen and the phosphorous and $\bar{z}_X$ is the average position of a segment x. This quantity is computed as a volume fraction-weighted average of the layers:

$$\bar{z}_X = \frac{\sum_{z=1}^{M} z\left(\varphi_X(z) - \varphi_X^b\right)}{\sum_{z=1}^{M}\left(\varphi_X(z) - \varphi_X^b\right)} \qquad [3]$$

Hence, $\bar{z}_X$ gives the average distance in units of lattice spaces ℓ of a segment type from the centre of the bilayer. The average angle for the PC membrane
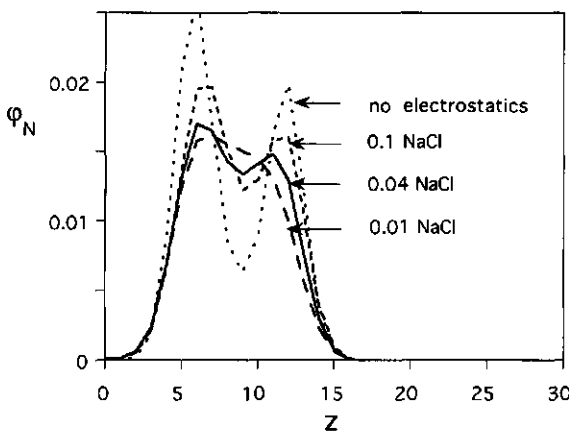
Figure 3. The volume fraction profile of the nitrogen in a DMPC bilayer embedded in aqueous electrolyte with varying ionic strength. The bulk volume fractions of NaCl are indicated. Also shown is the N profile for a membrane where all charge was removed (from PO, N, Na and Cl). Other parameters are as given in table I.

presented in figure 2 is $\alpha = 2°$.

In figure 2c only the phosphorus, the nitrogen and both the salt ions are plotted. Note that when NaCl has a bulk volume fraction of 0.04 the separate ions each have a bulk volume fraction of 0.02 that can be compared to a concentration of 1 M. Under these conditions electrostatic interactions are largely screened. The ion profiles beyond layer 15 are characteristic for the diffuse part of an electrical double layer. The local charge profile (figure 2d, dashed curve) is formed by depletion of the Na^+ ion (dotted line) rather than by accumulation of Cl^- (long dashes) because of the unfavourable interactions of the ions with the C segments around the nitrogen (figure 2b). Although the head group has no net charge, the small abundance of positive charge from the nitrogen that is pointing slightly outwards provokes a positive "surface" potential. In the middle of the head group area, around layer 9, the Na^+ has a local maximum, corresponding to a locally negative potential. This can be correlated with the dip in the nitrogen and the peak in the phosphate profile. As the carbon segments pull the positively charged nitrogen towards the hydrocarbon core of the membrane, a positive potential in the centre of the membrane is also found (figure 2d near layer $z = 1$). This in turn facilitates the enrichment of the centre of the membrane by chloride ions, more than by sodium ions. This may be part of the reason, chloride ions have a faster transport rate though PC bilayers than most positively charged ions.[31-33]
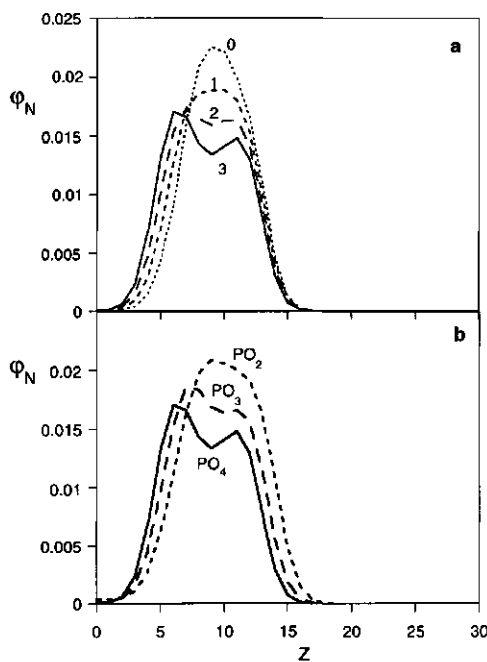
Figure 4. The volume fraction profile of the nitrogen segment in a DMPC bilayer upon decreasing the head group size. In figure (a): the bilayer-forming lipid changes from DMPE (0) by addition of CH_3 groups to the nitrogen until it becomes DMPC (3) (with 3 CH_3 groups on the nitrogen). The numbers in the graphs resemble the number of CH_3 groups at the nitrogen. In figure (b) the lipid is modified DMP^*C with P^* modified. We changed PO_4 to PO_3 and PO_2, respectively, while the total valence of the group remained −1, distributed over the P and O segments. The parameters were as in table I and the NaCl bulk volume fraction was 0.04.

The nature of the two-state distribution of the choline moiety is analysed in more detail by varying the salt concentration to 0.01 and 0.1 and by totally removing all charge from the segments (figure 3). Clearly, the electrostatic interactions tend to restrict the two opposite charges, (−) on the phosphate and (+) on the nitrogen, to the same layer(s), as could be expected. At lower salt concentrations ($\varphi_{NaCl}^b = 0.01$), the nitrogen distribution is just one peak with a small shoulder. At low ionic strength the energy cost of separating the two charged groups (N and PO_4) is prohibitive. Increasing salt concentration progressively screens the electrostatic attraction and the nitrogen obtains a broader, entropically more favourable distribution. The width of the N distribution
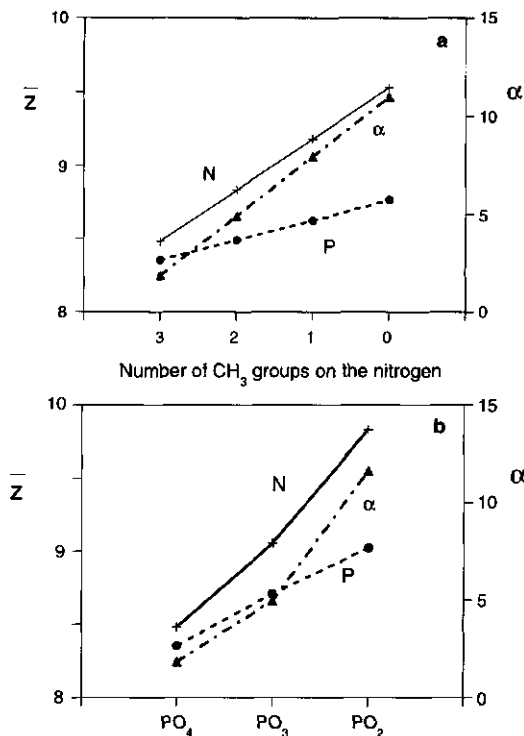
Figure 5. The average position ($\bar{z}$) of nitrogen (N) and phosphorus (P) segments and the angle (α) the head group makes with the membrane plane as a function of (a) the number of methyl groups connected to the nitrogen and (b) the number of oxygen segments around the phosphorous segment. The average positions are found by applying equation [3] to the profiles given in figure 4a.

is larger than that of the phosphorus group. This is explained by the fact that tail ends always have fewer restrictions than the middle segments. But why is there a dip half-way in the nitrogen profile?

In figure 4 we present what we believe is the answer to this question. Here the profile is shown with varying head-group size. In figure 4a the choline moiety is changed gradually to 2-aminoethanol by removing one CH_3 at a time and in figure 4b the phosphate group is changed by removing one or two oxygens, respectively, while keeping the total charge of the group $\nu = -e$ equally distributed over the remaining P and O segments. Diminishing the size of either the choline (figure 4a) or the phosphate group (figure 4b) makes the nitrogen profile change from a two-state to a one-state distribution. This leads to the

conclusion that, although the total volume fraction of the head group is less than 0.4, the volume interactions (packing constraints) are of the same order of magnitude as the electrostatic interactions.

From figure 5a we can see that the average distance from the membrane centre of the phosphorus segment increases with decreasing numbers of CH_3 groups around the N. At the same time the average angle of the head group increases. This effect can be attributed to a reduction of the head-group size. The lipids can come closer to each other and consequently the membrane grows thicker. The same effect is seen in figures 4b and 5b where the size of the phosphate group is modified.

The average angle of the P-N head group (figure 5) increases by 5°-10° upon reduction of the head-group size. This small shift can be attributed to the change of the N distribution from a double to a single conformation. In the single conformation, the position is half-way between the original two peaks at the position of the phosphate group. In the double conformation case the inner orientation is slightly preferred over the outer one. Thus the average location of the N shifts slightly outwards going from the double to the single conformation.

From a chemist's point of view it is interesting to study whether the orientation of the head group can be modified by grafting linear chains of hydrophilic segments (EO) of various lengths to the choline moiety. From a cell biologist's point of view these modified lipids are of interest for their use in *e.g.* drug-delivery systems like the so-called "Stealth" liposomes.[34] The results of such an investigation are shown in figures 6 and 7.

Several noteworthy observations can be made from these figures. We will divide our discussion into three parts. First, we will discuss the PC head group profiles. Next we turn to the effect of the EO tail on the membrane thickness and the head group orientation and finally attention will be paid to the EO tail itself.

In figure 6a we can see that, for shorter grafted tails, the N distribution favours the more outer orientation (EO chain length up to about 8). Note that this orientation has its maximum in the N-distribution further outwards than in a bilayer formed by unmodified DMPC. This is due to the hydrophilic nature of the EO segments. The Gibbs energy of the system is reduced when water completely surrounds the EO segments. To obtain a favourable water interaction, they stretch towards the water phase and pull the nitrogen outwards. This happens even when the number of EO segments attached to the choline group is low. In figure 7 this shows up as a maximum in the average position of the nitrogen, while the average position of the phosphorus segment only decreases with increasing EO chain length. This decrease is caused by the bulkier head group that has more lateral pressure (*i.e.* a higher u') and forces the head group area to

Figure 6. The volume-fraction profile of (a) the nitrogen and (b) the phosphorus segment in a bilayer of modified DMPC. One of the CH_3 groups was exchanged by a chain of EO segments (see figure 1). The size of the lattice was adapted to make sure that there was no interaction between the bilayers. The numbers in the graph show the number of EO segments in the chain attached to the nitrogen. In figure (c) the electrostatic potential profiles are plotted. In figures (d) and (e) the volume fraction profile of the water (d) and the EO segments (e) are shown. The parameters were as in table I and the NaCl bulk volume fraction was 0.04.

increase, causing the membrane core to become thinner. One other consequence of the increase in surface area per lipid molecule with longer EO chains is that the EO chain becomes less stretched. The long EO chain does not pull as strongly at the N, and hence the nitrogen can repopulate the inner state of the distribution. Consequently the average P-N angle (α) decreases: see figure 7.

It is no surprise that the membrane thickness measured as the outer border of the EO segments increases with increasing EO tail length (see figure 6e). But because of the increase of the lateral pressure the EO tails exert on each other with increasing tail length, the area per chain decreases and, consequently, the thickness of the hydrocarbon core and the local segment density of charged segments decrease. Obviously, the electrostatic potential is also affected (figure 6c). Note that the choline bends inward again with an EO tail length of 128 with the consequence that, in this case the potential in the centre of the membrane (layers 0 and 1) is again positive, while, for shorter EO chains
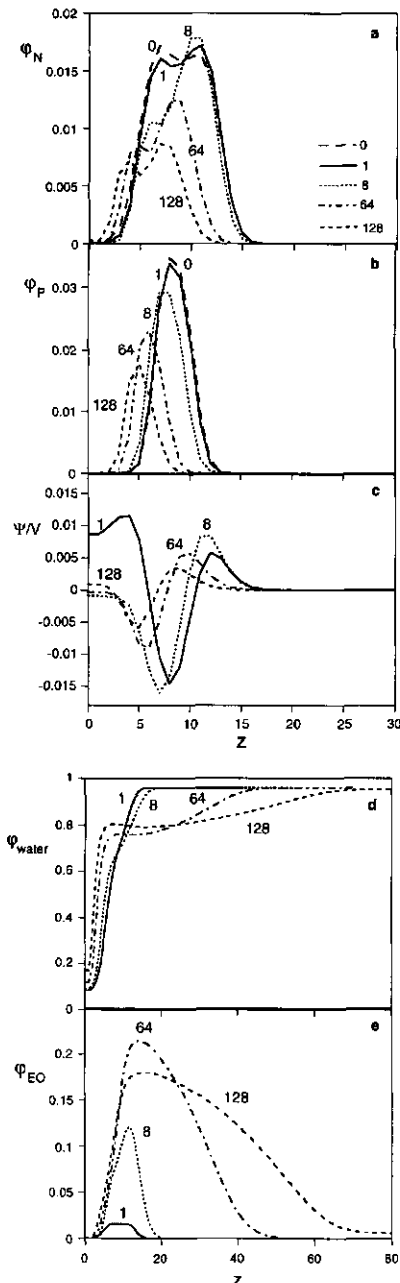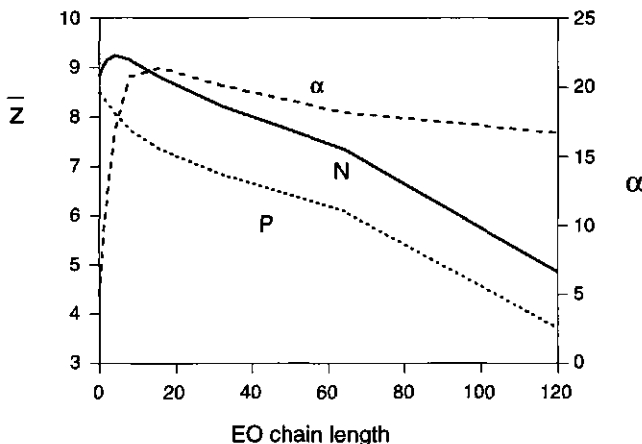
Figure 7. The average position ($\bar{z}$) of the nitrogen (N) and the phosphorus (P) segment and the angle (α) the head group makes with the membrane plane as a function of the EO chain length grafted to the nitrogen segment of DMPC. The average positions were found by applying equation [3] to the profiles given in figures 6a and 6b.

(8 and 64), the electrostatic potential is slightly negative.

In parts d and e of figure 6 the volume fraction profile of the water and the EO segments are shown, respectively. It is clear that with increasing EO chain length the water in the outer head-group region is partly replaced by the EO chains. Close to the centre of the membrane the decrease of the thickness of the hydrocarbon core and the increase of its water content upon increasing EO chain length can be observed. The EO segment profile resembles a polymeric brush. Polymer brushes, end-grafted polymers, have been described extensively.[35-38] The grafting density σ and the tail length N determine the height of the brush H: $H \propto N\sigma^{-\frac{1}{3}}$. In good solvent conditions, the profile is parabolic. Roughly the same trends are found for our EO brush, although there are some effects that should be noted. First of all, our EO tail is not very long so that deviations from the parabolic profile are noticeable, especially at the very end of the profile.[37] Secondly, with our brush the grafting density is reduced when the EO tail length is increased. This is the reason for the observation in figure 6e that the maximum in the profile for the longest tail (128) is lower than that of 64 segments. A third complication in our system, also causing a slight deviation from the parabolic profile, is that the EO chain is not uniformly grafted at an impenetrable sharp interface. Our head-group region is both penetrable by EO segments and somewhat diffuse.

We conclude that the P-N dipole can be lifted out of the flat conformation by a hydrophilic group, but that this group should not be too large.
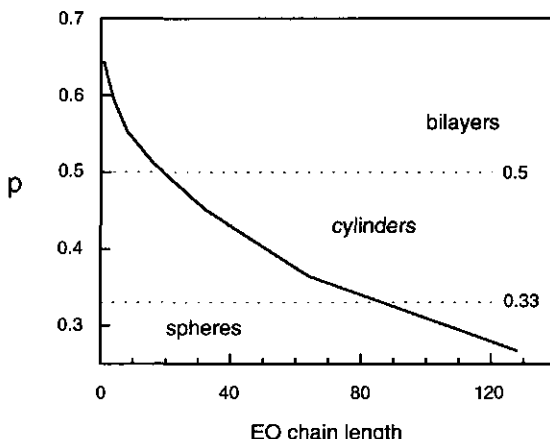
Figure 8. The packing parameter $p = v/(a_0 l_c)$ as a function of the EO chain length grafted to the nitrogen segment of DMPC. The hydrocarbon volume and the critical chain length were computed according to Israelachvili et al.[4]: $v = 2(27.4 + 26.9n)$ Å^3 and $l_c = (1.5 + 1.265n)$ Å with the number of carbon atoms in the alkyl chains $n = 14$. The surface area per chain was computed from the system of figure 6.

It is of interest to examine whether these modified lipids will or will not remain in a lamellar phase for the whole range of EO chain lengths. As a first indication that the lamellar phase does not remain the preferred geometry with increasing chain length we have plotted the packing parameter p as a function of this chain length in figure 8. The packing parameter p is calculated using the formulae given by Israelachvili et al.[4] for the hydrocarbon volume $v = 2(27.4 + 26.9n)$ Å^3 and the critical hydrocarbon chain length $l_c = (1.5 + 1.265n)$ Å with the number of carbon atoms in the alkyl chains $n = 14$. The remaining parameter needed to calculate p is the surface area per lipid molecule a_0. This value is often difficult to estimate. One can either measure it or, alternatively, calculate it as discussed in this paper. Using our calculated a_0 values, we predict that for intermediate EO chain lengths (20 < EO chain length < 80) cylindrical and for long EO tails (EO chain length > 80) spherical micelles are the preferred structures. The transitions as predicted by the value of p and indicated in figure 8 must not be interpreted as being extremely sharp. In fact, the shape transitions depend on the overall surfactant concentration in the system, *e.g.* the micelles may be spherical at low but lamellar at high concentrations. A complete analysis of these transitions is possible in the SCAF approach, but we will not do this here.
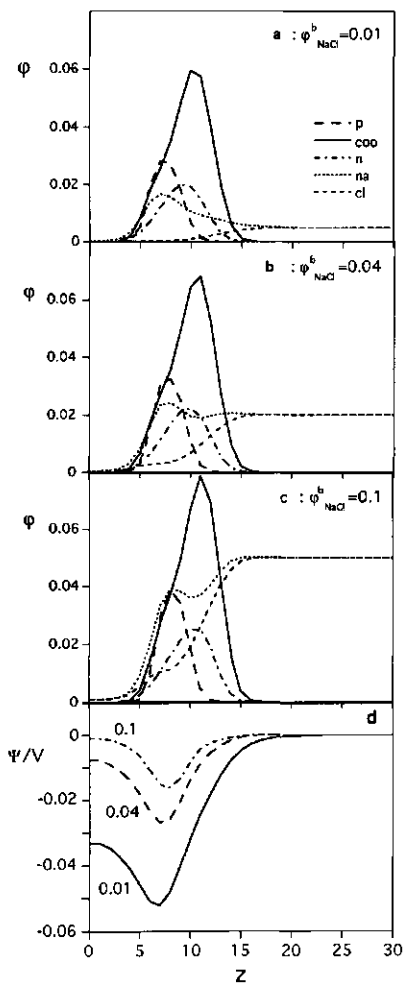
Figure 9. Segment distributions of some of the head group segments in a DMPS bilayer at different salt concentrations. Bulk volume fractions of salt are: (a), 0.01; (b), 0.04 and (c), 0.1. The resulting electrical potentials are shown in figure (d). The χ parameters, segmental valences and dielectric constants were as in table I.

We now shift our attention to membranes formed by dimyristoylphosphatidyl-serine (DMPS). In figure 9 the segment density profiles of some head group segments are shown at bulk volume fractions of NaCl of $\varphi_{NaCl}^{b} = 0.01$, $\varphi_{NaCl}^{b} = 0.04$ and $\varphi_{NaCl}^{b} = 0.1$. Here the nitrogen (dot-dashed curve) does not have a distribution with two maxima. This is partly because it lacks the methyl groups. The positively charged N is now positioned spatially between the two
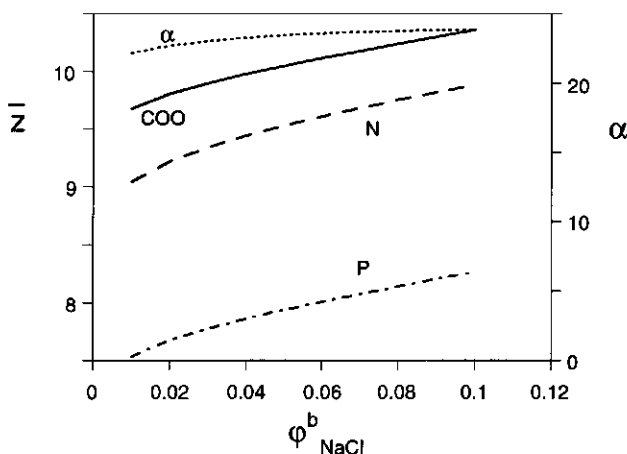
Figure 10. The average position (in layers) of the charged head group segments of DMPS and the tilting angle (α) of the head group (eqn [2]) as they depend on the salt bulk volume fraction φ_{NaCl}^{b}.

negatively charged groups. A similarity with dimyristoylphosphatidylcholine (DMPC) molecules is that the width of the distribution of the nitrogen is much broader than that of the phosphate. The phosphate is closer to the glycerol backbone, which is situated at the interface between the hydrocarbon and the water, and, therefore, is highly restricted. The distribution of the carboxylic groups (COO, solid line) is very broad as this group consists of three segments, their local density is also about three-fold higher than that of N.

The changes in head group conformation and orientation with the salt concentration are less spectacular than with DMPC but in DMPS membranes a different phenomenon draws our attention. The head group of DMPS is negatively charged and therefore the positive Na ions penetrate the head group area. Comparison of the segment density profiles for different salt concentrations reveals that PS head groups are also packed tightly together. As a result, especially at high salt concentrations, there is no positive adsorption of salt as one would expect from the electrostatic charge on the DMPS, but a depletion is found instead. The negative Cl ion is simply expelled more than the positive Na. In this way the electrostatic potential is lowered without an accumulation of salt at the membrane surface! The local concentrations ($\varphi(z)$) of Na$^+$ and Cl$^-$ in the head group area do not depend strongly on the concentration of salt in the bulk. Nevertheless, the small changes cause the electrostatic potential (figure 9d) to drop considerably from over −50 mV for $\varphi_{NaCl}^{b} = 0.01$ to just about −16 mV for

$\varphi^b_{NaCl} = 0.1$. Due to the screening of the electrical potential the head groups can come slightly closer together. This causes, in turn, an increase of the membrane thickness (figure 10). The average position of the phosphate, nitrogen and carboxylic groups increases with increasing salt concentration. As can be seen in figure 10 the increase in membrane thickness has no consequence for the average orientation of the head groups: the curves are parallel and the head group tilting angle (α) is constant.

Conclusions

Although head groups in DMPC do not completely separate the water from the hydrocarbon phase, it is evident that packing constraints in the head-group region contribute strongly to the Gibbs energy of the system. We find that at relatively high ionic strength the packing effects dominate, causing the nitrogen of the PC membrane to adopt a double conformation. One of the conformations is tilted towards the water phase, the other to the hydrocarbon phase; the two states are found in roughly equal numbers.

We have modified phosphatidylcholine by adding a hydrophilic tail to the nitrogen. We find that with increasing length of the hydrophilic tail, the hydrophobic core of the membrane reduces in size monotonically. For the orientation of the head group we predict an increase in head group tilting angle α at low grafted tail length and a decrease in α for longer tails. This behaviour is not monotonic, which can be attributed to the change in behaviour when the grafted tails start to interact laterally with each other.

The thickness (and area per chain) of DMPS membranes strongly depends on the salt concentration. The thickness increases with increasing salt concentration due to a more effective screening of the electrostatic interactions. The head group orientation (tilting angle) is, on the other hand, insensitive to the ionic strength.

At very high ionic strength we found a remarkable way to screen charges in the charged head-group region of DMPS. Both ions adsorb negatively in the head group area. As the anions are depleted more than the cations we see, in effect, that the ions compensate locally for the charge unbalance in the head-group region.

The overall conclusion is that self-consistent-field interpretations of membrane structures are very promising, because they can not only reproduce familiar features, but also predict the consequences of certain modifications in the molecular architecture.

Acknowledgements

Literature

1. Helfrich, W., Naturforsch., 1973 **28c** p. 693.
2. Helfrich, W., Naturforsch., 1978 **33a** p. 305.
3. Barneveld, P.A., J.M.H.M. Scheutjens and J. Lyklema, Langmuir, 1992 **8** p. 3122-3130.
4. Israelachvili, J.N., S. Marčelja and R.G. Horen, Quart. rev. of Biophys., 1980 **13**(2) p. 121-200.
5. Israelachvili, J.N., D.J. Mitchel and B.W. Ninham, J. Chem. Soc. Faraday Trans II, 1976 **72** p. 1525-1568.
6. Scheutjens, J.M.H.M. and G.J. Fleer, J. Phys. Chem., 1979 **83** p. 1619-1635.
7. Berendsen, H.J.C., B. Egberts, S.-J. Marrink and P. Ahlström, in *Membrane Proteins: Structures, Interactions and Models,* Pullman, A., Editor. 1992, Kluwer academic press: Dordrecht, The Netherlands
8. Egberts, E. and H.J.C. Berendsen, J. Chem. Phys., 1988 **89**(6) p. 3718-3732.
9. van der Ploeg, P. and H.J.C. Berendsen, Molecular Physics, 1983 **49**(1) p. 233-248.
10. Meijer, L.A., F.A.M. Leermakers and A. Nelson, Langmuir, 1993 **10** p. 1199-1206.
11. Leermakers, F.A.M. and J.M.H.M. Scheutjens, J. Chem. Phys., 1988 **89** p. 6912-6924.
12. Böhmer, M.R., O.A. Evers and J.M.H.M. Scheutjens, Macromolecules, 1990 **23** p. 2288-2301.
13. Smit, B., Phys. Rev. A, 1988 **37** p. 3431-3433.
14. Leermakers, F.A.M. and J.M.H.M. Scheutjens, J. Chem. Phys., 1988 **89** p. 3264-3274.
15. Barneveld, P.A., D.E. Hesselink, F.A.M. Leermakers, J. Lyklema and J.M.H.M. Scheutjens, Langmuir, 1994 **10** p. 1084-92.
16. Björling, M., *Polymers at Interfaces.* 1992, PhD thesis University of Lund, Sweden.
17. Besseling, N.A.M., *Statistical Thermodynamics of Fluids with Orientation-Dependent Interaction; Applications to Water in Homogeneous and Heterogeneous Systems.* 1993, PhD thesis Agricultural University Wageningen.

18. Besseling, N.A.M. and J.M.H.M. Scheutjens, J. Phys. Chem., 1994 in press.

19. Besseling, N.A.M. and J. Lyklema, J. Phys. Chem., 1994 in press.

20. Mouritsen, O.G., K. Jorgensen, J.H. Ipsen, M.J. Zuckermann and L. Cruzeiro-Hansson, Physica Scripta, 1990 **T33** p. 42-51.

21. Caillé , A., D.A. Pink, F. De Verteuil and M.J. Zuckermann, Can. J. Phys., 1980 **79** p. 2027.

22. Hill, T.L., *Thermodynamics of Small Systems.* Vol. 1 and 2. 1963, 1964, New York: Benjamin.

23. Hall, D.G. and B.A. Pethica, in *Nonionic Surfactants,* Schick, M.J., Editor. 1976, Marcel Dekker: New York

24. Leermakers, F.A.M., *Statistical Thermodynamics of Association Colloids.* 1988, PhD thesis Wageningen Agricultural University.

25. Tanford, C., *The Hydrophobic Effect: Formation of Micelles and Biological Membranes.* 1973, New York: John Wiley.

26. Leermakers, F.A.M., P.P.A.M. van der Schoot, J.M.H.M. Scheutjens and J. Lyklema, in *Surfactants in Solution,* Mittal, K.L., Editor. 1989, Plenum Publishing Corporation: New York p. 43-60.

27. Tocanne, S.-F. and J. Teissié, Biochim. Biophys. Acta., 1990 **1031** p. 111-142.

28. Gutman, M. and E. Nachliel, Biochim. Biophys. Acta., 1990 **1015** p. 391-414.

29. Leermakers, F.A.M., J.M.H.M. Scheutjens and J. Lyklema, Biophys. Chem., 1983 **18** p. 353-360.

30. Seelig, J. and A. Seelig, Quarterly reviews of Biophysics, 1980 **13**(1) p. 19-61.

31. Papahadjopoulos, D. and J.C. Watkins, Biochim. et Biophys. Acta, 1967 **135** p. 639-652.

32. Alberts, B., *et al.*, *Molecular Biology of the Cell.* second ed. 1989, New York and London: Garland Publishing, Inc. 1219.

33. Stein, W.D., *Transport an Diffusion across Cell Membranes.* 1986, Orlando: Academic.

34. Needham, D., *et al.*, J. Liposome Research, 1992 **2**(3) p. 411-430.

35. Milner, S.T., T.A. Witten and M.E. Cates, Macromolecules, 1988 **21** p. 2610.

36. Zhulina, E.B., V.A. Priamitsyn and O.V. Borisov, Polymer Sci. USSR, 1989 **31** p. 205.

37. Wijmans, C.M., J.M.H.M. Scheutjens and E.B. Zhulina, Macromolecules, 1992 **25** p. 2657-2665.

38. Israëls, R., F.A.M. Leermakers, G.J. Fleer and E.B. Zhulina, Macromolecules, 1994 **27** p. 3249-3261.

Chapter 2

Modeling of the
Electrolyte Ion - Phospholipid Layer Interaction[*]

Abstract

The self-consistent anisotropic field theory for chain molecules in inhomogeneous systems has been applied to the analysis of ionic behavior at the lipid-water interface of free standing phospholipid bilayers and surface-adsorbed phospholipid monolayers. Fundamental in the theory is that the conformations of lipid molecules are generated with a rotational isomeric state approximation on a lattice and weighted according to Boltzmann statistics where the local self-consistent field potential is computed using Flory-Huggins χ-parameters and averaged contact fractions. Electrostatic energies are also incorporated (in a Poisson-Boltzmann way) into the model so that quite complex molecules, in this case zwitterionic and charged phospholipids are considered. Results show that lipid head group P-N orientations in phosphatidylcholine (PC) monolayers and bilayers are angled from the layer plane in two probable conformations, whereas the head groups of phosphatidylserine (PS) in PS monolayers and bilayers have only one preferred conformation which is tilted toward the solution. The interaction of potentially permeant cations with the lipid was studied in the presence of screening electrolyte which is present at about 10^3 times the permeant ions' volume fraction in solution. Because of the form of the potential profile in both PC and PS layers, bulk electrolyte cations associate electrostatically with the phosphate group in both lipids and to a lesser extent with the carboxyl group in PS and themselves modify the potential profile across the lipid layer. The attraction of cations to the polar groups is greater with negatively charged PS than with zwitterionic PC and increases with the charge on the cation. Although there is a large difference between the potential profiles across monolayers of PC and PS in a monovalent cation 1:1 electrolyte, the difference in potential profiles across the two lipid layers PC and PS respectively is not so great in 2:1 and 3:1 electrolytes. This is reflected in the adsorption of permeant cations at the lipid-water interface.

Introduction

A previous paper[1] used the self-consistent field theory to model the structure of an adsorbed phospholipid monolayer on a mercury electrode. This was done not only to gain an insight into the structure of the phospholipid monolayer but also to understand better the occurrence of certain well-defined phase transitions in response to potential change. A good agreement between theoretical predictions and experiment[2] was obtained which led to a clarification of the lipid structure and interactions between lipid molecules. However, the simulated lipid molecules were a relatively crude representation and the model took no explicit account of charge effects. This theory has since been developed and has become more sophisticated. Now not only Flory-Huggins (FH) contact energies are taken into account but also electrostatic potentials. The possibility is available now of working with quite complex molecules. We have used GOLIATH, a computer implementation of the self-consistent anisotropic field (SCAF) theory, discussed below, which is specialized in the analysis of self-assembling interfacial phenomena.

Much experimental work has now been carried out looking at ionic permeability in both unmodified[3] and modified[4,5] phospholipid layers adsorbed onto mercury electrodes. This has been done because these adsorbed layers have proved to be an excellent new type of biological membrane model enabling very precise measurements on phospholipid monolayer permeability to ions to be performed. Additional concurrent experiments have shown that ionic interactions in the lipid surface region are important in influencing ionic permeability in negatively charged lipid layers[6] and lipid layers with ion channels.[7] Indeed, such lipid surface charge effects are of general significance in biological membrane studies with relation to their role in controlling ion transport[8-10] and the activation of voltage-gated ion-channels.[11] By the same token, ionic and charge interactions in the polar region of a phospholipid layer and the way in which these relate to the composition of the adjacent bulk solution are of enormous biological significance.[9,10,12] In order to understand these interactions better, we have used the GOLIATH computer program to simulate the ionic interactions in the lipid surface region. In the following we describe the results of calculations where both zwitterionic and negatively charged phospholipid molecules have been built from uncharged and charged monomer segments. We have investigated their interactions with ions by studying bilayers and monolayers in different electrolyte solutions.

Theory

We consider lipid layers consisting of densely packed self-associated chain molecules in an aqueous environment. Any theory for the description of such

$(H_2C)_{16}CO_2$ —— CH_2

$(H_2C)_{16}CO_2$ —— CH

CH_2-O —— P —— O-$(CH_2)_2$-$\overset{\oplus}{N}(CH_3)_3$

with O, $\ominus$, O on phosphorus

1
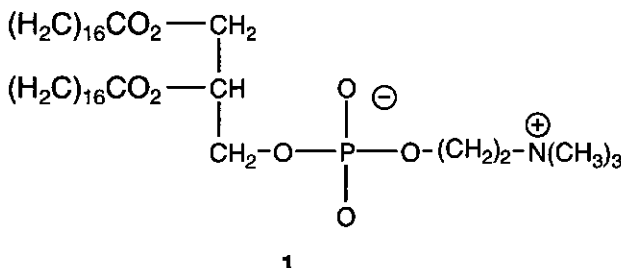
layers should include the relevant energetic interactions (unfavorable tail-water and favorable head group-water contacts) and entropic contributions [intramolecular (conformational) and intermolecular (configurational) degrees of freedom]. An exact theory including all correlations is not yet feasible. Hence approximate methods are being used. A successful approach is based on the method to enumerate the partition function using a SCAF approach.

In the SCAF theory the statistical weights of all conformations of a test chain molecule on a lattice are determined by way of Boltzmann statistics. In addition to this an anisotropy factor that takes into account the fact that densely packed chains tend to line up with each other, weights each conformation of the test chain. Conformations are generated by a second order Markov approximation also known as the rotational isomeric state (RIS) scheme. The local segment potentials used in the Boltzmann factors contain three contributions: a space filling potential; contact energies averaged over three adjacent lattice layers on the basis of FH χ-parameters; an electrostatic contribution determined by the charge density and dielectric permitivity profile which, in turn, depend on the density profiles.

An iterative Newton computer algorithm ensures that the segment densities (also called volume fractions) are consistent with the segmental potentials. Only the SCAF solution for which the boundary conditions are met is accepted. In Appendix A the closed set of equations used in the GOLIATH program is presented.

Procedure

The layer thickness (ℓ) of the lattice was set to 0.3 nm. A lattice of 50 layers from a reflecting boundary for a free-standing bilayer and from an adsorbing surface for an adsorbed monolayer was used.

Two types of lipid molecules were considered in which, according to a united atom approach, each monomer segment, $e.g.$ -CH_2- is written as one unit:

(1) A zwitterionic phosphatidylcholine (PC) type molecule with a structure depicted as **1**. The charge on the phosphate group was smeared out over five atoms of phosphorus and oxygen, each represented by one segment. This is not

$$(H_2C)_{16}CO_2 - CH_2$$
$$(H_2C)_{16}CO_2 - CH$$
$$CH_2-O-P-O-CH_2-CH-C$$

2
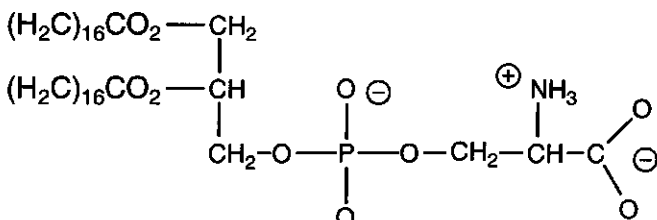
strictly correct since it makes the phosphate group rather large but it does take account of the electronegativity of the esterified oxygen atoms and renders the $-PO_4^-$ group as a singly charged unit consistent with its low intrinsic pK_a value of <2.25.[10,13] This was a first approximation. Future studies will vary the distribution of negative charge within the phosphate group in accordance with ideas of molecular resonance to see how this affects the ionic interactions. The positive charge on the choline group rests only on the nitrogen atom.

(2) A phosphatidylserine (PS) type molecule with a structure depicted as **2**. Note that the terminal carboxyl group occupied three segments with smeared negative charge. The PS type molecule was introduced into the model system in the form of a salt neutralized with a univalent metal cation (M^+).

The surface to which the lipid was adsorbed was considered a fixed plane. For the solvent, water with dielectric constant 80 was simulated. In modeling the salt distribution, we have always considered two electrolytes (a) one containing a permeant ion whose behavior on the lipid surface is of critical importance with respect to its potential permeability in the lipid film and (b) a screening electrolyte, of about 10^3 times higher volume fraction as the electrolyte containing the permeant ion. This terminology is used since in concurrent experimental work the permeability of an ion in a lipid layer is always measured in the presence of an excess screening electrolyte.[6,7] The symbols used in this study for permeant cations and electrolyte cations with their respective valencies are as follows: permeant cations, Tl(I), Cd(II), Eu(III); electrolyte cations, Na(I), Mg(II), La(III). We have also considered the distribution of electrolyte anions at the lipid/water interface labeled with their respective valencies as follows: X(I), ClT(III).

All volume fractions of screening salt (cation + anion) were set at 10^{-2} whereas those of the permeant salt (cation + anion) were generally set at 10^{-5}. So the only difference between screening and permeant cations is their (bulk) volume fraction. Again the point of introducing two ion types with the same interaction parameters is to facilitate comparison with the experiments where the two ions can be distinguished.[6,7]

Table 1. Summary of Flory-Huggins (FH) Interaction χ–Parameters between Segments, Ions (M) Surface (Hg) and Solvent (H_2O).

χ	Hg	H_2O	CH_2	CO	O	P	N	M
Hg	0	4.8	0	1	4.8	4.8	4.8	4.8
H_2O	4.8	0	1.6	0	−2	−2	−2	−2
CH_2	0	1.6	0	1	4	4	4	4
CO	1	0	1	0	0	0	0	0
O	4.8	−2	4	0	0	0	0	0
P	4.8	−2	4	0	0	0	0	0
N	4.8	−2	4	0	0	0	0	0
M	4.8	−2	4	0	0	0	0	0

Note that all ions have the size of a lattice site. Thus the electrostatic part of the model evolves to a modified Poisson-Boltzmann approach. The finite size of the ions is important because they invade the head group region and compete for the available space. Table 1 lists the χ-parameters between the segments considered in this study. Several of these parameters are the same as those previously employed. Thus interactions between water and the surface were given as 4.8 to simulate the hydrophobicity of mercury.[1] The same value of this χ-parameter was also applied to ionic interactions with the surface. Water interaction with the hydrophobic CH_2 segments has the χ-parameter of 1.6 as before but ionic interaction with these segments was set at 4 to reflect the lower permeability of ions compared to water in the lipid hydrocarbon phase.[14] The interaction of the -CH_2- segments with the surface is set to 0, as before and all ionic interactions with water were set at −2. The CO_2 acyl group esterified by the glycerol backbone was an uncertainty to model. It carries no charge but is always considered as part of the polar group due to its polarizability.[15] As a first approximation we treated it as only one segment and its FH interactions with all segments, ions and water were set as zero except its interaction with the –CH_2– segment and with the surface which was given as 1 representing its lower hydrophobicity than these entities.

Results

Equilibrium Membrane in Solution
First a free liquid crystalline bilayer membrane was modeled with 0.01 volume fraction of univalent 1:1 salt in solution. The bilayer membrane was simulated so that it could attain its most thermodynamically favorable thickness under the set
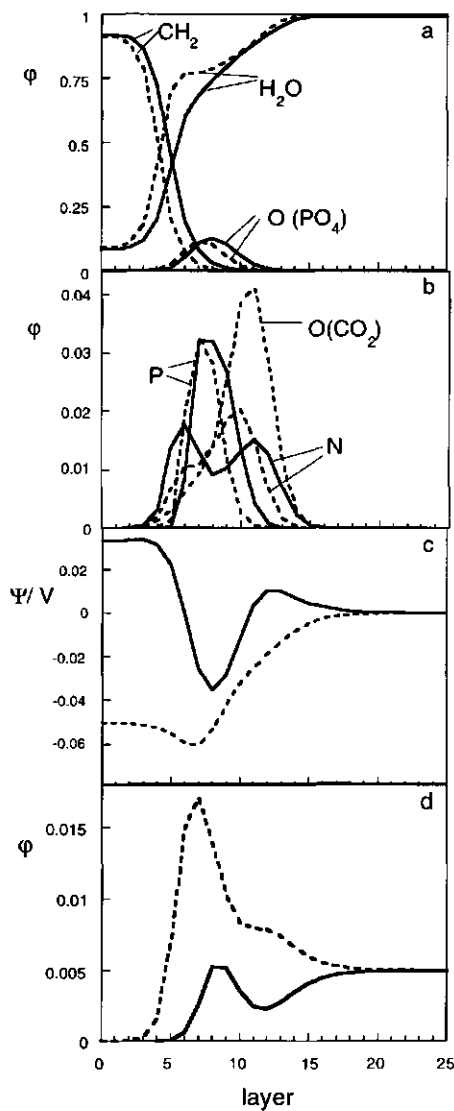
Figure 1. Segment volume fraction profiles for half a lamellar bilayer membrane: (a) tail segments (CH_2), the solvent (H_2O) and the oxygen (O) segments associated with the phosphate moiety, (b) the phosphate (P), nitrogen (N) of the head group and the oxygen (O) associated with the CO_2 group of PS, (c) the potential profile and (d) the volume fraction profile of electrolyte ion, Na(I) in 10^{-2} volume fraction electrolyte salt Na(I)X. Continuous curve, phospholipid PC; broken curve, phospholipid PS. The midplane of the bilayer is situated between layer zero and layer one.

conditions. In later studies, dealing with the adsorbed monolayer system, the obtained thickness for half a bilayer was used throughout for a given lipid and input prior to calculation. Parts a and b of figure 1 show the volume fraction versus distance profile of half of the bilayer membrane of PC and PS. The volume fraction profile of the O segments surrounding the P segments is used to denote the position of the head groups. The structures resemble those previously modeled.[1] We can also see the head group structures in more detail where the individual segments are portrayed. If we consider in the first instance the structure of PC (continuous curves in figure 1), we find that there is on average a more or less parallel orientation of the P-N dipoles to the layer plane. Note the double peak in the distribution of the N segment (figure 1b). This phenomenon is a result of a complex balance between steric (space filling), conformational (entropic) and energetic contributions. Electrostatic and contact energies favour the P and N to be in the same plane. However, the space filling constraint opposes this. The splitting up is an entropic favorable compromise. Thus, the choline group is bent toward the phosphate group and this bent configuration has two alternate conformations. This has been experimentally observed and also discussed for PC.[15]

We can see in figure 1b that the probability for the outer conformation is slightly smaller than that for the inner one. This distribution can be influenced in several ways. As an example we show in figure 7b that this can be done by changing the hydration of the charged groups *i.e.* the χ-parameter between water and the charged groups. With a decrease of the hydration (less negative χ-value) the flat conformation of the head group tends to gain importance. Note that when less water is associated with the head groups, their effective size reduces and the lipids can come closer to each other. This in its turn has the effect that the equilibrium membrane is thicker and thus the adsorbed amount in figure 7b increases to $\theta = 6.826$ compared to $\theta = 5.695$ with χ values from table 1. If the hydrophilicity of the ionic groups is further reduced, the membrane loses its thermodynamic stability: There is no composition for which the surface tension vanishes.

It is quite clear that if the P-N dipole of PC were exactly parallel to the interface and if the two charged groups were entirely equivalent in electronic and molecular structure, there would be no potential profile across the monolayer. The angular displacement of the choline group relative to the phosphate group gives rise to the positive potential peak on the outermost side of the membrane and a positive potential excursion on the inner membrane side of the phosphate group (figure 1c). In between there is a negative potential peak coinciding with the phosphate moiety.
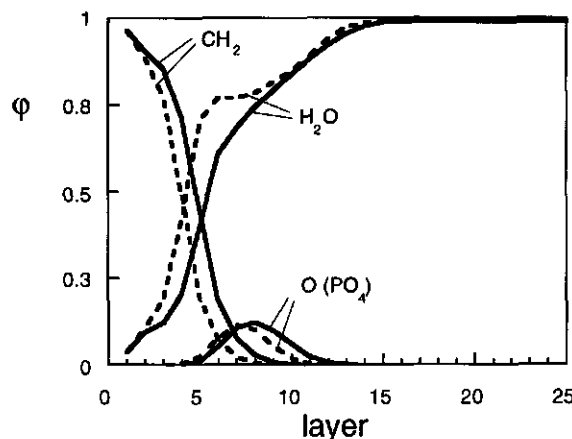
Figure 2. Segment volume fraction profiles for a phospholipid monolayer adsorbed on a hydrophobic surface in 10^{-2} volume fraction electrolyte salt, Na(I)X. Continuous curve: phospholipid PC, broken curve: phospholipid PS. The hydrophobic surface is situated in layer zero.

The orientation of the PS polar group is slightly different to that of PC (broken curves in figure 1). The negative charge on the serine moiety is oriented out of the plane of the membrane toward the solution (figure 1b). This pulls the N moiety with it so that only a small number of lipids have a head group conformation slightly bent toward the hydrocarbon core leaving a small shoulder in the volume fraction profile with PS. In this instance the potential profile is dominated by the negative charge which instigates a large drop in potential toward the phosphate moiety and a small positive recovery toward the center of the monolayer (figure 1c). We observe that the orientation of the PS groups is such that the positive charge carried by the amine moiety is always overlapped by negatively charged groups in the profile along the layer normal. For this reason there is no positive excursion in potential on the outer side of the membrane. We note also that half the equilibrium membrane thickness, $\theta = 4.746$, of PS is less than that of PC, $\theta = 5.695$, due to the negatively charged head groups and their repulsion maintaining a thinner membrane. These values of θ were subsequently used throughout in the adsorbed phospholipid monolayer simulations except in figure 7b.

The volume fraction of electrolyte cation associated with the head group follows the potential profile (figure 1d). Note the initial dip in volume fraction of Na(I) on the solution side of the PC layer corresponding to the initial positive potential peak. Further into the polar group region, there is an association of Na(I) with the negative potential peak. Henceforth, we refer to this as an adsorption peak of the ion within the polar region of the lipid layer. With PS there is also an accumulation
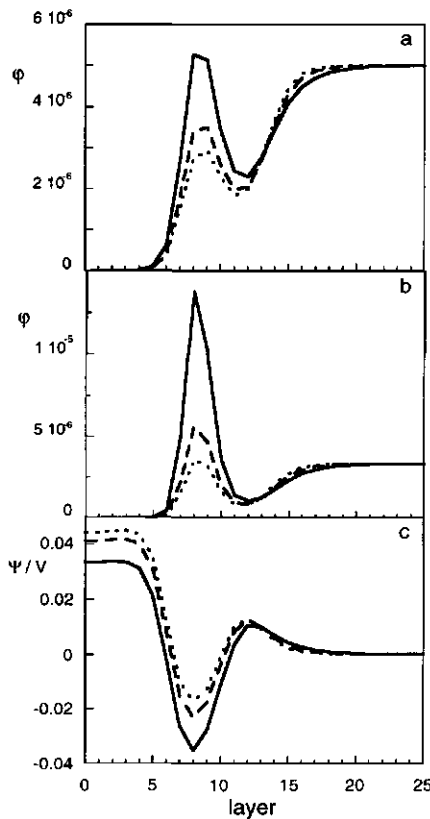
Figure 3. Permeant ions, (a) Tl(I) volume fraction and (b) Cd(II) volume fraction and (c) potential profiles across PC monolayer adsorbed on a hydrophobic surface in electrolyte solutions of Na(I), continuous curve, $\varphi^b = 5.0 \cdot 10^{-3}$; Mg(II), broken curve, $\varphi^b = 3.3 \cdot 10^{-3}$; and La(III), dotted curve, $\varphi^b = 2.5 \cdot 10^{-3}$.

of Na(I) associated with the negative potential peak but no initial drop in Na(I) volume fraction at the PS layer-water interface. A three times higher volume fraction of Na(I) is associated with PS than with PC.

Adsorbed phospholipid layers

Figure 2 shows the profiles of phospholipid layers of PC and PS adsorbed on mercury. The similarity to half a bilayer is readily apparent except for interactions close to the mercury surface (compare figure 1a and figure 2).

Figures 3 and 4 show profiles of permeant ion Tl(I) and Cd(II) volume fractions and the electrostatic potential along the adsorbed PC and PS monolayer normals, respectively, in the presence of screening electrolyte cations with increasing charge. Immediately evident in figure 3 is that the adsorption peaks of Tl(I) and of
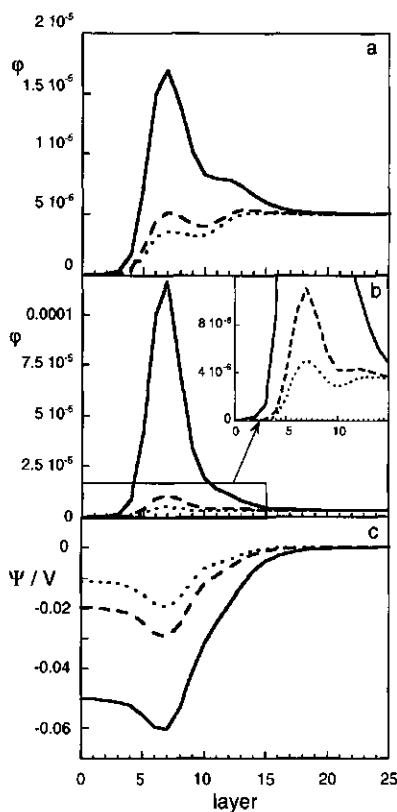
Figure 4. Same as figure 3 but across PS monolayer adsorbed on a hydrophobic surface.

Cd(II) are associated with the negative potential peak in the PC layer normal profile. This adsorption peak is very much larger for divalent Cd(II) than for univalent Tl(I). Also evident is the suppression of the negative potential peak in divalent Mg(II) electrolyte and even further in trivalent La(III) electrolyte. The adsorption of the permeant ion thus follows the magnitude of the negative potential peak. From figure 4 we note that Tl(I) is enriched by a factor of 3 in the lipid polar groups of PS compared to the polar groups of PC like Na(I) was in free standing bilayers. Similarly Cd(II) is enriched by a factor of about 8 in PS compared to PC. This is because the net charge on the PS head group has to be compensated whereas PC has no net charge. Additionally in PS layers, divalent and trivalent electrolyte cations depress the negative potential peak and adsorbed volume fraction of cations much more than in PC layers. In La(III) electrolyte, this occurs to such an extent that the negative potential peaks in the layer normals of
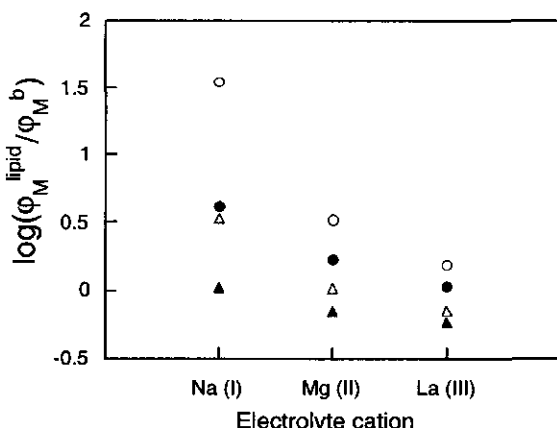
Figure 5. Logarithm volume fraction peak of permeant cation adsorbed on lipid surface minus logarithm volume fraction of permeant cation in solution $(\log(\phi_M{}^{lipid}/\phi_M{}^b))$ versus the electrolyte cation whose volume fractions are: $5.0 \cdot 10^{-3}$, $3.3 \cdot 10^{-3}$ and $2.5 \cdot 10^{-3}$ for Na(I), Mg(II), and La(III), respectively: (O) permeant cation Cd(II), lipid PS; (●) Cd(II), PC; (Δ) Tl(I), PS; (▲) Tl(I), PC.

PC and PS are almost of the same magnitude. The same can be said of the volume fractions of adsorbed permeant cations.

In figure 5, the above effects are summarized and the surface excess of permeant cation is plotted against the screening electrolyte cation charge. Here we plot this cationic surface excess as the logarithm of the ratio of the peak volume fraction of permeant cation associated with the lipid to the volume fraction of permeant metal ion in bulk solution. We see quite clearly in the first case the effect of charge on the permeant metal cation increasing its interaction with the lipid, second the effect of the negative charge on PS increasing the lipid's interaction with the permeant cation, and finally the effect of the increasing charge on the screening ion in increasing the similarity of the adsorption behavior of all permeant ions. These effects arise since the screening cation competes with the permeant cation for the lipid surface. This is also seen in figure 6 where the surface excess of the permeant ion Eu(III) on the lipid is plotted against the volume fraction of the electrolyte ion La(III) in solution. Na(I) was also present in the electrolyte at a constant volume fraction of $5 \cdot 10^{-3}$. We observe that with a higher volume fraction of La(III) in the electrolyte, Eu(III) is displaced from the lipid surface. Accordingly at $2.5 \cdot 10^{-4}$ volume fraction La(III) in the solution, the surface excess of Eu(III) is almost the same on the PS layer as on the PC layer in the absence of La(III).

Finally it is interesting to observe that the presence of higher valent electrolyte
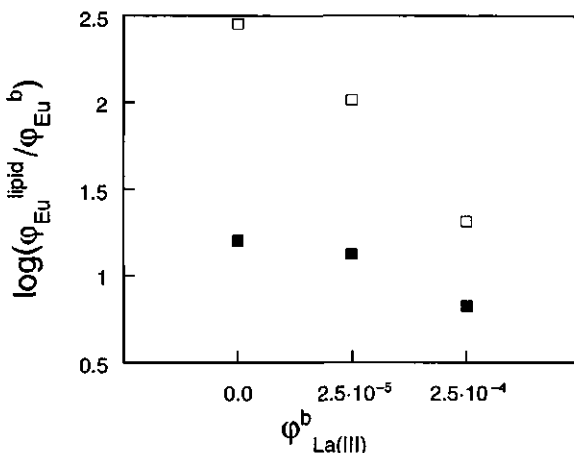
Figure 6. Logarithm volume fraction peak of Eu(III) adsorbed on (□) PS and (■) PC surface minus the logarithm of volume fraction of Eu(III) in solution [$\log(\varphi_{Eu}^{lipid})/\log(\varphi_{Eu}^{b})$] versus the volume fraction (φ) of La(III) in the electrolyte (volume fraction of Na(I)X, 10^{-2}).

ions alters somewhat the conformation of the polar groups of PC (figure 7a). Thus trivalent electrolyte cations increase the resolution of the two conformations of PC. Lanthanide ions have indeed been shown experimentally to influence the orientation of the polar groups of PC through their adsorption.[16,17]

The profiles of electrolyte anions are also interesting with respect to their charge (figure 8). On PC head groups, the anions associate in the region of the positively charged groups. With more highly charged anions this association increases. There is little influence, however, on the permeant cation (Tl(I)) volume fraction profile and the potential profile (compare with parts a and c of figure 3).

Discussion

Although a number of approximations and simplifications have been undertaken in this model, several important concepts emerge. The significance of the electrostatic potential profile in cationic adsorption within lipid layers has become apparent and the influence on this from the electrolyte ion is of important implication. Thus, the electrical potential gradient will determine the chemical activity of ions adjacent to the hydrocarbon phase. Cation binding to phospholipid layers has always been of interest and is a complex phenomenon in which chemical binding and electrostatic adsorption have been considered separately.[9,10,12,17] Indeed, the strength of cation binding to the lipid has already been shown to depend greatly on the charge on the lipid and the valency of the cation.[9,10] The fact that the model used in this study shows this order of cation
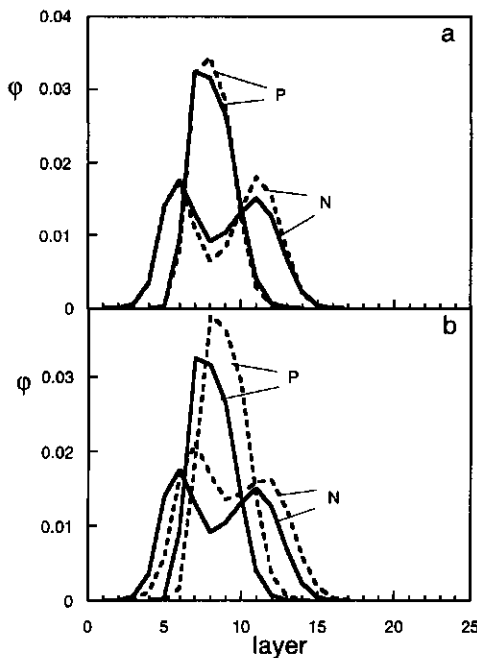
Figure 7. Head group segment volume fraction of the P and N segments for a PC monolayer adsorbed on a hydrophobic surface: (a) continuous curve, in Na(I) ($\varphi^b = 5 \cdot 10^{-3}$) electrolyte; broken curve, in La(III) ($\varphi^b = 2.5 \cdot 10^{-3}$) electrolyte; (b) continuous curve as in (a), broken curve with χ-parameter between water and charged groups set to -1, other χ's equal to values in table 1, the adsorbed amount $\theta = 6.826$, half the thickness of the equilibrium membrane.

binding within the context of electrostatic interaction questions the validity of separating the chemical and electrostatic factors. In a similar argument, binding to a PC layer was previously thought to be driven by some chemical affinity since any positive charge adsorbed on a net neutral surface will hinder further adsorption.[17] Experimentally at the molecular level however, no distinction was seen between chemical binding and electrostatic adsorption.[17] The present study predicts that significant electrostatic adsorption of cations occurs in response to the potential profile across the lipid layer which depends on the orientation of the polar group. These ideas have been discussed in earlier reviews in a speculative manner.[10] This topic is always important in biological membrane studies since the concentration profile of adsorbed ions in the head group region of lipids will determine the flux of ions through channels in the membrane.

The results from this study therefore indicate that fixed charge in the polar
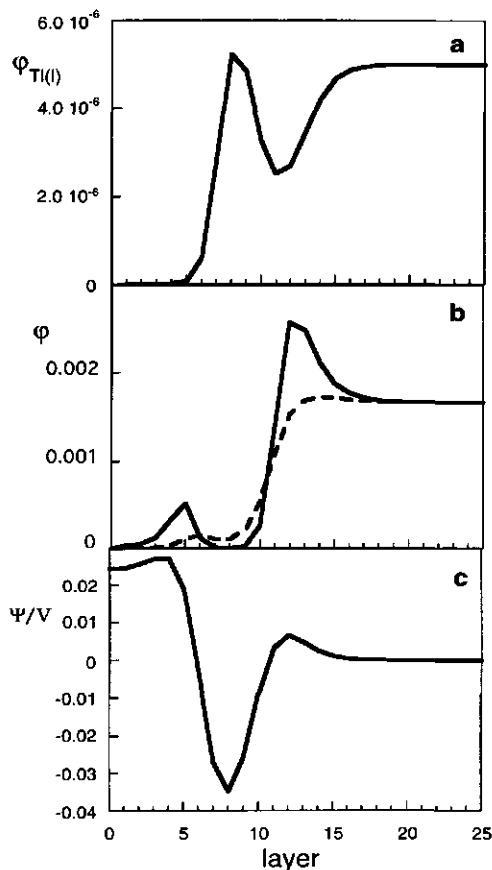
Figure 8. Volume fraction profile of (a) Tl(I) and (b) electrolyte anions (X(I), continuous curve and CIT(III), broken curve) and (c) potential profiles across PC monolayer adsorbed on hydrophobic surface. With 10^{-2} bulk volume fraction [Na$_3$CIT(III) + Na(I)X] as electrolyte.

group region of lipid layers and modified lipid layers could have a marked effect on the cationic flux through these layers. More importantly, this model shows conceptually the way in which fixed membrane charge exerts its effect. This is significant since the influence of fixed lipid charge on lipid layer[6] and ion channel[7-9] permeability has already been experimentally shown to exist and qualitatively the effects are similar to those predicted by the model.

Conclusions

The SCAF theory simulates both free standing bilayer and surface-adsorbed monolayer structures when detailed lipid molecular forms and segment:segment interactions are input. Using realistic parameters, we show that two major

conformations of the head group of PC can exist whereas P-N orientations in PS layers are slightly angled outward from the layer plane in one conformation. Adsorption of higher valent electrolyte cations increases the resolution, while decreased hydration of the charged groups decrease the resolution of the head group conformations in PC layers. In PC layers the angulation of the P-N group from the layer plane in each of the two conformations gives rise to a potential profile with positive and negative peaks along the layer normal. Because of the form of the potential profile in both PC and PS, cations associate electrostatically with the phosphate group and to a lesser extent with the carboxyl group in PS. Divalent electrolyte ions, and to a greater extent trivalent permeant ions, show a higher affinity for the lipid polar groups than monovalent permeant ions. Permeant cations have a very much greater affinity for negatively charged PS than for zwitterionic PC in a monovalent screening electrolyte. This difference is decreased in divalent screening electrolytes and further in trivalent screening electrolytes. This occurs because the permeant ion volume fraction profile follows the potential profile which is set not only by the type and orientation of the lipid polar groups but also by the association of the screening electrolyte cation with the polar groups.

Acknowledgements

Appendix A.

The Self Consistent Anisotropic Field Theory

In this Appendix we limit our discussion to linear chain molecules of type i with segments numbered from $s = 1$ to $s = N_i$ in an inhomogeneous system. A statistical thermodynamic method is used to calculate the statistical weight of all conformations of each chain in a segmental potential field generated by all the other molecules.

To represent the configurations of such chains composed of segments, a rotational isomeric state (RIS)[18] scheme is used on a three choice lattice. This allows the distinction between the *trans* and *gauche* configurations. We use a tetrahedral lattice, that can be represented in two dimensions as a square lattice as show in figure 9, with lattice spacing ℓ. The four directions that exist are indicated: h denotes the direction from one layer (z) to the next $(z + \ell)$, f and g refer to two different directions within a layer and e is used for the direction from one layer (z) to the previous one $(z - \ell)$.
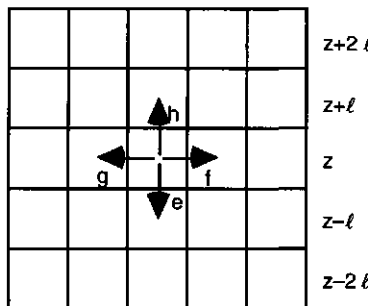
Figure 9. The two-dimensional square lattice representation with the four directions indicated (e, f, g, and h).

A typical segment in a chain is connected by two bonds to the rest of the chain. The volume fraction of a segment number s in molecule i that has a connection in direction α (e, f, g, or h) and one in direction β (e, f, g, or h) is computed as

$$\varphi_i\left(z, s_{12}^{\alpha\beta}\right) = C_i \, \frac{G_i\left(z, s_1^{\alpha\beta}\right) G_i\left(z, s_2^{\alpha\beta}\right)}{G_i\left(z, s^{\alpha\beta}\right)} \qquad [1]$$

The subscripts 1 and 2 designate that there is a chain end connected to the first or the second bond of the segment, respectively. C_i is a normalization constant discussed below. The chain end distribution functions $G_i\left(z, s_1^{\alpha\beta}\right)$ is defined according to the recurrent relation:

$$G_i\left(z, s_1^{\alpha\beta}\right) = G_i\left(z, s^{\alpha\beta}\right) \sum_{\gamma''} \lambda^{\gamma''-\alpha''-\beta''} G_i\left(z', s_1'^{\gamma'\alpha'}\right) G^{\alpha''}\left(z|z'\right) \qquad [2]$$

where $s_1' = s - 1$, indicating the chain generation from s = 1 to s = N_i and correspondingly for $G_i\left(z, s_2^{\alpha\beta}\right)$:

$$G_i\left(z, s_2^{\alpha\beta}\right) = G_i\left(z, s^{\alpha\beta}\right) \sum_{\gamma''} \lambda^{\alpha''-\beta''-\gamma''} G_i\left(z', s_2'^{\beta'\gamma'}\right) G^{\beta''}\left(z|z'\right) \qquad [3]$$

with $s_2' = s + 1$ for the reversed chain generation.

A prime on α, β, or γ is added to designate the connecting direction and a double prime denotes any of the two directions α or α' according to table 2, where also the layer z' is defined.

In this way the chains are "grown" from the free segment weighting factors, $G_i\left(z, 1_1^{\alpha\beta}\right) = G_i\left(z, 1^{\alpha\beta}\right)$ and $G_i\left(z, N_2^{\alpha\beta}\right) = G_i\left(z, N^{\alpha\beta}\right)$. The unconnected weighting factors are independent of the orientation of the segments:

Table 2. Direction α and the Connecting Cirection α' and the Relations to z'.

α (layer z)	α' (layer z')	z'
e	h	$z - \ell$
f	g	z
g	f	z
h	e	$z + \ell$

$$G\left(z, s^{\alpha\beta}\right) = \begin{cases} G(z,s) & \text{if } \alpha \neq \beta \\ 0 & \text{if } \alpha = \beta \end{cases} \qquad [4]$$

By putting this weighting factor to zero when $\alpha = \beta$ direct back folding is prevented. The chain ends have only one bond connected and eqn [1] simplifies

$$\varphi_i\left(z, 1_{12}^{\alpha\beta}\right) = \varphi_i\left(z, 1_2^{\alpha\beta}\right) = C_i \frac{G_i\left(z, 1_1^{\alpha\beta}\right)G_i\left(z, 1_2^{\alpha\beta}\right)}{G_i\left(z, 1^{\alpha\beta}\right)} = C_i G_i\left(z, 1_2^{\alpha\beta}\right) \qquad [5]$$

and

$$\varphi_i\left(z, N_{12}^{\alpha\beta}\right) = \varphi_i\left(z, N_1^{\alpha\beta}\right) = C_i \frac{G_i\left(z, N_1^{\alpha\beta}\right)G_i\left(z, N_2^{\alpha\beta}\right)}{G_i\left(z, N^{\alpha\beta}\right)} = C_i G_i\left(z, N_1^{\alpha\beta}\right) \qquad [6]$$

If segment number s of molecule i is of type A, than $G_i(z,s)$ can also be written as $G_A(z)$ which simply is the Boltzmann equation in which the segmental potential consists of three contributions

$$G_A(z) = \exp\left(u'(z) - \sum_B \chi_{AB}\left(\tfrac{1}{3}\varphi_B(z - \ell) + \tfrac{1}{3}\varphi_B(z) + \tfrac{1}{3}\varphi_B(z + \ell) - \varphi_B^b\right) - \frac{ev_A\Psi(z)}{k_BT} \right)$$

$$[7]$$

where the summation B runs over all segment types and the super script b refers to the values in the bulk.

The first part of the segmental potential, $u'(z)$, is a Lagrange parameter chosen such that $\sum_A \varphi_A(z) = 1$ for all z. It is equal for different types of segments and is in effect a hard core potential.[19]

The second part takes into account the nearest neighbour interactions averaged equally over layers $z + \ell$, z and $z - \ell$.[20] In eqn [7] χ_{AB} is the well-known Flory-Huggins (normalized) exchange energy parameter.

The third term in the segmental potential is of electrostatic origin,[21,22] wherein

v_A is the valence of the segment A, e the elementary charge, k_B the Boltzmann constant, T the absolute temperature, and $\Psi(z)$ the local electrostatic potential. The latter is obtained through Gauß' law: $\oint EdA_s = q/\varepsilon$ with q the charge enclosed in surface A_s and ε the dielectric permitivity constant of the medium. Both q and ε are computed from the volume fraction profiles $q(z) = e\sum_A v_A \varphi_A(z)$ and $\varepsilon(z) = \sum_A \varepsilon_A \varphi_A(z)$.

Since $E = -\nabla\Psi$, the electrostatic potential can be expressed in terms of local charge and the potential in adjacent layers:

$$\Psi(z) = \frac{C(z - \ell, z)\Psi(z - \ell) + q(z) + C(z, z + \ell)\Psi(z + \ell)}{C(z - \ell, z) + C(z, z + \ell)} \qquad [8].$$

Where $C(z, z + \ell)$ is the capacity of the system formed by plates at z and $z + \ell$, while the permitivity changes at $z + \ell/2$ and is given by:

$$C^{-1}(z, z + \ell) = \frac{1}{2\ell}\left(\frac{1}{\varepsilon(z)} + \frac{1}{\varepsilon(z + \ell)}\right) \qquad [9].$$

With the boundary conditions $\Psi^b = 0$ and $\Psi(\ell) = \Psi(0)$ and $\Psi(M) = \Psi(M+\ell)$ this automatically yields the condition of electroneutrality, both in the system and in the bulk.

Returning to eqns [2] and [3], $\lambda^{\alpha''-\beta''-\gamma''}$ is the *trans* or *gauche* probability depending on the directions α'' and γ'' and the energy difference U^{tg} between a *gauche* and a *trans* configuration:

$$\lambda^{\alpha''-\beta''-\gamma''} = \begin{cases} 1 - 2\big/\big(2 + \exp(U^{tg}/k_B T)\big) & \text{if } \alpha'' = \gamma'' \\ 1\big/\big(2 + \exp(U^{tg}/k_B T)\big) & \text{otherwise} \end{cases} \qquad [10].$$

Further, the anisotropy weighting factor $G^{\alpha''}(z|z')$ expresses the fact that densely packed chains tend to line up with each other.[23] When the density of bonds in direction α'' (between layer z and z') is given by $\varphi^{\alpha''}(z|z')$, this quantity is expressed as

$$G^{\alpha''}(z|z') = \frac{1 - \varphi^{\alpha''b}}{1 - \varphi^{\alpha''}(z|z')} \qquad [11].$$

We assume the bulk to be isotropic, so $\varphi^{\alpha''b}$ is the same for every direction α'' and therefore: $\varphi^{\alpha''b} = \frac{1}{2}\sum_i \varphi_i^b\left(1 - \frac{1}{N_i}\right)$. Obviously $\varphi^{\alpha''}(z|z')$ can be computed again from the $\varphi_i\left(z, s_{12}^{\alpha\beta}\right)$ profile by

$$\varphi^{\alpha''}(z|z') = \sum_i \sum_{s=2}^{N_i} \sum_\beta \varphi_i\left(z, s_{12}^{\alpha\beta}\right) \qquad [12]$$

The set of equations listed above is closed. The normalization constants C_i in eqn [1] are related to input quantities. For all molecules except the lipids we use φ^b as an input parameter (grand canonical environment). The normalisation constant C_i then has the form:

$$C_i = \frac{\varphi_i^{\alpha''\beta''b}}{N_i} = \frac{\varphi_i^b}{N_i \sum_\beta \sum_{\alpha\neq\beta} 1} \qquad [13]$$

For the lipids we usually have $\theta_i = \sum_z \sum_s \sum_\beta \sum_\alpha \varphi_i\left(z, s_{12}^{\alpha\beta}\right)$, the amount of molecules i in the system per unit area as an input quantity (canonical system):

$$C_i = \frac{\theta_i}{N_i \sum_z \sum_\beta \sum_\alpha G_i\left(z, N_1^{\alpha\beta}\right)} \qquad [14]$$

The boundaries of the system are chosen such that in case of a fluid membrane the weighting factors and the volume fraction in the layers just outside the system ($z = 0$ and $z = M + \ell$) are chosen the same as those in the first layer and the last layer, respectively. In other words there are reflecting boundary conditions.

In case of adsorption on an impenetrable wall, the boundary at $z = 0$ is treated differently: All volume fractions in this layer are set to zero except for the segment type that represents the wall, this is set to unity. Consequently the weighting factors for all segments except for the type that represents the wall are zero in this layer and the weighting factor for the wall is zero anywhere but in layer $z = 0$.

Further, the electrical potential should not change on the border of the system and is zero in the bulk: $\Psi^b = 0$, $\Psi(\ell) = \Psi(0)$, and $\Psi(M) = \Psi(M+\ell)$ (the wall is not charged). Finally all lattice sites must be filled: $\Sigma_A \varphi_A(z) = 1$.

The field $\{G_A(z)\}$ is conjugated to the density profiles $\{\varphi_A(z)\}$: We can calculate $\{\varphi_A(z)\}$ from an initial guess of $\{G_A(z)\}$ and update the field in a Newton iteration scheme such that it becomes self consistent with the density profiles which satisfy the boundary conditions.[18,19,22]

Furthermore, from $\{\varphi_A(z)\}$ and $\{G_A(z)\}$, it is possible to calculate the partition function for the system[19,22] and from that other thermodynamic quantities such as surface tension and chemical potentials.

Literature

1. F.A.M. Leermakers and A. Nelson, *J. Electroanal. Chem.*, **1990**, *278*, 53-72.
2. A. Nelson and F.A.M. Leermakers, *J. Electroanal. Chem.*, **1990**, *278*, 73-84.
3. A. Nelson and H.P. van Leeuwen, *J. Electroanal. Chem.*, **1989**, *273*, 183-200.
4. A. Nelson, *J. Electroanal. Chem.*, **1991**, *303*, 221-236.
5. A. Nelson, *J. Chem. Soc., Faraday Trans.*, **1991**, *87*, 1851-1856.
6. A. Nelson, *J. Chem. Soc.,Faraday Trans.*, **1993**, *89*, 2799-2805.
7. A. Nelson, *J. Chem. Soc.,Faraday Trans.*, **1993**, *89*, 3081-3090
8. W.H. Green and O.S. Andersen, *Annu. Rev. Physiol.*, **1991**, *53*, 341-359.
9. G. Cevc, *Biochim. Biophys. Acta*, **1990**, *1031*, 311-382.
10. S-F. Tocanne and J. Teissié, *Biochim. Biophys. Acta*, **1990**, *1031*, 111-142.
11. B. Hille, *Ionic Channels of Excitable Membranes*; Sinauer Associates: Massachusetts, 1984; p. 316.
12. S. McLaughlin, *Annu. Rev. Biophys. Chem.*, **1989**, *18*, 113-136.
13. M. Gutman and E. Nachliel, *Biochim. Biophys. Acta*, **1990**, *1015*, 391-414.
14. L. Stryer, *Biochemistry*; W.H. Freeman and Co.: New York, 1981; p. 215.
15. H. Hauser, I. Pascher, R.H. Pearson and S. Sundell, *Biochim. Biophys. Acta*, **1981**, *650*, 21-51
16. H. Hauser, W. Guyer, P. Skrabel and R.J.P. Williams, *Biochim. Biophys. Acta*, **1978**, *508*, 450-463.
17. J. Seelig, P.M. Mcdonald and P.G. Scherer, Biochemistry, **1987**, *26*, 7535-7541.
18 F.A.M. Leermakers and J.M.H.M. Scheutjens, *J. Chem. Phys.*, **1988**, *89*, 3264-3274.
19 O.A. Evers, J.M.H.M. Scheutjens and G.J. Fleer, *Macromolecules*, **1990**, *23*, 5221-5233.
20 J.M.H.M. Scheutjens and G.J. Fleer, *J. Phys. Chem.*, **1979**, *83*, 1619-1635.
21 P.A. Barneveld, J.M.H.M. Scheutjens and J. Lyklema, *Colloids and Surf.*, **1991**, *52*, 107-121.
22 M.R. Böhmer, O.A. Evers and J.M.H.M. Scheutjens, *Macromolecules*, **1990**, *23*, 2288-2301.
23 F.A.M. Leermakers and J.M.H.M. Scheutjens, *J. Chem. Phys.*, **1988**, *89*, 6912-6924.

Chapter 3

Modelling the Interactions Between Phospholipid Bilayer Membranes with and without Additives

Abstract

We have investigated the interaction between bilayer membranes on the basis of the self-consistent-anisotropic-field (SCAF) theory. The method is applied to dimyristoylphosphatidylcholine (DMPC) lamellae in the presence and in the absence of additives, with and without applied lateral tension and as a function of the ionic strength in solution.

The interaction curve between free-standing DMPC membranes is non-monotonous. Two repulsive regions, one of electrostatic and one of steric origin, bracket an entropic attraction range. We show that this attraction is enhanced by applying a lateral stress to the membranes. The minimum in the interaction curve is only found at not too high ionic strength. The attraction is caused by an alteration of the head-group conformations when the two bilayers come in close contact. In isolated films, the head groups have a conformation parallel to the membrane surface, but on close approach they cross the gap between the membranes intercalating the head groups of the other membrane. In this way they gain conformational entropy and therefore the free energy of interaction is negative.

We show that upon the addition of alcohols (additive : DMPC = 1 : 5 volume fraction) the interaction curves remain virtually unaltered. The interaction curves are qualitatively different for DMPC bilayers to which positively or negatively charged surfactants are added; these layers become fully repulsive. For cationic surfactants the repulsion range is shifted to larger separations than for anionic surfactants. This behaviour is caused by the pronounced effect of ionic surfactants on the orientation of the head groups of DMPC membranes. For negatively charged surfactants the head group is pulled inwards towards the membrane interior, whereas the opposite occurs in the presence of the positively charged additive. These results are in line with NMR experiments found in the literature.

Introduction

Membranes are the borders between life and death. All living cells have a membrane that separates the cell interior from the, often hostile, surroundings. Mostly, cells contain various organelles such as a cell nucleus, mitochondria, a vacuole, an endoplasmic reticulum and chloroplasts. Many of these cell compartments are also enveloped by membranes, sometimes even by a double membrane, and they may contain various membrane structures inside them. The complex topology persists by the existence of membranes and it is essential for maintaining the local chemical environment required for all kinds of natural processes. Membranes serve as active barriers, over which transport of molecular compound is carefully controlled. Membranes also provide the interfaces on which proteins adsorb such that these biologically active complexes find optimal operational conditions.

Biomembranes are composed of many kinds of molecules, such as lipids, proteins, cholesterol and several other additives. The amphipolar phospholipid molecules are in the majority; they are composed of two apolar tails and one polar phosphate-containing group attached to a glycerol backbone. These molecules form spontaneously a two-dimensional fluid system composed of two sheets. The driving force for this membrane formation is the phase separation of the apolar tails with the water, very similar to the demixing of oil and water. The apolar tails dislike the polar aqueous environment and, trying to escape from it, they stick together pointing their polar heads to the outside of the aggregates. Due to the specific shape of most lipid molecules the aggregate's geometry is roughly planar. Not all molecules partition readily into the membranes, and the semi-permeable character is easily explained by its hydrophobic interior and its continuous 2D structure.[1]

Despite the abundant literature on biological membranes, there is only limited theoretical insight into the fundamental properties of bilayer membranes on a molecular level. Not many techniques are available that enable the modelling of these self-assembling structures on such small length scales. One very interesting approach is molecular dynamic (MD)[2-5] simulations. From such simulations, it is possible to obtain a large amount of information on the lipid aggregates, but, because of a lack of computer power, one can only follow a small portion of such a structure for a few nanoseconds. Another problem is that in an MD simulation one cannot reach equilibrium membrane lamellae even when one allows for the adaptation of the simulation box in the equilibration procedure. We will return to this point, as we will study the equilibrium conditions of bilayer membranes in detail below. An alternative method to obtain information on the equilibrium

structure of bilayer membranes is to make use of statistical thermodynamical methods based on self-consistent-field approximations. The obvious advantage of the self-consistent-field modelling of the bilayer membrane is that a large parameter space can be probed, much larger than in MD. Moreover, one can study true equilibrium membranes.

We employ such a model for idealised membranes composed of dimyristoyl-phosphatidylcholine (DMPC), one of the most frequently encountered lipids in biomembranes. DMPC is a lipid with a zwitter-ionic head group without any net charge. We have investigated free-standing membranes composed of these lipids in a previous publication.[6] The head groups of DMPC molecules were found to have an average conformation parallel to the membrane surface. However, at high salt concentrations we have predicted that there is a possibility that the PC head groups assume simultaneously two preferred conformations, one tilted slightly towards the hydrophobic interior and the other folded towards the water phase.

Membrane-membrane interactions will always be of interest for biological systems because many biochemical processes depend on such interaction. For example, some cell organelles contain double-membrane envelopes. The 'contact' between these two bilayers, which might be protein-mediated, is believed to be of crucial importance for the functioning of these organelles.[7] Another typical example is a chloroplast in which grana stacks, composed of closely packed (attractive) membranes are in equilibrium with free floating, repulsive stroma lamellae.

There are several experimental techniques that are being used to learn more about interacting membranes. The surface-force apparatus, developed by Israelachvili and Adams,[8] is often used. In principle it measures mica-supported bilayers. The forces are measured mechanically and the distance between the surfaces is obtained optically. Marra et al.[9,10] and several others[11-14] have made an extensive study with this set-up. The method is best to probe the repulsive interactions in bilayers, as the surfaces jump uncontrolled to the next stable region when the gradient of the force exceeds the spring constant. An alternative method was developed by Parsegian and co-workers.[15-17] Their system is a multi-lamellar lipid phase in equilibrium with a water phase. The lamellar spacings, under osmotic stress, are determined by X-rays. The method gives access to the repulsive parts of the force-distance profile. MacIntosh and Simon reviewed with detail the various contributions to the repulsive part of the interaction curve of phospholipid membranes with this technique.[18] Evans[19-21] has developed the pipette aspiration method. Here a micro pipette is used on which a huge lipid vesicle is carefully attached. Then a second vesicle, also attached to a pipette, can be brought into contact with the former. One then can measure the

deformation of the vesicles shape under a microscope. For instance, one can obtain the depth of the minimum in the interaction curve, when the membranes attract each other. We also mention that indirect information on the interaction between membranes is found by analysing the swelling behaviour of concentrated lipid solutions.

In a rigorous proof for thermodynamic stability it has to be shown that the membranes do not attract each other. If they would, then free-standing membranes would not be the preferred entities, and one should model multi-bilayer aggregates. Therefore we shall now study the bilayer-bilayer interaction behaviour in detail. We will show how the membrane-membrane pair interaction is affected by the ionic strength and the presence of surfactant additives. Moreover, we will examine how the interaction of two bilayers is modified by an applied lateral stress. We will show that a given, finite, surface tension reduces the electrostatic repulsion between bilayers and increases the attraction between them, even when we neglect undulations of the bilayer sheets. We will also assume that the Van der Waals attraction between two bilayers is additive to the interaction that will be presented, so that the overall force can straightforwardly be evaluated from the given interaction curves. We will first discuss the equilibrium conditions for self-assembling systems. Then we will embark on the thermodynamics of interacting bilayers in the absence of undulation forces. This discussion will be followed by a brief outline of the principles of evaluating thermodynamic equations in a SCF framework. Then we will present our results and finish up with our main conclusions.

Thermodynamics of Small Systems

Thermodynamic criteria for equilibrium self-assembled structures are known for some time now. The most rigorous treatment is due to Hall and Pethica[22] presented in the context of non-ionic surfactants. These surfactants were assumed to self-assemble in non-interacting entities. These authors made use of the thermodynamics of small systems as developed by Hill.[23] As we will show below, the analysis is general and can be extended to interacting, ionic systems. However the interaction between aggregates has its intregueties as we will show below.

We will consider the condition that there are N (surfactant, lipid) aggregates in the system. On a not too small length scale we may assume that the energy of the system is a linear homogeneous function of N. Let ε be the conjugated variable for N. In the nomenclature of Hall and Pethica N is the number of small systems and ε is called the subdivision potential. We can write:

$$dU = TdS - pdV + \sum_i \mu_i dn_i + \epsilon dN. \qquad [1]$$

Where i is the index referring to the molecules in the system and all other quantities have their usual meaning. At constant T and p it is convenient to define the Gibbs energy $G = U - TS + pV$, then the usual Legendre transformation gives

$$dG = -SdT + Vdp + \sum_i \mu_i dn_i + \epsilon dN = \sum_i \mu_i dn_i + \epsilon dN \qquad [2]$$

The optimal number of small systems is now easily found by:

$$\left(\frac{\partial G}{\partial N} \right)_{p,T,n_i} = \epsilon = 0 \qquad [3]$$

and the stability condition is:

$$\left(\frac{\partial \epsilon}{\partial N} \right)_{p,T,n_i} \geq 0 \qquad [4]$$

Thus, we see that the Gibbs energy of the system is just given by the sum of the chemical potentials of the molecules times the number of molecules in the system. There is no excess energy in the system associated with the formation of membranes.

The formidable task of statistical thermodynamics is to evaluate ϵ from a suitable theory, and then select out of the many possible aggregate structures only those which obey the equilibrium and stability constraints. In the self-consistent-field theory we use the following procedure. First, we will make use of a lattice of which the lattice sites are of the size ℓ comparable to the smallest building block (CH_2) of the molecules. This implies a united atom approach. Consequently we cannot obtain information on smaller length scales than ℓ. Next, we will employ a mean-field approximation in this lattice in such a way that effectively density profiles in one direction are obtained. The mean field averaging can be over shells in a spherical lattice, resulting in spherical micelles or vesicles, or over flat layers, leading to perfectly flat bilayers. In this paper we consider the flat geometry. Finally, we fix the lattice onto the membrane, so that the bilayer remains stationary on the lattice.

Restricting ourselves to lamellae we disregard two sources of entropy. First, we do not account for the translational entropy of the aggregates and, second, we ignore the undulation entropy.[24,25] We can evaluate the sub-division potential being the sum of the excess grand potential (eqn [14]) and the translational and undulational entropy terms that were deliberately left out of the analysis
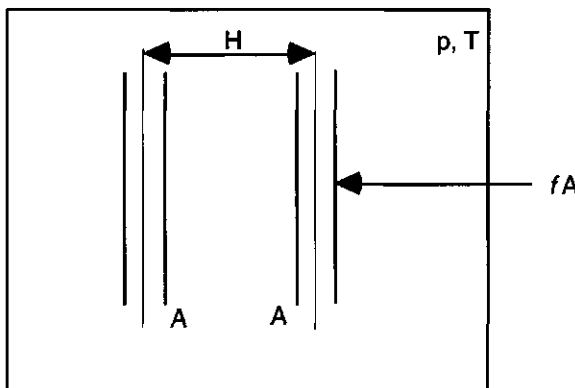
Figure 1. System of two interacting membranes with surface area A and inter membrane (core-core) distance H embedded in a bulk with given temperature T and pressure p. The external force f is indicated. In our theory we do not model the interaction between two membranes, but, due to the reflecting boundary conditions, the interaction between many bilayers.

($\varepsilon = \gamma A +$ entropy terms). For large membranes we can safely neglect the translational entropy for any finite membrane volume fraction. The entropy associated with undulations depends on the rigidity of the bilayers, parameterised by k_c, the mean bending modulus. De Gennes[26] has shown that a membrane can be considered flat on a length scale ξ, which is an exponential function of k_c: $\xi \propto \exp(4\pi k_c / k_B T)$, where k_B is Boltzmann's constant. Parts of the surface with the area ξ^2 can be considered to move independently, having their own translational entropy. We have shown before that for lipids with two tails such as DMPC the membranes are rather stiff having k_c of order 20 $k_B T$.[27] This order of magnitude is often cited in the literature[25,28,29] and thus we can safely assume that the undulational entropy is small for our system. Consequently, we can write $\varepsilon = \gamma A = 0$ meaning that, to a good approximation, free floating membranes have a vanishing surface tension. In the following we will therefore replace εdN by γdA in the relevant equations.

We note that formally we should, for absolute thermodynamic stability, also scan all possible aggregate geometries and check which of these has the lowest Gibbs energy. The aggregate shape with $\varepsilon = 0$ and the lowest chemical potential of the lipids is the preferred one. Such a full analysis is possible in the frame work of a self-consistent-field theory, but is not elaborated here.

Thermodynamics of Interacting Membranes

In the above we have ignored the possibility that the bilayers have interaction with each other. Especially when there are long range electrostatic interactions in the system calculations on isolated membranes have only limited meaning. In MD simulations this problem also presents itself; it poses a serious problem. Usually one employs a simulation box with periodic boundary conditions in all three directions. In this box one sheet of the bilayer is positioned near one boundary and the other sheet near the opposite one, so that one half bilayer feels the other half not only through the apolar part of the membrane but also through the water phase. The resulting attractive or repulsive force is not measured: one allows the box to adjust its size according to the condition that the integral of the lateral pressure over the system equals the atmospheric pressure. But, this is only correct when the bilayers do not interact. In fact, it is virtually impossible to model thermodynamically equilibrated (interacting) membranes with MD. This difficulty is not present in self-consistent-field calculations as will be proven below.

We define a system consisting of a number of parallel stacked membranes (see figure 1 where we have schematically drawn a pair of these membranes) with surface A each. These membranes are held at membrane-membrane distance H (defined by the core-core distance) by an external force fA. We choose f to be positive when the membranes repel each other. We can add this interaction term to the Gibbs energy and thus we may write at constant p and T:

$$dG = \sum_i \mu_i dn_i + 2\gamma dA - fAdH \qquad [5]$$

Upon integration of eqn [5] we have

$$G = \sum_i \mu_i n_i + 2\gamma A \qquad [6]$$

Differentiating eqn [6] and comparison with eqn [5] leads, after division by A, to a Gibbs-Duhem equation:

$$\sum_i \frac{n_i}{A} d\mu_i + 2d\gamma = -fdH \qquad [7]$$

which gives, upon integration, access to the interaction 'energy', $\Delta_{int}G(H)$, per surface area:

$$\frac{\Delta_{int}G(H)}{A} = -\int_{H'=\infty}^{H} fdH' = 2\gamma(H) - 2\gamma(\infty) + \sum_i \int_{\mu_i'=\mu_i(\infty)}^{\mu_i(H)} \frac{n_i}{A} d\mu_i' \qquad [8]$$

We found in the previous section that the stability condition for equilibrium, free-floating membranes is that the surface tension is vanishing. If we apply this condition (method **a**) we get, as interaction 'energy':

$$\frac{\Delta_{int}G_a(H)}{A} = \left(-\int_{H'=\infty}^{H} f\,dH'\right)_{p,T,\gamma} = \left(\sum_i \int_{\mu_i'=\mu_i(\infty)}^{\mu_i(H)} \frac{n_i}{A} d\mu_i'\right)_{p,T,\gamma} \qquad [9]$$

One could also consider the option that the two approaching membranes interact at constant chemical potentials (method **b**). This case implies that there is an infinitely large bulk in equilibrium with the membrane system such that, if molecules are included in or expelled from the membrane system during the interaction, this does not lead to a change in the composition of the bulk. As is the case, for instance, in a surface force apparatus experiment. At constant chemical potential, the second term on the right hand side of eqn [8] cancels and therefore we find that the interaction energy is the change in surface tension in the membranes:

$$\frac{\Delta_{int}G_b(H)}{A} = \left(-\int_{H'=\infty}^{H} f\,dH'\right)_{p,T,\mu_i} = 2\gamma(H) - 2\gamma(\infty) \qquad [10]$$

The interaction curves as computed with eqns [9] and [10] both are experimentally accessible. In an osmotic stress experiment on multi-layer lipid systems, the results obey eqn [9], and, with the surface force apparatus the equivalent of eqn [10] is measured. Calculations on both approaches were performed and compared.

In the above we have assumed that during the interaction of the membranes full equilibrium was maintained, thus that the necessary equilibration could take place. Under experimental conditions it is not always possible to realise this. For example, in a surface force apparatus, where the surface area of a membrane is fixed, one can encounter the case that the surfaces are brought together so fast that the lipids have no time to diffuse to the bulk (under repulsive conditions) or diffuse from the bulk to the interface (under attractive conditions). Under these conditions of restricted equilibrium one should always expect a more repulsive interaction force than as predicted by the equations given above. It is possible to mimic these situations in a SCF analysis by imposing that at fixed surface area A some of the molecules in the system can not leave the gap between the two surfaces, whereas all other types of molecules can. In this case neither the local chemical potentials nor the surface tension can be kept constant during the interaction process. If only the lipid molecules are constrained and the other

molecules are in equilibrium with the surrounding bulk, the chemical potentials of all molecules, except the lipids can be considered constant, because the bulk concentration (CMC) of lipids is very low. All terms referring to molecules with constant μ drop out of the integration of eqn [8]. The integration over the chemical potential of the lipids remains, but is easily carried out because n_{lipid} is fixed:

$$\frac{\Delta_{int}G_c(H)}{A} = \left(-\int_{H'=\infty}^{H} f\,dH'\right)_{p,T,n_{lipid}/A,\mu_{i\neq lipid}}$$

$$= \left\{2\gamma(H) - 2\gamma(\infty) + \frac{n_{lipid}}{A}\left[\mu_{lipid}(H) - \mu_{lipid}(\infty)\right]\right\}_{p,T,n_{lipid}/A,\mu_{i\neq lipid}} \qquad [11]$$

Application of the eqns [9], [10] and [11] is only possible if one has an accurate way to evaluate local chemical potentials, excess amounts of molecules in the inhomogeneous system and the surface tension of the membrane system. In the following paragraph we will briefly outline the theory which we have used to obtain these quantities.

Self-Consistent-Field Theory

As explained above, we make use of self-consistent-field approximations for which we can write the partition function of the inhomogeneous lipid systems. From this quantity we can derive all thermodynamic and mechanical quantities of the system, including the density profiles of all the components and the corresponding segment potential energies. The details of the theory have been presented elsewhere,[27,30-32] here we will give the background information needed for the interpretation of the results.

As explained above, we discretise the space and the number of conformations by allowing segments to be positioned only at given coordinates defined by a regular flat lattice with lattice spacings ℓ and coordination number Z. The lattice sites are organised in parallel flat layers, numbered z = 0, 1, 2, ..., M, M + 1. Each layer contains L sites. Obviously $A = L\,\ell^2$ and the membrane spacing H is twice the value of M ℓ. We will assume that all monomeric species in the system each occupy one lattice site. Larger molecules, like phospholipids or other chain molecules are supposed to be composed of units, often called segments, also of the size of the lattice sites. The N_i units in the chain molecule are numbered s = 1, 2, ..., N_i. The architecture of the molecules may vary from linear to extremely complex, multiple branched 'animals', and there is virtually no limit to the maximum chain length that can be handled in this theory. Moreover, the segments in the chain molecules may vary with respect to their hydrophobicity, their electrostatic charge and dielectric properties.

In a self-consistent-field theory one assumes that there is a potential energy field $u_A(z)$ for each segment type A at a coordinate $z = 1, ..., M$. The potential $u_A(0) = u_A(1)$ and $u_A(M+1) = u_A(M)$ due to the reflecting boundary conditions between layers $z = 0$ and $z = 1$ and between $z = M$ and $z = M + 1$. Conjugated to this set of potentials are the segment volume fraction profiles $\varphi_A(z) = N_A(z)/L$ (the ratio between the number of segments of type A in layer z and the overall number of sites in the layer) for all segment types A and layer numbers $z = 1, ..., M$. Again, the reflecting boundary conditions dictate that $\varphi_A(0) = \varphi_A(1)$ and $\varphi_A(M + 1) = \varphi_A(M)$. Below we will discuss briefly how $u_A(z)$ is found from $\varphi_A(z)$ and the other way around. Here we note that we will assume that the system is incompressible, which leads to the constraint $\sum_A \varphi_A(z) = 1$, for each layer z.

The thermodynamic quantities can be evaluated, when the self-consistent-field solution, that is the point for which the densities and the potentials are consistent with each other, is known. The number of molecules per lattice site follows directly from the density profiles:

$$\frac{n_i}{L} = 2\frac{\theta_i}{N_i} = 2\frac{\sum_{z=1}^{M}\varphi_i(z)}{N_i}. \tag{12}$$

Where the factor 2 is added because the number of molecules as defined above is the amount of molecules in the space $z = 1, ..., H/\ell$ and θ_i is the amount of molecule i per lattice site in half that space. The chemical potentials of the molecules are constant throughout the system. Therefore, it does not matter where these quantities are evaluated. We choose to do this in the homogeneous bulk phase b that is in equilibrium with the membranes. With k_B as Boltzmann's constant it can be written as:

$$\frac{\mu_i - \mu_i^*}{k_B T} = \ln\varphi_i^b - \left[(Z-1)N_i + 1\right]\ln\left[1 + \frac{-1 + N_i\sum_j \frac{\varphi_j^b}{N_j}}{(Z-1)N_i + 1}\right] - \frac{N_i}{2}\sum_A\sum_B\left(\varphi_{Ai}^* - \varphi_A^b\right)\chi_{AB}\left(\varphi_{Bi}^* - \varphi_B^b\right). \tag{13}$$

The reference state of the chemical potentials is a homogeneous phase of pure component i and is indicated by an asterisk. The bulk volume fraction of segments of type A is given by φ_A^b, and $\varphi_{Ai}^* = N_{Ai}/N_i$ is the fraction of A segments in the chain i. The short range interactions are accounted for by a Bragg-Williams approximation parameterised by Flory-Huggins contact energy parameters, χ_{AB},

which are defined between unlike segments A and B. A positive value of this parameter means that the segments A and B repel each other and a negative value indicates attraction. In the bulk phase the electrostatic potential is zero so electrostatic contributions do not occur in eqn [13]. The second term on the right hand side of eqn [13] reduces to the usual Flory-Huggins term for large Z. The quotient in the logarithm is then small and one can approximate $\ln(1+x)$ by x.

The surface tension (derived from the excess grand potential, Ω^σ) of the inhomogeneous (membrane) system is:

$$\frac{\gamma A}{k_B T} = \frac{\Omega^\sigma}{k_B T} = L \sum_{z=1}^{M} \left[\begin{array}{l} -\sum_A \varphi_A(z) \ln G_A(z) + 2 \ln G(z\,|\,z) + \dfrac{\ln G(z\,|\,z-1) + \ln G(z\,|\,z+1)}{2} - \\ \frac{1}{2} \sum_A \sum_B \chi_{AB} \left\{ \varphi_A(z)\left(\langle\varphi_B(z)\rangle - \varphi_B^b\right) - \varphi_A^b\left(\varphi_B(z) - \varphi_B^b\right) \right\} + \dfrac{q(z)\Psi(z)}{2k_B T} \end{array} \right]$$

[14].

In eqn [14] we have used several quantities that were not introduced yet. The angular brackets indicated an averaging of the segment density over three successive layers according to $\langle\varphi_B(z)\rangle = \frac{1}{3}\left[\varphi_B(z-1) + \varphi_B(z) + \varphi_B(z+1)\right]$. The quantities $G(z|z')$, where $z' = z - 1$, z, or $z + 1$ are called anisotropic weighting factors. They depend on the local density of bonds in a given direction dictated by the coordinates z and z'. These quantities can be computed directly from the ranking number-dependent density distributions. The anisotropy weighting factors with $z' \neq z$ are divided by 2 to prevent double counting, while the multiplication by 2 for $z' = z$ accounts for the two possible bonds per segment that are parallel to the lattice layers. The electrostatic contributions contain the electrostatic potential, Ψ, and the total charge in layer z, q(z), which is calculated as the sum over the volume fractions in the layer times the valence of the segments involved, v_A: $q(z) = e\sum_A v_A \varphi_A(z)$, with e denoting the elementary charge. Finally eqn [14] contains $G_A(z)$, which is called the free segment distribution function. The free segment distribution functions are exponential functions of the segment potential energy $u_A(z)$:

$$G_A(z) = e^{-u_A(z)/k_B T}.$$ [15]

The segment potential energy contains three terms. The first is a space filling potential, the second gives the contribution of short range nearest neighbours contact energies to the segment potential energy and the third is due to electrostatics:
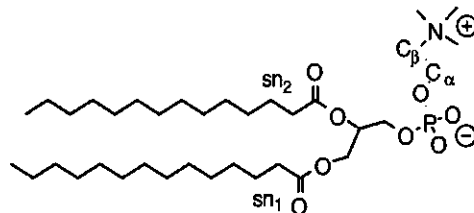
Dimyristoylphosphatydylcholine (DMPC)
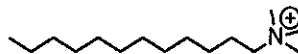
dodecyltrimethylamonium (DTA)
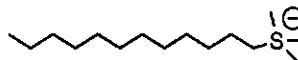
dodecyltrimethylsulfide (DTS)

OH
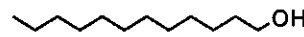
dodecanol

Figure 2. Some of the molecules used in the calculations. In the computations the charges on the phosphate are evened out over all oxygens and the central P segment. The charges of the nitrogen and the sulphur are localised to the respective segments.

$$\frac{u_A(z)}{k_B T} = u'(z) + \sum_B \chi_{AB}\left(\langle \varphi_B(z) \rangle - \varphi_B^b \right) + \nu_A e \Psi(z) / k_B T \qquad [16]$$

The volume filling potential is normalised such that it equals zero in the homogeneous bulk solution, where the whole segment potential is zero.

With the weighting factors $G_A(z)$ and $G(z|z')$ one can compute the segment densities. We use a rotational isomeric state (RIS) approximation to generate chain conformations. This scheme is used on a lattice with coordination number $Z = 4$. In this method we account for segment-correlations along the chain of the molecules. Sequences of four consecutive segments cannot overlap and we can control the local chain stiffness by assigning an energy difference between a local *gauche* and a *trans* conformation (the *trans* conformation is usually lower in energy). We note that segments that are more than four segments along the chain apart from each other, are allowed to occupy the same lattice site. Computing fully self-avoiding conformations is in itself possible but this will not significantly improve the description, because in our method we cannot at the same time

correct for the fact that two segments of neighbouring chains are sitting on the same site. There are two mechanisms in our theory that correct for this excluded volume problem. First of all we have the constraint that each layer with L lattice sites contains exactly L segments. The second correction is through the anisotropic weighting factors $G(z|z')$. A high value for $G(z|z')$ induces local alignments of segment bonds along the $z \rightarrow z'$ direction. This means that chain crossings, which cause the double occupancies of lattice sites, are systematically suppressed especially at high densities. Here we must note that bonds that are parallel to the plain of the lattice, are assumed to be distributed isotropically (mean field approximation). So self-avoidance is indirectly accounted for, at least to a certain extend.

Procedure

In order to apply the above scheme to lipid membranes, one has to select a suitable self-consistent-field solution of the equations, because there may be several mathematically acceptable SCF solutions (e.g. a homogeneous segment distribution throughout the system is always one of the solutions). We choose a numerical procedure, starting with initial guesses of $G_A(z)$ values such that an inhomogeneous density distribution develops near layer $z = 1$. Then automatically the symmetry plane of the bilayer will line up with the symmetry plane of the lattice, which is the reflecting boundary between layers $z = 0$ and $z = 1$. For a given amount of lipids (and other components) in the system, the weighting factors are modified by successive approximations using a numerical Newton-type method until a self-consistent solution is obtained. This numerical procedure guarantees electroneutrality both in the bulk and in the inhomogeneous membrane system as a whole and the exact space filling. Equilibrium free-standing membranes were found by varying the amount of lipids $\theta_i = n_i N_i / L$ in the layers $z = 1, ..., M$ iteratively until the equilibrium constraint $\gamma = 0$, and the stability constraint $\partial \gamma / \partial \theta_i < 0$ are obeyed. In case of doped membranes the amount of additive was coupled to the amount of lipid by keeping the $\theta_{additive}/\theta_{lipid}$ ratio constant. Care was taken to take M large enough so that a free membrane does not 'feel' the other membrane positioned at $z = 2M$.

For the calculations of the interaction curves, the chemical potentials and the surface tension are first computed for the case that the membranes are far apart. Then the membrane separation is, step by step, reduced until the membranes contact each other. In this last procedure we fix either the chemical potentials, or we remove any interaction-induced surface tension by changing the composition in the system, or we fix the number of lipids in the system depending on the mode of interaction we choose.

Table I. The parameters of the various segment types used in this study.

		H_2O	C	O	PO	S	N	Na	Cl
ε_r		80	2	80	80	80	80	80	80
ν		0.0	0.0	0.0	−0.2	−1.0	+1.0	+1.0	−1.0
χ	H_2O	0.0	1.6	0.0	−1.0	−1.0	−1.0	−1.0	−1.0
	C	1.6	0.0	1.6	2.6	2.6	2.6	2.6	2.6
	O	0.0	1.6	0.0	0.0	0.0	0.0	0.0	0.0
	PO	−1.0	2.6	0.0	0.0	0.0	0.0	0.0	0.0
	N	−1.0	2.6	0.0	0.0	0.0	0.0	0.0	0.0
	Na	−1.0	2.6	0.0	0.0	0.0	0.0	0.0	0.0
	Cl	−1.0	2.6	0.0	0.0	0.0	0.0	0.0	0.0

Parameters

The theory outlined above is implemented in a computer program called GOLIATH. The systems discussed in this paper consist of: DMPC as shown in figure 2, water, modelled as monomers, salt ions referred to as Na^+ and Cl^-, and, in some cases, the surfactant molecules dodecyltrimethylammonium (DTN^+) and dodecyltrimethylsulphide (DTS^-) with Cl^- and Na^+ as their counter ions, respectively. We have also considered surfactant molecules dodecylammonium (DA^+) and dodecylsulphide (DS^-) which lack the CH_3 groups surrounding the charge carrying unit. In figure 2 we have also drawn the dodecanol molecule that we have used as a model for an uncharged (rather hydrophobic) surfactant.

The system size was chosen large enough to prevent, where needed, bilayer interaction (usually M = 40 layers). The lattice spacing, ℓ, was set to 0.3 nm. The salt distributions are normalised with a given bulk volume fraction. The energy difference between a *gauche* and a *trans* state was set at 1 $k_B T$, irrespective of the segment types involved. Further segment properties were chosen as given in table I. The relative dielectric constants of all components except for the hydrocarbon (C) were taken as $\varepsilon_r = 80$, the value found in bulk water. The relative dielectric constant of hydrocarbon was set to $\varepsilon_r = 2$, corresponding to the value found in bulk hydrocarbon fluids.

Regarding table I, the contact energy between hydrocarbon and water reflected in χ_{C,H_2O}, is the most critical parameter for membrane formation as it is the driving force for self-assembly. The value was chosen to be $\chi_{C,H_2O} = 1.6$, similar to that validated by earlier studies[6,31-33] and in accordance with other estimates found in the literature.[34] This value is also consistent with the
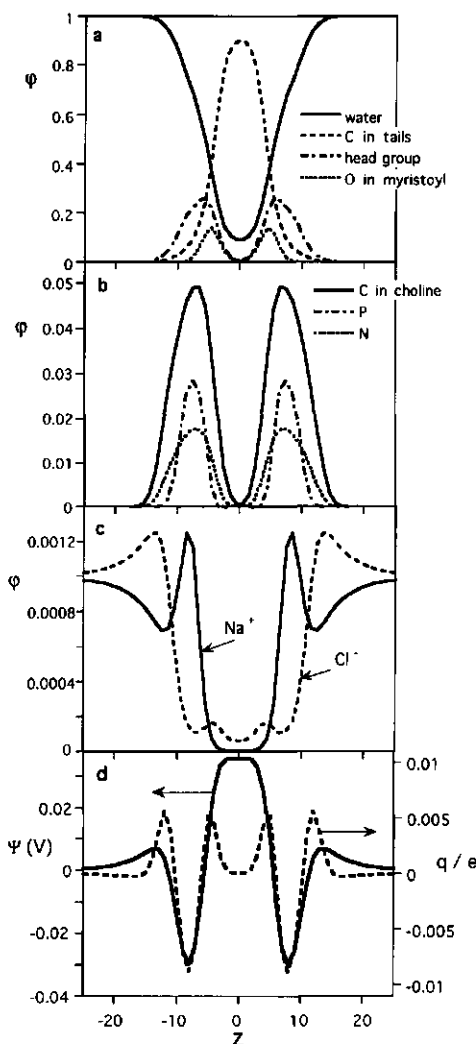
Figure 3. Segment density, electrostatic potential and charge profiles though a cross-section of a free-standing non-interacting DMPC membrane. The bulk volume fraction of NaCl, $\varphi^b_{NaCl} = 0.002$; ε_r and χ are as in table I. The centre of the membrane is at $z = 0$. Figure (a) shows the overall segment distribution of the main components: the water, the hydrocarbon and the head-group segments as well as the oxygen from the myristoyl (tetradecanoyl) ester. Figure (b) shows detailed segment distributions for the phosphate, the nitrogen and the C segments in the choline group. In figure (c) the distributions of the salt ions are shown and in figure (d) the electrostatic potential and the total charge profiles across the membrane are presented.

dependencies of the CMC on the surfactant tail length.[27] The uncharged polar segments (O) are set to be energetically equal to water with respect to their interaction with hydrocarbon. Charged components (N, Na, Cl, P and the O from the phosphate group) have a favourable χ of −1 with water to mimic their tendency to be solvated by water and an unfavourable one with the hydrocarbons of +2.6 for the lack of solvation in hydrocarbon. Other interactions are kept zero for the sake of simplicity, but these choices are not critical.

The phosphate group is modelled being composed of five units. Since this group has a low intrinsic pK_a value of < 2.25 [35,36] it has a net negative charge of −1 at neutral pH. This charge is assumed to be equally distributed over all five segments. Thus, effectively we put a charge of −0.2 on each of these units.

Results

We will start by discussing liquid-crystalline DMPC membranes. Firstly non-interacting bilayers will be examined and the main features of these DMPC membranes, which were published earlier are reviewed.[6] DMPC molecules have zwitter-ionic head groups and it will be shown that the electrostatic effect determine to a large extent the membrane head-group properties. Next, attention is given to the interaction of DMPC bilayers at various salt concentrations. We further show that it is possible to investigate fixed membranes and some results are shown of membranes that have a finite surface tension. We will also show that the head-group region dominates the membrane-membrane interaction. It is therefore interesting to see how the head-group conformations can be altered and how this affects the colloidal stability of the bilayers. To this end we will discuss the addition of some surfactants to DMPC membranes and show their influence as a function of their charge.

Free Standing Non-Interacting Membranes

Figure 3 shows the density profiles through a cross section of a free-standing, non-interacting, DMPC membrane at intermediate salt volume fraction of $\varphi_{NaCl} = 0.002$. This corresponds to a concentration of about 50 mM. At this salt concentration the Debye screening length is of the order of the distance between the positive nitrogen and the negative phosphate in the head group. The electrostatic attraction forces dictate that the nitrogen is on average in the same layers as the phosphate group (figure 3b). The phosphate-group distribution is rather narrow because the phosphates are situated just at the head group-tail boundary in the DMPC molecule.[31] At higher salt concentrations the nitrogen distribution changes into a two-state distribution (not shown), with one orientation closer to the membrane centre and the other one more directed towards the water

phase. The lower the salt concentrations the more the nitrogen profile resembles that of the phosphate group, both with respect to shape and position.[6,32] However, the profiles of the nitrogen and the phosphate do not match perfectly and the resulting net charge separation leads to a potential profile across the membrane. The profiles of the salt ions (Na^+ and Cl^-) results from a compromise between the electrostatic and nearest neighbour interactions. Ions prefer the water phase over the hydrocarbon core of the bilayer, but locally they follow the electrostatic profile. The overall structure of the membrane (figure 3a) is dominated by the water molecules and the lipid tails. The head groups are between these two phases, but the sum of all the volume fractions of the head-group constituents (including the C segments surrounding the nitrogen) never surpasses a local volume fraction of 0.4. This implicates that, contrary to the classical picture of a lipid bilayer, the hydrocarbon-water contacts are the most frequently occurring ones. Nevertheless, for the membrane described in figure 3, the surface tension is zero.

In earlier work[31] we have analysed the tail region of the bilayer in more detail. It was found that the two tails of each DMPC molecule have small differences in their conformations. The sn_1 tail is positioned a fraction of a nm deeper into the membrane than the sn_2 tail. It was also found that the segments of the latter have a slightly narrower distribution than those of the former. We found that the distribution of segments becomes wider the further they are positioned from the head-tail-connection in the molecule. It was also found that the segment order parameter becomes lower towards the tail ends. A further noteworthy result of our theory is that it predicts a first-order gel-to-liquid phase transition[31] where the low temperature gel state is characterised by the fact that virtually all the lipid tails are in the all-*trans* configuration. In this paper we restrict ourselves to membranes in the high temperature, fluid state.

Free-Standing Interacting Membranes

The colloidal stability of free-standing bilayers is the topic of the following discussion. In the interaction curves to be presented, the distance H between the membranes is calculated by multiplying the number of layers with the lattice spacing ℓ, which was set to 0.3 nm. This choice is a compromise between the aspect ratios of the segments, the long range of the electrostatic interactions and the C-C bond length in a molecule.

We first check the consistency of our theoretical analyses. As outlined in the theory, the interaction energy per surface area can be obtained in several ways. In figure 4 we have brought together the three methods as they emerge from our theory:

    a   The change of chemical potential times the number of molecules in the
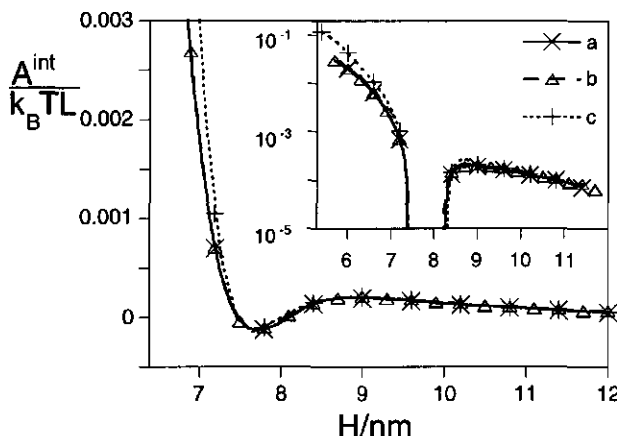
Figure 4. The interaction curve between two free-standing DMPC bilayers. A comparison between the three approaches outlined in the theory: **a** according to eqn [9], **b** to eqn [10], **c** to eqn [11]. The ε_r and the χ-parameters are as in table I. The salt bulk volume fraction was 0.002. The inset shows the repulsive part on bilayer contact in a log-linear plot.

system upon interaction at constant surface tension: $\gamma = 0$ (eqn [9]).

    b   The change in excess free energy at constant chemical potential (eqn [10]).

    c   The sum of the change in surface tension and the amount per surface area times the change of the chemical potential of the lipid molecules at constant amount of lipid in the system (eqn [11]).

It is clear from figure 4 that the first two approaches have nearly the same outcome, and that method number **c** gives more repulsive interaction curves at contact. This is in line with expectations, as in this last method we force the lipids to remain in the bilayers of which the surface area was fixed, whereas the other two methods allowed the lipids to escape, irrespective of the mode of interaction used, either to an infinitely large bulk solution or by altering the membrane surface area. Methods **a** and **b** only start to become different from each other at extreme compression of the bilayers. Under these conditions method **b** tends to be slightly more repulsive (not shown).

The interaction curve at the (modest) salt concentration considered, has three regimes. Bringing two membranes from a large separation into contact leads first to a repulsive, then to an attractive and finally to again a strong repulsive region. The two repulsive parts are the easiest to understand. The one where the membranes are closest together is due to steric interactions. At these short separations the membranes really touch each other (remember the distance between the membranes is defined from the core of one of the membranes up to

the centre of the other one). The logarithmic plot in the inset of figure 4 shows that here the interaction curves are fairly exponential. This is also found experimentally and has been attributed to protrusion or hydration forces.[28,29,37] We find a decay length of approximately 0.5 nm, which is in good agreement with the measurements.[28,29] In our calculations we have the full set of conformations of the lipids. Thus statistically protrusions are included. Our calculations suggest that the repulsion is not typical for the solvent (water) but is linked to the mechanical properties of the lipid matrix.

We note that recently Besseling has shown that hydration forces can both be repulsive or attractive.[38] Besseling developed a lattice gas model for water using a quasi-chemical approximation with orientation dependent interactions. He showed that attractive forces are expected when the water density near the surface deviates from its bulk value. Repulsive hydration forces on the other hand, originate from a disturbance of the (collective) orientation of the water molecules near a surface.[39] In a Bragg-Williams theory, water is modelled as isotropic molecules which cannot orient themselves. Therefore, the repulsive hydration forces are not taken into account in the present calculations.

The second repulsive regime, positioned at larger spacings, where the membranes first start to interact, is due to the electrostatic interactions (double-layer overlap) and may be described by classical DLVO theory.[40,41] As the positive and negative parts of the head groups do not lie exactly in the same plane, an electrostatic surface potential is built up (see figure 3) and as a consequence the membranes repel each other with the typical exponential dependence as can be seen from the inset. Here the decay length is given by the Debye screening length. We note that orientation correlations between the dipoles of the PC groups on the two opposing bilayers is neglected in our mean-field theory. These correlations can diminish the electrostatic repulsion.

At intermediate membrane-membrane spacing attraction is observed. This attraction has an entropic origin, as can be understood as follows. At large membrane-membrane separation the phosphate-choline vector is, to a good approximation, parallel to the membrane surface. This restriction in orientation is entropically unfavourable. When the membranes are brought closely together, the choline moiety can, without an energy penalty, gain entropy by crossing the gap between the membranes. In this way the choline group can take positions between the phosphate groups of both opposing bilayers. Thus, the Gibbs energy of the system reduces and the membranes attract each other. If this minimum is deep enough we should characterise free PC membranes as thermodynamically unstable, and whether they are colloidal stable may depend on the electrostatic repulsion and the Van der Waals attraction. The latter term has been omitted from
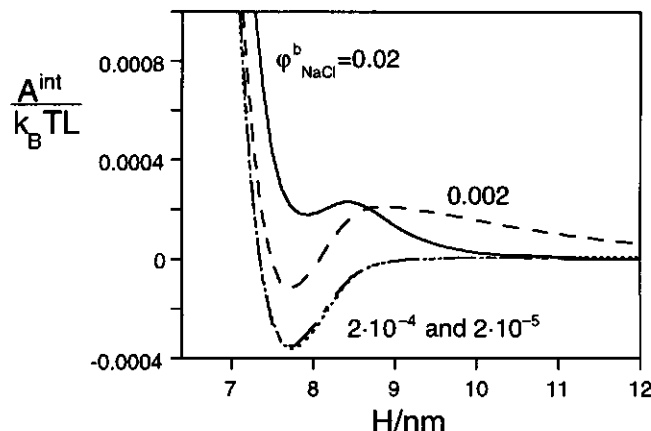
Figure 5. The interaction curve between two free-standing DMPC membranes at various salt concentrations as indicated, computed by the method described by eqn [10]. Other conditions as in figure 4.

the analysis.

Changing the salt concentration *both* to lower *and* higher ionic strengths removes the electrostatically generated repulsive barrier (figure 5) though for different reasons. Upon a decrease of the salt concentration the Debye screening length increases and, hence, the electrostatic penalty upon tilting the head group out-of-plane is increased. Therefore, the head group is positioned even more perfectly parallel to the membrane surface and no electrostatic surface potential is generated anymore. As a result of the lack of charge separation in the head-group region, the corresponding repulsive part of the interaction curve disappears. A second consequence of the low ionic strength condition is that the entropic attraction, as explained above, becomes more pronounced. However, one can not align the head group more than perfect to the membrane surface and therefore there is a limit to the depth of the attractive well. Decreasing the ionic strength from $\varphi^b = 0.0002$ to $\varphi^b = 0.00002$ does not lead to a further deepening of this well. Upon an increase of the salt concentration the Debye screening length is decreased to less than the distance between the phosphate and the nitrogen in the head group of a PC molecule. Approaching membranes have their surface potential screened very well and again the repulsion disappears. This effect is very well known from the DLVO theory. At high ionic strength the electrostatic attraction between the phosphorous and the choline group becomes negligible and the head group can tilt out of the plane of the membrane without an electrostatic penalty. In this regime the entropic attraction upon approach of two membranes is annihilated because there is simply no entropy to gain.

$$\frac{A^{int}}{k_B TL}$$
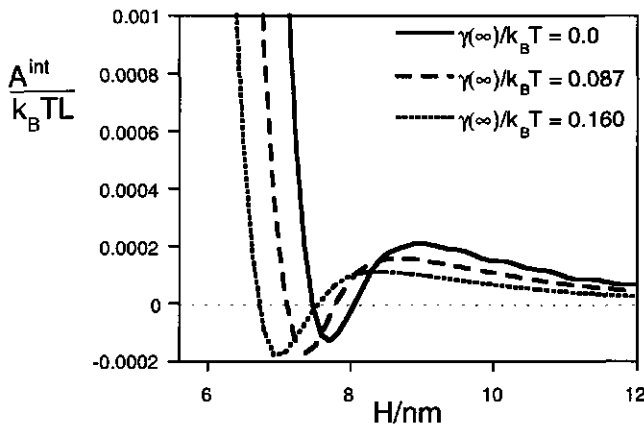
Figure 6. The interaction between two membranes at various surface tensions, $\gamma(\infty)$. The salt bulk volume fraction was 0.002 and the other parameters were as in table I.

When we now include the Van der Waals attraction in our discussion, clearly free, fluid, equilibrium, DMPC membranes are attractive under most electrolyte conditions as is found experimentally.[11] But there may be a regime of moderate ionic strengths where the electrostatic repulsion may overcome the Van der Waals attraction, which would then result to a colloidal stable membrane system.

We now might speculate upon an explanation for an existing paradox in lipid swelling experiments. It is known that lipids swell less with water applied from a saturated vapour than from excess water.[28,29,42,43] One of the reasons can be that a local minimum in the interaction curve, as discussed above, is keeping the lipids in close contact when the lipid phase is swollen from the water applied from the gas phase, whereas the electrostatic repulsion is keeping the bilayers colloid-chemically stable in the case that the lipids are swollen in excess water.

Stretched Interacting Membranes

In the literature[11] not only free floating membranes, but also supported membranes and stressed membranes are considered. The characteristic difference between supported or stressed membranes is that these last structures have a finite surface tension. We will now consider these conditions with the current theory. The calculations were done as follows. First, a bilayer with a given surface tension was computed and the chemical potentials of all components were recorded and kept fixed during the subsequent reduction of the membrane-membrane spacing. Then the change in excess grand potential ($\propto$ surface tension) is the characteristic function for interaction (eqn [10]).

The results of these calculations are shown in figure 6. The consequence of the

finite surface tension on an isolated membrane is that its thickness is reduced. This is reflected in a general tendency of the interaction curves to shift to lower H-values. The stretched membranes (dashed and dotted curves) display steric repulsion at a shorter distance than the free floating membrane system (solid curve). The electrostatic repulsion at long distances diminishes upon increasing the membrane surface tension. This has two causes. Due to the larger surface area per lipid molecule at higher tensions the charge density on the membrane surface is lower and, therefore, the resulting electrostatic potential is reduced. Furthermore, because of the larger area per head group, the excluded volume problems in the head-group area are reduced, allowing the head groups to assume a conformation more parallel to the membrane surface. This again results in a lower electrostatic potential and a less strong repulsion. This last phenomenon, on the other hand, increases the entropy gain per lipid molecule when the two bilayers are brought in close contact, so that the attractive minimum in the interaction profile becomes more pronounced. Since the electrostatic repulsion is significantly reduced upon stretching of the membranes, the salt concentration regime where the membranes are electrostatically stabilised, becomes narrower and may eventually vanish. We conclude that PC membranes have a stress-induced increase in the entropic attraction between bilayers that occurs simultaneously with a stress-induced reduction of electrostatic repulsive interactions.

Additives in Non-Interacting Membranes

A single component membrane system with only one lipid present is never met in living systems. We have therefore studied the addition of foreign molecules to the DMPC membrane. We have considered five additives: two cationic surfactants with a positively charged nitrogen as the head group [dodecylammonium (DA) and dodecyltrimethylammonium (DTA)], two anionic surfactants with a negatively charged sulphide (S) as the head group [dodecylsulphide (DS) and dodecyltrimethylsulphide (DTS)], and one neutral molecule (dodecanol) (see figure 2). The difference between DA and DS on the one hand and DTA and DTS on the other are the three CH_3 groups around the charged segment N and S, respectively. The introduction of the methyl groups makes the head groups of these surfactants bulkier and the molecules as a whole become less polar. So, the affinities of DTA and DTS for the membranes will differ from those of the DA and DS molecules. To quantify this difference we use the partition coefficient K defined ideally as the quotient of the amount of additive per amount of lipid in the membrane and the amount of additive in the water per amount of water:
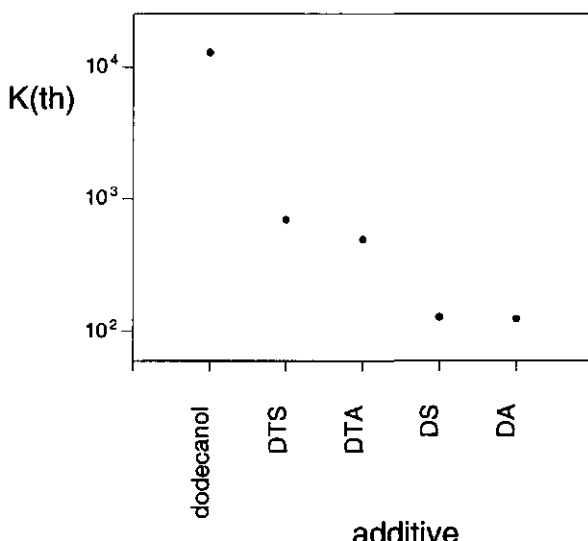
Figure 7. The partition coefficient as defined by eqn [18] for the following additives in a free-standing DMPC membrane: dodecanol, dodecyltrimethylsulphide (DTS), dodecyltrimethylammonium (DTA), dodecylsulphide (DS), dodecylammonium (DA). All parameters were set as in table I and the salt bulk volume fraction was 0.002 apart from the counterions associated with the ionic additives. The partition coefficients are computed at low additive concentrations to prevent disturbances of the DMPC membrane.

$$K(id) = \frac{\left[\varphi_{add}/\varphi_{lipid}\right]_{membrane}}{\left[\varphi_{add}/\varphi_{water}\right]_{water}}. \tag{[17]}$$

The subindices indicate the species involved and the square brackets the phases involved. The extension 9id0 is to differentiate this ideal definition from the theoretical calculations (th) as we will discuss below. A problem in calculating the partition coefficient is to define the extent of the membrane phase. Since there is no sharp interface between bulk water and the membrane we have defined the volume of the membrane as equal to the excess volume of lipids in the system. The amount of additive in the membrane is defined as the excess amount of additives in the system plus the bulk concentration times the volume of the membrane phase. Defining the excess amount with respect to the bulk solution per surface area of the membrane as θ^{σ} we arrive at the expression for K(th):
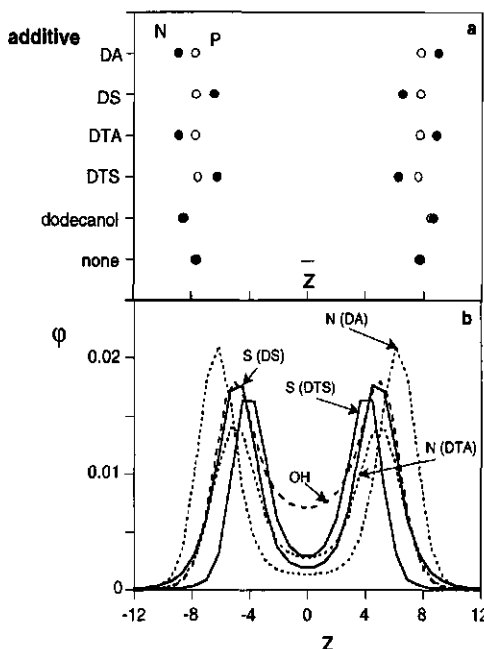
Figure 8. (a) The average positions $\bar{Z}$ of the main head-group segments of DMPC, N (closed circles) and P (open circles), with various additives in the membrane (see also figure 7) and (b) the volume-fraction profile of the main head-group segments of additives in a DMPC membrane. The centre of the membrane is at layer zero, the parameters were as in table I and the bulk volume fraction of salt was 0.002.

$$K(th) = \frac{\left(\theta_{add}^{\sigma} + \theta_{lipid}^{\sigma} \cdot \varphi_{add}^{b}\right)\varphi_{water}^{b}}{\theta_{lipid}^{\sigma} \cdot \varphi_{add}^{b}} \quad [18]$$

The partition coefficients of the five additives are presented in figure 7. The difference between the charged and the uncharged molecule is mainly due to the difference in contact energies (χ-parameters) between the charged N and S and the uncharged OH segment. Furthermore, DTS and DTA are more hydrophobic because they have three additional CH_3-segments and therefore their partition coefficients are higher than those for DS and DA. The third feature that draws the attention is that the negative additives have higher partition coefficients than the positive ones. The reason is that the potential in the membrane core in PC membranes is slightly positive due to the out-of-plane tilting of the head groups (some tilting towards the water phase and others to the membrane core). The more apolar DTS and DTA are more influenced by this phenomenon because, due

to their apolar nature, they reside more towards the centre of the membrane (around layer $z = 0$), whereas DS and DA position their head groups closer to the membrane head-group area, where the energy difference for positively and negatively charged segments is much less (see also figure 8b and figure 3).

As discussed above, the phosphate group has a rather narrow distribution. We can use this observation to define the thickness of the membrane by the average position of this unit of the head group. To compute this average position, $\bar{z}_X$, of a segment X we take the volume fraction-weighed average over the layers:

$$\bar{z}_X = \frac{\sum_{z=1}^{M} z\left(\varphi_X(z) - \varphi_X^b\right)}{\sum_{z=1}^{M} \left(\varphi_X(z) - \varphi_X^b\right)} \qquad [19]$$

In figure 8 we present results for various systems of which the amount of lipid was 5 times in excess of the amount of additive in the system. This is equivalent to a mole fraction of 0.41 for DA, DS and dodecanol and of 0.37 for DTA and DTS. The average position of the N and the P segment of DMPC in membranes with the various additives is plotted in figure 8a. We can conclude from figure 8a that the charged additives do not change the thickness of the membrane, whereas an uncharged surfactant, like dodecanol, does increase this quantity. This phenomenon is explained by the fact that the charged head groups of the surfactants exert an electrostatic repulsion that drives the charged molecules apart and prevents the membrane from becoming very thick. On the other hand dodecanol rather partitions (also with the head group) into the tail region of the bilayer (see figure 8b), which results in an outward push of the lipids leading to a thicker membrane compared to the undoped membranes.

In contrast to this, the head-group orientation of the PC molecules is not influenced by the uncharged dodecanol, while the charged additives have a very pronounced effect. This can be understood since the main reason for the head group to assume a flat conformation is the electrostatic attraction between P and N. Neutral surfactants do not alter this balance of forces in the head-group region. On the other hand, charged additives disturb this balance as the head-group region of the membrane becomes essentially charged. The positively charged surfactant can take over part of the screening of the phosphate group so that the choline unit can now tilt outwards. On the other hand, the negatively charged surfactants will pull the choline more towards the tail region, and the titling angle of the PC head group is now towards the hydrophobic region.

The effect of the charged additive on the head-group orientation of PC was
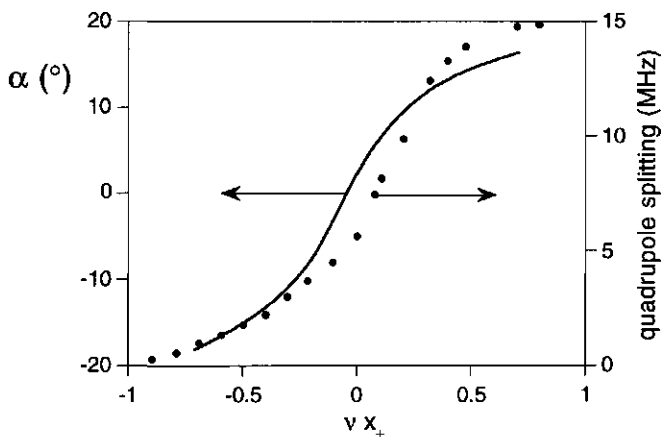
Figure 9. The average tilting angle of the DMPC head group (α, see eqn [20]) (drawn curve) and the quadrupole splitting of the deuterated carbon adjacent to the nitrogen in the DMPC molecule (the C_β position) as measured by Marassi and MacDonald[44] (dots) as a function of the valence, ν, times the mole fraction, x, of the surfactant in the membrane. Conditions were as in figure 6.

measured experimentally by Marassi[44] and Seelig.[45] In deuterium NMR experiments they determined the quadrupole splitting of DMPC deuterated at the C_α and also at the C_β position in the choline moiety (see figure 2). The quadrupole splitting is directly proportional to the order parameter of the atoms involved and is therefore related to the average orientation of the head groups. The quadrupole splitting was dependent on the mole fraction of charged surfactant added to the membrane and from this they concluded a change in head-group tilting.

To compare their results to our findings we calculated the average tilting angle α of the PC head group. Assuming that the P–O–C–C–N sequence is in the all-*trans* configuration we can compute the average angle that the head group makes with the plane of the membrane by:

$$\sin(\alpha) = \frac{\bar{z}_N - \bar{z}_P}{4} \tag{20}$$

The division by 4 is the number of bonds between the nitrogen and the phosphorous and $\bar{z}_N$ and $\bar{z}_P$ is the average position of the N- and the P-segment, respectively, as defined by eqn [19]. We have plotted this angle α in figure 9 as a function of the product of the mole fraction of the added surfactant and its valence. For the unperturbed membrane (mole fraction additive is zero) the angle α is slightly positive (the head groups point outwards). We observe that the curve is surprisingly symmetric around the mole fraction where the titling angle is zero. To
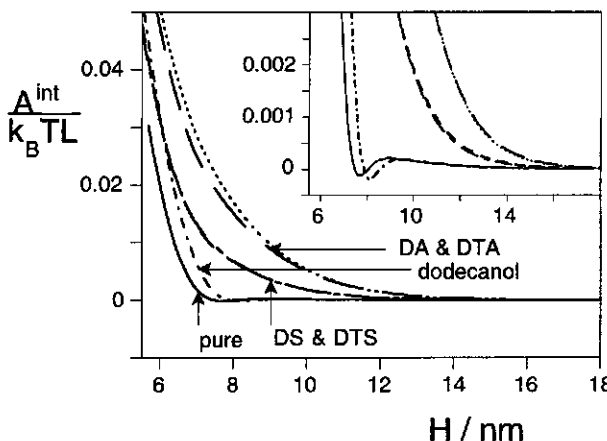
Figure 10. The interaction curve (method **b**; eqn [10]) of DMPC membranes with and without the additives indicated. The salt concentration and the other parameters were as in figure 8. In the inset we show the same data but now on a smaller energy scale.

obtain a flat average head-group conformation we need a small amount of anionic additives. The observed symmetry may partly be due to the chemical similarity of the surfactants used. The small deviation from perfect symmetry is expected because the head group, when it tilts towards the water phase, meets another environment than when it tilts towards the membrane interior. For low amounts of added surfactant we find that the tilting angle varies linearly with the surfactant concentration. For a higher mole fraction of additives the tilting angle levels off.

We have also plotted in figure 9 experimental NMR results for the effect of added surfactants on DMPC membranes, obtained by Marassi. There is a striking similarity between the trends found for the quadrupole splitting and our calculated head-group tilting angle. In the quadrupole splitting results there is a bending point found for a small added amount of cationic surfactants. A similar trend was found for the quadrupole splitting of DMPC deuterated at the C_α position (not shown). This implies that in the experimental conditions of Marassi the head groups in the pure DMPC membranes probably had a very small negative tilting angle. There is some asymmetry in the experimental data. The symmetry breaking can be caused by the difference in chemistry between the anionic and cationic surfactants used. We conclude from figure 9 that our calculations provide further evidence that the interpretation of the quadrupole splitting in terms of head-group tilt is justified.

In a previous publication,[6] we have predicted that the head-group conformation of a PC-like lipid to which we added a (large) hydrophilic chain will alter the head group orientation in a non monotonous way as a function of the length of the
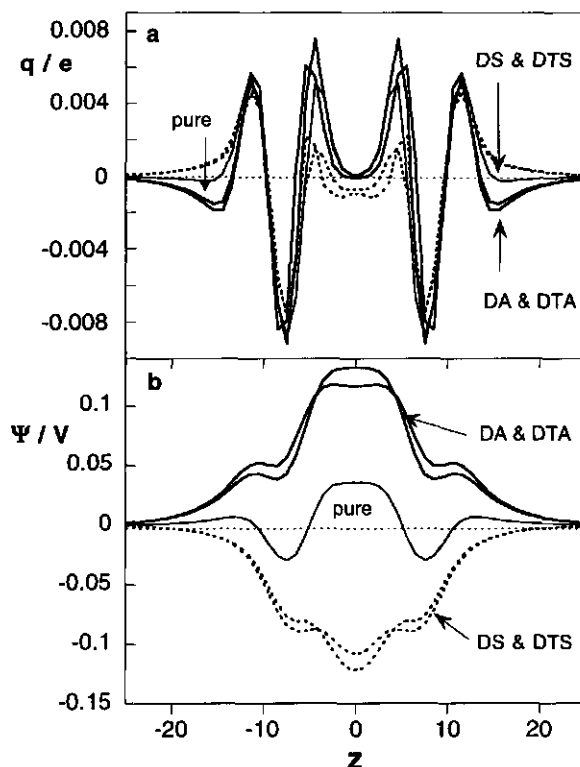
Figure 11. The total charge profile (a) and the resulting potential profile (b) in doped and pure non-interacting DMPC membranes as indicated. The membranes are the same as in figure 10 at infinite separation.

hydrophilic tail. NMR experiments as discussed above could be used to check our predictions.

Additives in Interacting Membranes

Additives not only influence the head-group conformations, they also have clear effects on the membrane interaction curves. This is shown in figure 10. Here we present interaction curves computed by method **b** (eqn [10]); the fixed chemical potentials case. Considering first the effect of dodecanol, we see again that the PC membrane with additive is thicker than without additives; in the interaction curve for PC membranes with dodecanol the steric repulsion sets in at a separation of about half a nm earlier than for membranes without any additives. Other features for dodecanol-doped membranes are very similar to the pure PC membranes, indicating that the PC head-group properties are effectively unaltered. The interaction curve for PC membranes with charged additives is

dominated by the electrostatic repulsion regime. As discussed above, the charged surfactants did not change the membrane thickness very much. This has the consequence that the interaction curves for dodecanol and DS and DTS cross each other at the position where the electrostatic repulsion regime yields to the steric one. A striking feature is the clear difference in the interaction curves between the anionic- and the cationic-doped DMPC membranes. Although both membranes have the same mole fraction of additive material in the membrane and the same absolute value of the charge (and therefore the same net surface charge density) it is clear that the cationics produce a repulsion shifted to larger membrane spacings. The clue to this phenomenon is found in figure 11. Here the total charge profile (figure 11a) and the potential profile (figure 11b) of these doped membranes are plotted. It can be seen from the charge profile that for DA and DTA the main difference in charge distribution with the pure membrane is located on the outside of the head-group region, while for DS and DTS it is located on the inside of the head-group region (compare figure 8b). A related difference shows up in the position and the height of the shoulder in the potential profile. For DA and DTA the potential rises at the membrane boundary but reaches a modest maximum value while the shoulder in the potential profile for DS and DTS sets in closer to the membrane core and reaches relatively high values. Hence, at a certain membrane-membrane distance H, in the DS and DTS cases the planes of charge of two approaching bilayers are further apart than in the DA and DTA. In figure 10 we notice that there is a profound electrostatic repulsion regime in the membrane systems that are doped with charged surfactants. The corresponding effects on the periphery of the DMPC membranes of the charge and electrostatic potential profiles are seen in figure 11. These parts of the charge distributions are known as the diffuse part of the electric double layer.

The large difference in partition coefficient and the differences in concentration in the tail region between DS and DTS do not show up in the interaction curves. Also for DA and DTA, which have even more influence on the membrane surface properties, the interaction curves are virtually the same. This is in line with our previous conclusion that the orientations of the DMPC head groups determine the details of the interaction curve. On the other hand, the interior of the membrane experiences the difference between the methylated and the non-methylated surfactant head group. As mentioned before, due to their more apolar nature the methylated additives preferentially enrich the hydrophobic centre of the membrane, giving rise to more enhanced electrostatic potential values in the membrane. The electrostatic potential profile is important for understanding the diffusion of charged species through the lipid bilayers. A local extreme in the potential profile results in a local maximum or minimum in the equilibrium

distribution of ionic compounds. A local minimum in the ion concentration is a rate-limiting factor in the passive ion flux.

In the above we have shown how additives affect the membrane-membrane interactions. For other membrane properties influenced by foreign molecules we do defer a more detailed analysis of the membrane-additive problem to future publications.

Conclusions

We have performed SCF calculations to predict the molecular details of both free-standing and interacting, liquid-crystalline DMPC membranes in aqueous solutions. In our calculations the interaction curve has three regimes: an attractive regime of entropic origin bracketed by two repulsive regimes, one of electrostatic and one of steric nature. When the bilayers are brought into close contact the repulsive steric forces are exponentially increasing, which might be linked to the so-called protrusion forces. The height of the repulsive region of electrostatic origin is non-monotonous dependent on the salt concentration. More specific, we have shown that it is possible to find a regime of intermediate ionic strength for which an electric double layer develops on the periphery of the bilayer, which gives rise to an electrostatic repulsion that is sufficiently long ranged and sufficiently strong to overcome the Van der Waals attraction. In this regime we thus expect colloid chemically stable DMPC membranes. We have also speculated that the non-monotonous interaction curve as found in DMPC membranes might explain the lipid swelling paradox that lipids tend to swell more strongly from excess water phase than from a saturated water vapour.

Single chain, neutral surfactants with small head groups do not change the head-group orientation in a DMPC membrane, but they do alter the membrane thickness. On the other hand, charged surfactants have no effect on the membrane thickness but modulate the lipid head-group conformation of DMPC molecules. In line with NMR findings we find that cationic surfactants push the choline moiety outwards, whereas anionic surfactants pull this group inwards.

Uncharged surfactants hardly modify the pair interaction between DMPC membranes, whereas charged surfactants have the effect that the electrostatic repulsion becomes much more pronounced. The sign of the charge on an added surfactant plays an important role in positioning the excess charge in the head-group region. With cationic surfactants the 'plane of charge' is located in the outer head-group region, while for anionics it is at the inner head-group region. This difference leads to a shift of the electrostatic interaction curve. At a specific membrane-membrane distance the electrostatic repulsion is larger for a system doped with a cationic surfactant than with an anionic one.

Acknowledgements

Literature

1. Singer, J.S. and G.L. Nicholson, Science, 1972 **175** p. 720-731.
2. Berendsen, H.J.C., B. Egberts, S.-J. Marrink and P. Ahlström, in *Membrane Proteins: Structures, Interactions and Models,* Pullman, A., Editor. 1992, Kluwer Academic Publishers: Dordrecht p. 457-470.
3. Egberts, E. and H.J.C. Berendsen, J. Chem. Phys., 1988 **89**(6) p. 3718-3732.
4. Van der Ploeg, P. and H.J.C. Berendsen, J. Chem. Phys., 1982 **76**(6) p. 3271-3276.
5. Van der Ploeg, P. and H.J.C. Berendsen, Molecular Physics, 1983 **49**(1) p. 233-248.
6. Meijer, L.A., F.A.M. Leermakers and J. Lyklema, Recl. Trav. Chim. Pays-Bas, 1994 **113** p. 167-175.
7. Van Venetië, R. and A.J. Verkleij, Biochim. Biophys. Acta, 1982 **692** p. 397.
8. Isrelachvili, J.N. and G.E. Adams, J. Chem. Soc. Faraday Trans. 1, 1978 **74** p. 975.
9. Marra, J., Biophys. J., 1986 **50** p. 815.
10. Marra, J. and J.N. Israelachvili, Biochemistry, 1985 **24** p. 4608.
11. Helm, C.A., J.N. Israelachvili and P.M. McGuiggan, Science, 1989 **246** p. 919-922.
12. Leckband, D.E., C.A. Helm and J. Israelachvili, Biochemistry, 1993 **32** p. 1127-1140.
13. Leckband, D.E., J.N. Israelachvili, F.-J. Schmitt and W. Knoll, Science, 1992 **255** p. 1419-1421.
14. Israelachvili, J.N. and H. Wennerström, Langmuir, 1990 **6** p. 873-876.
15. Parsegian, V.A., P.R. Rand, N.L. Fuller and D.C. Rau, in *Methods in Enzymology,* Packer, L., Editor. 1986, Academic Press: New York p. 400-416.
16. Parsegian, V.A., N.L. Fuller and R.P. Rand, Proc. Natl. Acad. Sci. U.S.A., 1979 **76** p. 2750.
17. LeNeveu, D.M., R.P. Rand and V.A. Parsegian, Nature, 1976 **259** p. 601.
18. MacIntosh, T.J. and S.A. Simon, Annu. Rev. Biophys. Biomol. Struct, 1994

23 p. 27-51.

19. Evans, E. and D. Needham, J. Phys. Chem., 1987 **91** p. 4219.
20. Evans, E. and M. Methcalfe, Biophys. J., 1984 **46**(423-425).
21. Evans, E.A., Colloids and Surfaces, 1990 **43** p. 327-347.
22. Hall, D.G. and B.A. Pethica, in *Nonionic Surfactants,* Schick, M.J., Editor. 1976, Marcel Dekker: New York p. 516-557.
23. Hill, T.L., *Thermodynamics of Small Systems.* Vol. 1 and 2. 1963, 1964, New York: Benjamin.
24. Helfrich, W., Naturforsch., 1973 **28c** p. 693.
25. Helfrich, W., Naturforsch., 1978 **33a** p. 305.
26. De Gennes, P.-G. and C. Taupin, J. Phys. Chem., 1982 **86**(13) p. 2294-2304.
27. Leermakers, F.A.M. and J.M.H.M. Scheutjens, J. Chem. Phys., 1989 **93** p. 7417-7426.
28. Rand, R.P. and V.A. Parsegian, Biochim. Biophys. Acta, 1989 **988** p. 351-376.
29. Rand, R.P. and V.A. Parsegian, in *The Structure of Biological Membranes,* Yeagle, P., Editor. 1992, CRC Press: Boca Raton p. 251-306.
30. Evers, O.A., J.M.H.M. Scheutjens and G.J. Fleer, Macromolecules, 1990 **23** p. 5221-5233.
31. Leermakers, F.A.M. and J.M.H.M. Scheutjens, J. Chem. Phys., 1988 **89** p. 6912-6924.
32. Meijer, L.A., F.A.M. Leermakers and A. Nelson, Langmuir, 1994 **10** p. 1199-1206.
33. Leermakers, F.A.M. and J.M.H.M. Scheutjens, J. Chem. Phys., 1988 **89** p. 3264-3274.
34. Tanford, C., *The Hydrophobic Effect: Formation of Micelles and Biological Membranes.* 1973, New York: John Wiley.
35. Tocanne, S.-F. and J. Teissié, Biochim. Biophys. Acta., 1990 **1031** p. 111-142.
36. Gutman, M. and E. Nachliel, Biochim. Biophys. Acta., 1990 **1015** p. 391-414.
37. Israelachvili, J.N. and H. Wennerström, J. Phys. Chem., 1992 **96** p. 320-351.
38. Besseling, N.A.M., *Statistical Thermodynamics of Fluids with Orientation-Dependent Interactions. Applications to Water in Homogeneous and Heterogeneous Systems.* 1993, PhD thesis Wageningen Agricultural University.
39. Marčelja, S. and N. Radic, Chem. Phys. Lett., 1976 **42** p. 129-130.
40. Deryagin, B.V. and L.D. Landau, Acta Physicochim. U.R.S.S., 1941 **14** p. 633.

41. Verwey, E.J.W. and J.T.G. Overbeek, *Theory of the Stability of Lyophobic Colloids.* 1948, Amsterdam: Elsevier.

42. Jendrasiak, G.L. and J.C. Mendible, Biochim. Biophys. Acta, 1976 **424** p. 149.

43. Jendrasiak, G.L. and J.H. Hasty, Biochim. Biophys. Acta, 1974 **337** p. 79-91.

44. Marassi, F.M. and P.M. MacDonald, Biochemistry, 1992 **31** p. 10031-10036.

45. Seelig, J., P.M. MacDonald and P.G. Scherer, Biochemistry, 1987 **26**(24) p. 7535-7541.

Chapter 4

Self-Consistent-Field Modelling of Complex Molecules with Atomic Detail in Inhomogeneous Systems.

Cyclic and Branched Foreign Molecules in DMPC Membranes.

Abstract

We have developed a detailed self-consistent-field model for studying complex molecules in inhomogeneous systems, in which all the molecules are represented in a united atom description. The theory is in the spirit of the approach developed by Scheutjens and co-workers for polymers at interfaces and self-assembly of surfactants and lipids into association colloids.

The theory is applied to lipid membranes composed of dimyristoylphosphatidylcholine (DMPC). In particular, we looked at the incorporation of linear, branched and cyclic molecules into the lipid bilayers being in the liquid phase. Detailed information on the properties of both the lipids and the additives is available.

For the classes of linear and branched alcohols and phenol derivatives we find good correspondence between calculated partition coefficients for DMPC membranes and experimental data on egg-yolk PC. The calculated partitioning of molecules of isomers, containing a benzene ring, two charged groups (one positive and one negative) and 16 hydrocarbon segments, into DMPC membranes showed variations of the partition coefficient by a factor of 10 depending on the molecular architecture. For zwitterionic additives we find that it is much more difficult to bring the positive charge into the membrane core than the negative one. This result can be rationalised from information on the electrostatic potential profile of the bare membrane, being positive in both the core and on the membrane surface but negative near the position of the phosphate groups. For several tetrahydroxy naftalenes we found that, although the partition coefficient is barely influenced, the average orientation and position of the molecule inside the membrane is strongly depends on the distribution of the hydroxyl groups on the naphthalene rings. The orientation changes from one

where the additive spans the membrane when the hydroxyls are positioned on (2,3,6,7) positions, to an orientation with the rings parallel to the membrane surface and located near the head group-hydrophobic core interface for the hydroxyls at the (1,3,5,7) positions.

We propose that, when our model is used in combination with octanol/water partitioning data, a very accurate prediction is possible of the affinity of complex molecules for lipid membranes.

Introduction

Membranes are one of the key structural components that sustain life. Life would not be possible without the lipid bilayer matrices, enriched with many proteins and a large number of apolar or amphipolar additives. These layers envelop each cell, preventing the uncontrolled mixing of the cell interior with the surroundings. Furthermore they compartmentalise the cell interior and in that way make it possible for a cell to create local environments necessary for its appropiate chemical performance. Membranes are semipermeable. Both passive and active transport processes are known to take place over the bilayer. Passive transport is controlled by the specific polar-apolar nature of the membranes. Active transport is possible as the membranes can embed various (macro-)molecules that can regulate, at the expense of Gibbs energy (*e.g.* ATP), the translocation of other molecules.

Singer and Nicholson proposed a fluid mosaic model to explain many membranes properties.[1] A two dimensional "sea" of lipids forms the matrix in which the proteins are floating. This complex set of many kinds of lipids, proteins and other additives play in concert to perform many vital functions. Most molecules that are part of the membrane are characterised by a polar and an apolar part. The apolar moieties tend to escape the aqueous phase and cluster together in a process called self-assembly. On the other hand, the polar parts of the molecules (the head groups) prefer the water phase and thus stay typically on the outside of the assembly. Such a molecular aggregate, in the surfactant literature known as a micelle, can have a spherical, cylindrical or flat shape, depending on the architecture and concentration of the molecules. All these structures have in common that there is one length scale that is of the order of twice the length of the apolar tails. Membranes are predominantly flat structures, where the polar head groups occupy on the average the same area per molecule as the tails do.

Membranes have a low mechanical resistance. Cells, without a cell wall, can easily be destroyed by a low osmotic pressure. The surface tension of lipid membranes in general, and of unsupported free membranes in particular, is

negligible.

The interior of the lipid matrix of membranes is comparable to a two-dimensional liquid alkane solution. The order in the chains is, however, larger than in a bulk alkane solution due to the fact that all carbon tails are attached to a head group that effectively anchors them to the hydrocarbon water interface. A membrane exhibits several phase transitions. The main one is often called the gel to liquid phase transition and is believed to be of first order in membranes of pure lipids. Most biologically active membranes are in the liquid crystalline phase rather than in the gel phase. Apparently, for appropriate biological functioning the lipid matrix should have a rather high degree of disorder and a fluid-like lateral mobility. The gel phase, in which all chains are frozen in an all-*trans* configuration and, relative to the fluid phase, have reduced lateral mobility, is usually avoided in living nature.

Investigating biomembranes is a rather specialistic task. It can be useful for the understanding of the main principles to study simplified model systems by successively reducing the number of different molecules in the aggregates. Understanding the behaviour of a two-dimensional lipid phase without additives is already an ambitious goal. At present the lipid-only membranes are still too difficult to fully comprehend. Typically, a further simplification is to consider systems containing only one kind of lipid molecule. For these highly simplified model membranes a fair amount of knowledge both on experimental and on theoretical aspects has been accumulated.[2]

Lipids can be subdivided into several groups. Phospholipids are a subset of lipids that are found to constitute over 90% of most biological membranes. For this reason, this class of lipids is most frequently studied. It also constitutes the class of lipids selected for the present study. They consist of a glycerol backbone on which two apolar tails, 12 to 24 carbon atoms long, and a polar head group are attached. The head group contains a phosphate group esterified to the glycerol and often some other polar group like choline, ethanol amine or glycerol.

The next step in the modelling of biomembranes is to study the effect of adding foreign molecules to the phospholipid matrix. By doing this, one can systematically study both the influence of the additives on the bilayer structure and the position, orientation and partition of these molecules. One can consider various types of additives, such as other (phospho-)lipids, ions or biologically active molecules, *e.g.* hormones or man-made drugs.

For the latter two classes of 'foreign' molecules a parameter of special interest is the partition coefficient. This quantity is defined as the ratio between the

concentration of a foreign molecule in the membrane phase and that in the water phase. The partitioning of the above mentioned molecules in the membrane matrix is important because it plays a role in the working mechanism of the drug or hormone. For example, the passive transport through the membrane is obviously strongly dependent on this partition coefficient. If the working site of a drug is known one can propose an optimal partition coefficient for such a drug. If one could predict partition coefficients from molecular details one would speed up the search for new drugs enormously. It is this ultimate goal, which has motivated us to perform the present study.

Well-controlled experiments on lipid bilayer systems are certainly not easy and the interpretation of the data is facilitated when good theories are available. In fact, the modelling per se is a useful alternative approach to obtain insight into the structure of lipid membranes. Theoretical modelling is nowadays possible with the help of fast computers.

Surprisingly little work has been done in recent years on the theoretical modelling of the molecular details of lipid membranes and, particularly, of additives therein. Due to the complexity of membranes there is still much progress to be made on this subject. There are a few theoretical techniques that have been applied with some success.

Molecular dynamics (MD) simulations of bilayers are at first glance the most exact. In these simulations Newton's equation is solved for interacting particles in a box. Since typically the fundamental time steps are very small (order of femto seconds), MD requires supercomputer power or massive parallel computing. Slow processes like the partitioning of additives into lipid bilayer membranes are not yet within reach. Nevertheless, one can get some information on the interactions between the lipid matrix and additives.[3-6]

Monte Carlo (MC) simulations form often an alternative technique to model condensed systems. In this approach only a selection of all possible conformations of the system is generated. The success of the method depends on the ability to generate enough probable system configurations. This can be done with the Metropolis algorithm. However, for densely packed layers the generation of most probable states is laborious and MC simulations of the full membrane problem are not known to us. The modelling of some sub-problem in of lipid membranes has been undertaken. Mouritsen et al.[7-9] approach a bilayer membrane as a two-dimensional sea in which the molecules can have several states. With state-dependent interactions they can calculate the lateral structure formation. There is however the difficulty of, a priori, determining the various states and corresponding interactions for a (new) molecule from its molecular

structure.

A fourth theoretical modelling option applied to lipid membranes, and used in this paper, is known under the term self-consistent-field (SCF) methods. SCF theories do not share the disadvantages of the former MD and MC simulations, *i.e.* they do not heavily depend on supercomputer power. The method is based on the reduction of the many-molecule problem to the problem of one molecule in the (external) field of mean force of all the others. In general, the external field is defined depending on the set of all conformations of all molecules and their interactions. The potential field, on its turn, determines the statistical weight of the conformations that make up the complete system. The fixed point solution of this implicit set of equations is referred to as the self-consistent-field solution, which typically depends on boundary conditions and space filling constraints.

Several people have elaborated various approaches along these lines to describe association of molecules into aggregates. Most of them use a lattice to limit the accessible number of conformations and make use of the given symmetry of the aggregates. They consider the aliphatic chains to be attached to the surface of the aggregate but do not allow solvent (water) to penetrate into the aggregate. The external field is mostly a pressure field that ensures that the core of the aggregate has a density comparable to that of liquid alkane.[10-14] Sometimes an order dependent field is introduced.[15,16] Marčelja showed that the gel to liquid phase transition could be modelled in this way. Additives in bilayers are either modelled as structureless isotropic monomers that mostly have no specific contact interaction with the lipid tails, or small chain molecules of the same type of units as the tail segments. The results are, despite these approximations, promising and give insight into the importance of the included field components.

The theory discussed in this paper includes not only volume interactions and an anisotropic field (of a different origin than used by Marčelja or Gruen), it also includes electrostatic interactions and contact interactions between unlike segments in a Bragg-Williams approximation, parametrised by way of Flory-Huggins χ-parameters. These interactions allow the lipids to self-assemble in a given geometry. Apart from the lattice geometry nothing is assumed about the segment position or orientation.

Several years ago simplified model membranes were investigated with this theory.[17-19] Although the molecular representation was rather crude, the main features of the tail region, *i.e.* the large degree of disorder and the fact that the segments closest to the hydrophobic-hydrophilic "interface" in the lipid molecules have the most narrow distribution, were reproduced, in line with MD predictions.

In order to relate to experiments, calculations were done on adsorbed phospholipid monolayers with a more realistic molecular description.[20] It was found that the zwitterionic nature of DMPC gives rise to a profile in the electrostatic potential which, in turn, causes cations to associate with the phosphate group. The association is the stronger the higher the valence of the ions is. These results were of interest in interpreting the ion permeability measurements of monolayers deposited on a mercury electrode, and used to conjecture that the concentration of ions in the head group area is a determining factor for their permeability through ion channels.[21,22]

More recently, we considered the head group conformations of (modified) DMPC and DMPS membranes.[23] The PC head group appeared to have, on the average, a conformation parallel to the membrane surface. In line with experimental data[24] it was found that, at high salt concentrations, the choline group distribution splits in two orientations, one closer to the hydrocarbon phase and the other closer to the water phase.

Despite these promising results, several shortcomings of our theory remain that deserve further attention. One of these is that, up to date, only flexible linear or branched molecules could be considered. Most biologically active additives to membranes have, however, some sort of rigid (ring) moiety as a part of their structure. Membranes are highly ordered systems (although not as high as some pictorial representations seem to imply), and thus a considerable difference in packing behaviour is expected between flexible and rigid species in the membrane. Furthermore, the position of different types of substituents on a ring structure is likely to be significant for, *e.g.*, the partitioning.

It is possible to extend our SCF theory such that the molecules can contain rigid fragments as we show in the present chapter. The incorporation of excluded volume correlations on the length scale of the rigid units is a natural extension of the previously implemented RIS scheme. In a RIS scheme four consecutive segments along the chain are non-overlapping and the local configuration is weighted with the *gauche-trans* energy. Incorporation of rigid fragments that contain an arbitrary number of units (atoms or united atom groups) in the chain statistics is facilitated by the fact that for these fragments all the relative coordinates of the atoms are fixed. One needs only to generate a proper set of conformations of the entire fragment and couple this to the flexible chain parts that might be connected to it.

In the following we will discuss in detail the theoretical framework to handle complex molecules with atomic detail in inhomogeneous systems. First we will present the partition function for the system. Next we will discuss the propagator

method to obtain the density profiles for flexible and branched chain molecules. We proceed by giving the details of the treatment of rigid structures within this propagator formalism. Results will be presented for the partition coefficients of linear and branched alcohols and phenols in DMPC membranes. The positional and orientational information of additives in DMPC membranes will be shown for a group of isomers containing a benzene ring with some substituents and of some, in various ways substituted, tetrahydroxy naftalenes. Finally, we will discuss the perspectives of our approach and present our conclusions.

Theory

Preliminary Considerations

As stated above, the SCF theory reduces the full membrane problem to one test molecule (*i.e.* lipid or additive) in the potential field of mean force of all the other molecules. In SCF theory the problem splits naturally into two: how to relate the potential fields to the densities and to relate the densities to the potential fields.

Both sub-problems can be tackled from the approximate partition function for the system. This quantity has been derived before and can be applied to the present system as well. Here the highlights of the derivation will be briefly reviewed. We start by introducing the parameters and key approximations.

The partition function is the sum over the probabilities of all sets of all conformations of all molecules in the system. To compute this properly, several quantities have to be defined. Molecules of different type (water, lipid, salt, additive) are numbered $i = 1, 2, \ldots$. Each molecule of type i consists of N_i units (segments). Each unit represents an atom or a group of atoms (*e.g.* CH_2 or OH). We use A, B,... to denote the types of segments. The segments in the molecule are referred to by ranking numbers $1, 2, \ldots, s_i, \ldots, N_i$ and linked to each other by bonds which, in turn, are numbered $1, 2, \ldots, \sigma_i, \ldots, N_{\sigma i}$, where $N_{\sigma i}$ denotes the number of bonds of molecule i. In linear or branched chains $N_{\sigma i}$ is one less than the number of segments N_i. If ring fragments are part of the molecule, $N_{\sigma i}$ increases by one for every closed ring in the structure. A conformation, c, is defined by the position in space of one segment (*e.g.* the first segment of the chain) and the subsequent orientation of all bonds in the molecule. Note that every configuration is L fold degenerated, because every first segment in a chain can occupy one of the L sites in layer z.

In order to keep the full set of all conformations, $\{n_i^c\}$, from becoming infinite, the system volume is discretised. A system of coordinates with spacings ℓ spans up a lattice in which flat layers are identified that accommodate L sites of equal
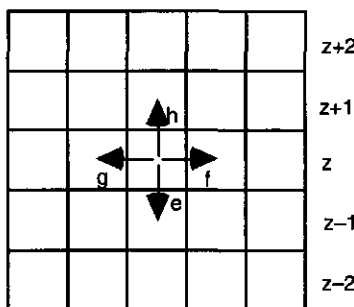
Figure 1. A two-dimensional square lattice representation of the tetrahedral (diamond) lattice used in this paper with the four directions indicated (e, f, g, and h).

volume ℓ^3 each. The layers are numbered 1, 2, ..., z, ...,M, with M being the total number of layers. All segments are assumed to fit exactly a lattice site. Within each layer a mean field approximation is applied as only the average occupation is recorded. The number of directions of the bonds is also limited: only four distinct directions are allowed for. A tetrahedral lattice is applied on which a three-choice propagation scheme is employed. This three-dimensional lattice can be mapped onto a two-dimensional square lattice which is shown in figure 1. In this two-dimensional representation the four bond directions e, f, g and h are indicated as vectors connecting segments in between layers z and z − 1 (e), within a layer z (f and g) and between layer z and z + 1 (h).

By the introduction of a lattice not only the counting of the conformations is simplified but also the geometry of the system, the length of the bonds and the size of the segments are fixed. These approximations can be relaxed in various ways. One way to do this is to reduce the lattice spacing while keeping the segment volume constant.[25] The assumption of a fixed bond length can be partly relaxed by allowing certain fragments with different bond lengths (like rigid rings) to have their segments on off-lattice sites. However, after the sampling of the conformations one needs to assign the segment to the layers and the bonds to one of the set of directions {e, f, g, h}.

To give every conformation the proper statistical weight, the energy of each conformation in the external field is determined. For a molecule in a given conformation every segment has a known z position. Depending on the segment type A of a unit, it feels the local segment potential energy, $u_A(z)$. The total potential energy of the molecule in that conformation is then found by the sum of the segment potential energies of all segments. Then the overall probabilities to find the segments of molecule i in conformation c on their respective positions is

related to the potential energy by a Boltzmann weighting factor. Directly linked to this probability is the number of molecules i in conformation c. This quantity is referred to by n_i^c.

The number of molecules i in conformations c follows the partition function which is maximised with respect to every n_i^c. If n_i^c is known, the approximate (mean field) partition function is available. From this all thermodynamic properties follow.

The Partition Function

Formally the grand canonical partition function for an open system, $\Xi(\{\mu_i\}, M, L, T)$, can be written as:

$$\Xi(\{\mu_i\}, M, L, T) = \Xi^* \frac{\sum_{\{n_i^c\}} \Omega(\{n_i^c\}) Q^\sigma \exp(U^{int}/k_B T) \exp(\sum_i n_i \mu_i / k_B T)}{\sum_{\{n_i^c\}} \prod_i \Omega_i^*(n_i) Q^{\sigma*} \exp(U^{int*}/k_B T) \exp(\sum_i n_i \mu_i^* / k_B T)} \qquad [1]$$

It is composed of a combinatorial factor Ω, an internal canonical partition function Q^σ, which takes the local bond configurations into account, the interaction energy U^{int} and the chemical potentials $\{\mu_i\}$. The corresponding reference states for every molecule (here we choose these to be the one component amorphous melts) are indicated by an asterisk. The absolute temperature is denoted by T and Boltzmann's constant by k_B.

The interaction energy U^{int} is split into two contributions with respect to the amorphous reference state of pure molecule i. One is of short range and extends over three consecutive layers. It is parametrised by the Flory-Huggins χ-parameter. The interaction parameter χ_{AB} is the dimensionless free energy involved in the exchange of a segment of type A from a pure A solution with a segment B from a pure B solution. So it is zero by definition for the exchange of segments of the same type. The other part of the interaction energy is of long range, extending over the whole system, and is of electrostatic origin. It contains the electrostatic potential $\Psi(z)$ which can be calculated, through Gauß' law, from the density profile, involving the dielectric permittivity profile, $\varepsilon_r(z)$ and the charge (valence) profile, $q(z) = \sum_A e v_A \varphi_A(z)$.[23,26,27] In this last equation v_A is the valence of segment A, $\varphi_A(z)$ the volume fraction of that segment at position z and e the elementary charge. The potential in the reference state is taken to be zero. The total interaction energy then reads:

$$\frac{U^{int} - U^{int*}}{k_B T} = \frac{1}{2} \sum_i \sum_z \sum_A \sum_B N_{Ai}(z) \chi_{AB} [\langle \varphi_B(z) \rangle - \varphi_{Bi}^*] + \sum_z \frac{L q(z) \Psi(z)}{2 k_B T} \qquad [2]$$
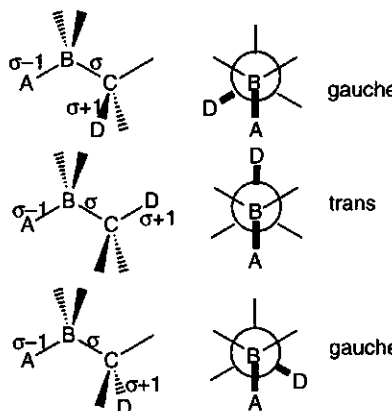
Figure 2. Illustation of the three possible local bond conformations in a linear chain. The central bond is denoted as σ, and A, B, C and D are four consecutive segments. Other segments in the chain are not shown.

In equation 2, $N_{Ai}(z)$ is the number of segments of type A that molecule i has in layer z. The angular brackets denote the averaging over three consecutive layers: $\langle \varphi_B(z) \rangle = \frac{1}{3}\varphi_B(z-1) + \frac{1}{3}\varphi_B(z) + \frac{1}{3}\varphi_B(z+1) \approx \varphi_B(z) + \frac{1}{3}\frac{\partial^2\varphi_B(z)}{\partial z^2}$.

The internal canonical partition function, Q^σ, takes into account the energetic and entropic contributions that the various conformations of a bond sequence can have. In this term only contributions of intra molecular interaction that are not accounted for in the (external) potential fields are included. More specifically in a linear chain it is the energy and entropy involved with the different *gauche* and *trans* conformations along the chain. In general, the local conformations (*gauche* and *trans*) are defined by the relative directions of the bonds in the immediate vicinity of one bond σ. It is assumed that the conformation of the rest of the chain does not influence the energy concerned with this 'local conformation'. The local conformation around bond σ is denoted by $q_{\sigma i}$ and the energy of a specific conformation as $u^{q_{\sigma i}}$. For a given conformation c of a molecule the local conformation around bond σ is denoted by $q_{\sigma i}^c$. So the conformation c of the full chain can be determined by the local conformations $\{q_{\sigma i}^c\}_\sigma$.

As an example, in a linear hydrocarbon chain $q_{\sigma i}$ for $1 < \sigma < N_{\sigma i}$ determines the relative directions of three consecutive bonds and therefore the relative positions of four consecutive segments. Such a fragment can have three local conformations, one *trans* and two *gauche* ones. In contrast to the two *gauche* ones, in the *trans* conformation the two bonds σ – 1 and σ + 1 are pointing in the same direction. By rotation around the central bond σ the bond sequence can
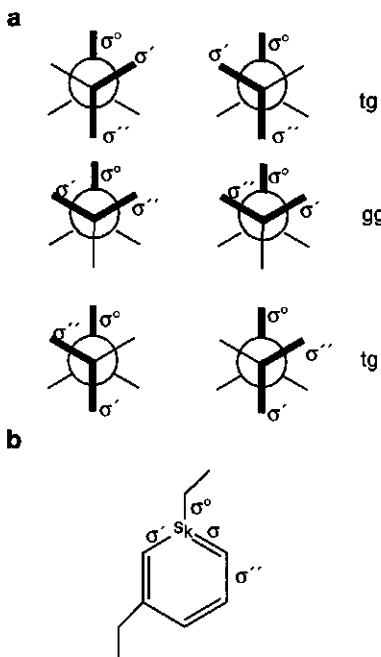
Figure 3. Diagram (a) presents the six possible local conformations close to a branch point with three bonds (three-node). There are four separate trans-gauche (tg) and two gauche-gauche (gg) conformations. Diagram (b) shows the only possible local bond conformation around a bond σ in a benzene ring. Here bond σ° is the 'outgoing' bond on segment s_k.

assume these local states (see figure 2). We denote the energy difference for the rotation from *gauche* to *trans* of the conformation $q_{\sigma i}$ as u^{g_σ}. We note that u^{g_σ} can vary along the chain.

The probability, $\lambda^{q_{\sigma i}}$, for a specific local conformation $q_{\sigma i}$ is related to the Boltzmann factor, containing the internal energy $u^{q_{\sigma i}}$. The proper normalisation is found by the sum of the Boltzmann factors of all possible local conformations around that bond σ, $\{q'_{\sigma i}\}$:

$$\lambda^{q_{\sigma i}} = \exp\left(-u^{q_{\sigma i}}/k_B T\right)/\sum_{q'_{\sigma i}} \exp\left(-u^{q'_{\sigma i}}/k_B T\right). \qquad [3]$$

For a linear chain part the probability to find a *gauche* conformation around bond σ then becomes: $\lambda^{q_{\sigma i}} = \lambda^{g_\sigma} = \exp\left(-u^{g_\sigma}/k_B T\right)/[2\exp\left(-u^{g_\sigma}/k_B T\right)+1] = 1/\left[2+\exp\left(u^{g_\sigma}/k_B T\right)\right]$. The probability to find a *trans* conformation is simply $\lambda^{t_\sigma} = 1-2\lambda^{g_\sigma}$. At the chain ends ($\sigma = 1$ and $\sigma = N_{\sigma i}$ respectively, for linear chains)

there is only one neighbouring bond ($\sigma = 2$ and $\sigma = N_{\sigma i} - 1$ respectively). Since all bonds have the same angles in a tetrahedral lattice, only one conformation exists which, according to equation 3, has a probability of unity.

In a branched chain there are more then two end-bonds σ for which $\lambda^{q_{\sigma i}} = 1$. Moreover, local conformations including a branch point have a specific problem. We have chosen in this chapter not to differentiate between occupancies between the f and g directions (isotropic distribution of bonds in a plane). For this reason no distinction can be made between the two chiral counterparts (changing two bonds will get the same statistical weight). Consequently, our calculations always represent racemic mixtures. As a result of this, the number of local conformations including a branch point equals six (see figure 3a). Let the branch point be defined by the three bonds σ, σ', and σ'' that come together. We *focus on bond σ which has, besides σ' and σ'', also $\sigma°$ as a neighbouring bond.* These four bonds (five segments) form the relevant fragment with conformations $\{q_{\sigma i}\}$. These conformations can be grouped into two sets according to their internal energy: one set for two *gauche-gauche* conformations with a higher energy and one set of four *trans-gauche* conformations with a lower energy. In calculating the probability for a specific *gauche-gauche* conformation only the energy difference u^{gg_σ} is needed: $\lambda^{q_{\sigma i}} = \exp\left(-u^{gg_\sigma}/k_B T\right)/[2\exp\left(-u^{gg_\sigma}/k_B T\right) + 4]$ $= 1/\left[2 + 4\exp\left(u^{gg_\sigma}/k_B T\right)\right] = \lambda^{gg_\sigma}$. The probability to find a *trans-gauche* conformation then is simply: $\lambda^{tg_\sigma} = \frac{1}{4} - \frac{1}{2}\lambda^{gg_\sigma}$.

A similar way of reasoning applies for a segment (node) where four branches come together (four-node). In this case five bonds and six segments are involved in the relevant fragment with conformations $\{q_{\sigma i}\}$. Now no energetic difference is made between the three bonds on the branch point (σ', σ'', σ''') next to bond σ. So the same internal energy is assigned to all viable conformations of these five bonds. Therefore, the probability for each of the six local conformations is equal to $\lambda^{q_{\sigma i}} = \frac{1}{6}$. Again, to simplify the calculations, here too an isotropic occupancy of the f and g directions is imposed. This has the result that molecules with a branch point with four connecting bonds are calculated as racemic mixtures. Equation 3 can also be applied to bonds in rigid fragments (see figure 3b). In these fragments there is obviously only one local conformation allowed and thus the denominator of equation 3 extends over just this one conformation and consequently $\lambda^{q_{\sigma i}} = 1$ for all bonds inside the rigid unit.

We have now specified the local probability factor that is assigned (with equation 3) to each bond in the (complex) molecules. The product of these probabilities over all bonds for a molecule i in a given conformation c can be

evaluated and this quantity is subsumed in $Q^\sigma/Q^{\sigma*}$. For a trimer, the unnormalised contribution to this part of the partition function is unity. The two bonds have only one local conformation each. Taking into account the rotational freedom of the whole molecule, a normalisation constant, $\lambda^{\alpha\beta}$, is found. Such a trimer can have 3Z conformations, where Z represents the number of different bond directions: the first bond has Z directions to choose from and the second than has only 3 alternatives left. In the same way molecules with more bonds also have 3Z degrees of rotational freedom. The natural logarithm of the internal canonical partition function with respect to the reference state now reads:

$$\ln\left(\frac{Q^\sigma}{Q^{\sigma*}}\right) = \sum_i \sum_c n_i^c \ln\left(\frac{1}{3Z} \prod_\sigma \frac{\exp\left(-u^{q_{\sigma i}^c}/k_B T\right)}{\left[\sum_{q_{\sigma i}} \exp\left(-u^{q_{\sigma i}}/k_B T\right)\right]}\right) = \sum_i \sum_c n_i^c \ln\left(\lambda^{\alpha\beta} \prod_\sigma \lambda^{q_{\sigma i}^c}\right)$$

[4]

Next the term Ω in the partition function Ξ will be discussed. This quantity has been derived by Leermakers and Scheutjens.[19] Their result also applies to our system even when we adopt complex shaped molecules:

$$\ln\left(\Omega/\Omega^*\right) = -\sum_i \sum_c n_i^c \ln\frac{n_i^c N_i}{L} + \frac{L}{2}\sum_z \sum_{\alpha''} \left[1 - \varphi^{\alpha''}(z \mid z')\right]\ln\left[1 - \varphi^{\alpha''}(z \mid z')\right]$$
$$-ML\sum_i \sum_{\alpha''}\left(\varphi_i - \varphi_i^{\alpha''*}\right)\ln\left(1 - \varphi_i^{\alpha''*}\right)$$

[5]

In this equation $\varphi^{\alpha''}(z \mid z')$ is the fraction of maximum bond density possible in orientation α'' starting in layer z and ending in layer z' (cf. figure 1 and table 1). Below we use $\varphi^{\alpha''b}$ which is the fraction of possible bonds in orientation α'' in the bulk defined as: $\varphi^{\alpha''b} = \left[Z\sum_i \varphi_i^b (N_{\sigma i}/N_i)\right]^{-1}$.

The factor Ω takes into account the number of ways the set of all the conformations $\{n_i^c\}$ can be put into the system. Here, not only the random mixing of the conformations, provided every layer is filled with L segments, is considered, but in addition the entropy of placing bonds in the lattice is included. It was recognised by DiMarzio that parallel bonds located at the same z coordinate, cannot block each other.[28,29] This notion enables one to rather accurately calculate the vacancy probability needed for the packing of the chains in the lattice. In effect an anisotropic field is created which has the property that, when it is large (due to the fact that many bonds have a given orientation) it will force other bonds to assume this orientation too. This cooperative behaviour is responsible for the gel-to-liquid phase transition in bilayer membranes.[19] The

two terms in equation 5 which depend on α'' are the result of this anisotropic weighting of the bonds in the lattice.

We note that in equation 5 the bond orientations α'' are limited to the primary orientations e'', f'', g'' and h'' as indicated by figure 1. The following procedure is adopted to place rigid structures in the system. If such a fragment of a molecule contains units that do not exactly fit onto the lattice layers, a representative set of conformations is sampled (see appendix). A segment in a fragment that is in a given conformation feels the external potential field of the layer in which the centre of that unit resides. In this procedure the bonds in the ring can have other orientations than defined by $\alpha'' \in \{e, f, g, h, e', f', g', h'\}$. We use the ansatz that these bonds are assigned to the bond orientation α'' that is closest to the direction of the bond of interest. More details will be given below.

With this procedure equation 5 can conveniently be calculated. Again the rounding errors can be systematically reduced by refining the lattice spacings while keeping the size of the units constant.

We return once more to equation 1: The chemical potentials μ_i still need to be discussed. In an equilibrated system, the chemical potentials do not depend on the spatial coordinate. In the bulk phase, denoted with the superscript b, no gradients in the densities occur, which facilitates the computation of these quantities. The chemical potential can be derived from the canonical partition function for a homogeneous system and written as a function of bulk values and reference state values only.[19] Here we have a slightly modified version which is correct even when the molecules contain closed rings or another exotic internal structure (see appendix).

$$\frac{\mu_i - \mu_i^*}{kT} = \ln\varphi_i^b - \frac{N_i}{2}\sum_A\sum_B\left(\varphi_{Ai}^* - \varphi_A^b\right)\chi_{AB}\left(\varphi_{Bi}^* - \varphi_B^b\right) - [ZN_i - N_{\sigma i}]\ln\left[1 + \frac{N_{\sigma i} - N_i\sum_j\dfrac{N_{\sigma j}\varphi_j^b}{N_j}}{ZN_i - N_{\sigma i}}\right]$$

[6]

The first term, $\ln\varphi_i^b$, is the ideal mixing term with φ_i^b the volume fraction of molecule i in the bulk phase. The second term in equation 6 accounts for the contact interactions between unequal segment of types A and B with respect to the reference state of a melt of pure molecules of type i, denoted by the asterisk. The last term in equation 6 is the modified Flory-Huggins mixing term which takes inter- and intramolecular correlations between bonds into account. The bond correlations that are included in the present theory account for the fact that a step in a certain direction cannot be blocked by one of the segments on bonds

in the same direction. In the limit that the lattice coordination number Z, equivalent to the number of different allowed bond directions, is large, the quotient in the logarithm is small and ln(1+x) can be approximated by x. The chemical potentials reduce to the classical FH ones, provided that there are no ring fragments in the molecules (then $N_{\sigma i} = N_i - 1$) of the system.

We have now specified the quantities of the partition function of equation 1 and proceed by maximising this function with respect to the number of molecules in a given conformation. To find the equilibrium set of conformations of the molecules in the system, under the constraint that all lattice layers are exactly filled [$\sum_i \varphi_i(z) = 1$], we introduce Lagrange multipliers $u''(z)$ to define the unconstrained function f:

$$
f = k_B T \ln\left(\Omega / \Omega^*\right) + k_B T \ln\left(Q^\sigma / Q^{\sigma*}\right) - \left(U^{int} - U^{int*}\right) +
$$
$$
\sum_i n_i\left(\mu_i - \mu_i^*\right) + \sum_z u''(z)\left[L - \sum_i \sum_c n_i^c N_i^c(z)\right]
$$
[7]

Now in the equilibrium distribution of the set of conformations the derivative $\partial f / \partial n_i^c$ equals zero for every conformation n_i^c. After some straightforward mathematics we find that the equilibrium number of molecules i in conformation c in the system can conveniently be expressed by:

$$
n_i^c = L C_i \lambda^{\alpha\beta} \prod_{s=1}^{N_i} G_i^c(z,s) \prod_{\sigma=1}^{N_{\sigma i}} \left[\lambda^{q_{\sigma i}^c} G_i^c(z,\sigma)\right]
$$
[8]

Where $G_i^c(z,s)$ is the free segment weighting factor for segment s of molecule i in layer z. The superscript c fixes the z coordinates for all the segments and the directions of the bonds. This free segment weighting factor is given by the Boltzmann factor of the potential energy field u(z) and, if segment s of molecule i is of type A, is given by:

$$
G_A(z) = \exp\left[-\frac{u'(z)}{k_B T} - \sum_B \chi_{AB}\left\langle\varphi_B(z) - \varphi_B^b\right\rangle - \frac{v_A e\Psi(z)}{k_B T}\right]
$$
[9]

where $u'(z) = u''(z) - u''^b$ so that the segment weighting factor is properly normalised to unity in the bulk. We return below to the consequences of the fact that $G_A(z) = 1$ in the bulk. The Lagrange parameter in the bulk u''^b reads:

$$
u''^b / k_B T = -1 - \sum_{\alpha''} \ln\left(1 - \varphi^{\alpha''b}\right) - \frac{1}{2}\sum_A \sum_B \chi_{AB}\varphi_A^b\varphi_B^b
$$
[10]

The u'(z) term in equation 9 does not depend on the segment type. It can be regarded as a hard core potential that takes excluded volume effects into account, since it arises from the Lagrange multipliers that satisfy the constraint that each layer of L lattice sites is exactly filled with L segments. The last factors in equation 8, $G_i^c(z,s)$, are the anisotropic bond weighting factors arising from the combinatorial factor Ω. They depend on the orientation (direction) of the bond σ. If this bond starts in layer z and ends in layer z' (having direction α'' in conformation c) it is given by:

$$G_i^c(z,\sigma) = G^{\alpha''}(z \mid z') = \frac{1 - \varphi^{\alpha''b}}{1 - \varphi^{\alpha''}(z \mid z')} \qquad [11]$$

Next, the normalisation constant C_i needs to be defined. For an open system where we use the grand canonical partition function, it is:

$$C_i = \frac{\varphi_i^b}{N_i} \qquad [12]$$

and in the case the number of molecules of type i in the system is fixed, *i.e.* a closed system where we use the canonical partition function, it is:

$$C_i = \frac{\theta_i}{N_i G_i(N_{i1})} \qquad [13]$$

In this equation $G_i(N_{i1}) = \sum_c \lambda^{\alpha\beta} \prod_s G_i^c(z,s) \prod_\sigma \left[\lambda^{q_{\sigma i}^c} G_i^c(z,\sigma)\right]$ is the total weighting factor per lattice site of all the molecules of type i in the system and $\theta_i = \sum_z \varphi_i(z) = \sum_c n_i^c N_i / L$ is the total amount of molecule i per lattice site. Below a more convenient expression for $G_i(N_{i1})$ will be given.

We have now outlined a way to calculate the partition function for a very large set of conformations that all the molecules in the system can assume. Before discussing the generation of the equilibrium set of conformations by the so-called propagator method we pause for an intermezzo.

Intermezzo

In connection with equation 9 we mentioned that the free segment weighting factor equals unity in the bulk. The consequence of this fact is that all molecules in the bulk are assumed to behave ideally (Flory-Huggins-like). This means that *e.g.* polymer molecules will have unperturbed Gaussian dimensions: $R_g \sim N_i^{0.5}$. As also can be seen from the equation for the chemical potentials, only the overall segment composition (the number of segments of a given type and the

number of bonds) is important in the bulk, the exact molecular architecture is not relevant to compute μ in our model. This implies that in our model the Helmholtz energy of the molecules in the water phase is, for a given overall composition, constant for a given set of isomers. Hence, differences in partition coefficients found within a group of isomers as predicted in the results section is solely due to the architecture dependent interactions of the additive within the membrane phase. There are several ways to correct for this imperfection of the theory. One could, *e.g.*, combine the theoretical prediction with experimental data for octanol-water partitioning of the molecule under consideration. Alternatively, one could improve the SCF modelling in this point. Other modelling techniques such as MD are also feasible for isolated molecules in an aqueous environment.

Introduction to Chain Propagation Schemes

Table 1. Collection of the direction α and the connecting direction α' combined with the relations of α to z'.

α (layer z)	α' (layer z')	z'
e	h	z$-$1
f	g	z
g	f	z
h	e	z+1

For flexible chains it is extremely difficult to generate all possible conformations without making approximations. In fact, the probability for a given chain to be in a specified conformation is usually not really an interesting quantity to know. More interesting are the density profiles $\{\varphi\}$ that result from the whole set of conformations $\{n_i^c\}$. It was shown before by others, and we will do this as well, that the partition function can also be written in terms of volume fraction profiles.[30] Then it is sufficient to calculate the weighted sum over all conformations. This weighted sum can be approximated by making the chains only locally self-avoiding (Markov approximation). In this scheme there are efficient methods available to find the density profiles. These methods are known as propagation schemes. In a Markov approximation the simultaneous generation and weighting of all conformations is carried out. We note that, if the statistical weight of a specific conformation needs to be computed, it is of course easily done with equation 8.

The chain propagation method will now be presented. First, the use of this method for linear chain molecules will be discussed. From that the extension to branched molecules will be made and finally more exotic molecules with complex structures, *i.e.* both with rigid and flexible parts will receive proper attention.

Propagator Method for Flexible Linear Chains

In the following we will present efficient methods to evaluate the statistical

weight of the full set of conformations of chains with limited bond flexibility. As stated above (cf. equation 4), to incorporate *gauche-trans* energy differences in the chain one only needs to consider three consecutive bonds at a time. This is achieved in the rotational isomeric state (RIS) scheme. In this scheme a bond can have four separate orientations within the lattice: $\alpha'' = e'', f'', g''$ or h'' (see figure 1 and table 1). In each orientation α'' we distinguish two directions α' and α. The direction e denotes the direction from one layer, z, to the previous one, $z - 1$; f and g denote the two separate directions within a layer and h denotes the direction from one layer, z, to the next one, $z + 1$ (cf. figure 1). The bonds *on* a segment are numbered σ_1 and σ_2 with the first bond, σ_1, pointing to the neighbouring segment with the lower ranking number and the second one, σ_2, to the neighbouring segment with a higher ranking number. Below we use the notation s_{12} where the '1' denotes σ_1 and the '2' σ_2. The volume fraction of a segment s of molecule i with σ_1 in direction α and σ_2 in direction β is the sum over all conformations c with segment s in layer z and the bonds in these directions of the number of molecules in such conformations. Defining $q_i^c\left(z, s_{12}^{\alpha\beta}\right)$

= 1 when the molecule in conformation c has segment s in layer z with its bonds 1,2 in the indicated directions α, β, respectively and zero otherwise we may write:

$$\sum_c \frac{q_i^c\left(z, s_{12}^{\alpha\beta}\right) n_i^c}{L} = \varphi_i\left(z, s_{12}^{\alpha\beta}\right) = C_i \lambda^{\alpha\beta} \frac{G_i\left(z, s_1^{\alpha\beta}\right) G_i\left(z, s_2^{\alpha\beta}\right)}{G_i(z, s)} \qquad [14]$$

In equation 14 the free segment weighting factor $G_i(z,s) = G_A(z)$ if segment s in molecule i is of type A which is defined as in equation 9. The subscripts 1 and 2 on the segment number s denote if either σ_1, or σ_2, or both σ_1 and σ_2 are connected to the rest of the chain. The end segment weighting factors $G_i(z, s_1^{\alpha\beta})$ and $G_i(z, s_2^{\alpha\beta})$ are defined recursively as follows:

$$G_i\left(z, s_1^{\alpha\beta}\right) = \sum_{\gamma'} \left[G_i\left(z', s_1'^{\gamma'\alpha'}\right) \lambda_{\sigma i}^{\gamma'' - \alpha'' - \beta''}\right] G^{\alpha''}(z \mid z') G_i(z, s) \quad s > 2 \qquad [15a]$$

$$G_i\left(z, s_2^{\alpha\beta}\right) = G_i(z, s) G^{\beta''}(z \mid z') \sum_{\gamma'} \left[\lambda_{\sigma i}^{\alpha'' - \beta'' - \gamma''} G_i\left(z', s_2'^{\beta'\gamma'}\right)\right] \quad s < N_i - 1 \qquad [15b]$$

The z' refers to z, $z - 1$ or $z + 1$, depending on the bond direction (see table 1), the prime on the segment number s indicates that the ranking number of a segment next to segment s defined by the chain architecture should be used. In a linear chain this is $s - 1$ for the preceding and $s + 1$ for the following segment. The $\lambda_{\sigma i}^{\alpha'' - \beta'' - \gamma''}$ in equation 15 is the same as $\lambda^{q_{\sigma i}}$ in equation 3 with the local bond conformation $q_{\sigma i}$ written specifically as the three consecutive bond

directions α''-β''-γ''. If γ' equals α'' the three bonds have a *trans* configuration and $\lambda_{\sigma i}^{\alpha''-\beta''-\gamma''}$ can be written as $\lambda^{t_{\sigma i}}$. Direct backfolding is excluded because if either γ'' or α'' equals β'', $\lambda_{\sigma i}^{\alpha''-\beta''-\gamma''} \equiv 0$. When $\alpha'' \neq \gamma''$ and $\alpha'' \neq \beta''$ and $\gamma'' \neq \beta''$ the configuration is *gauche*, and $\lambda_{\sigma i}^{\alpha''-\beta''-\gamma''}$ can be written as $\lambda^{g_{\sigma i}}$. Applying the relations of equation 15 recursively all end segment probabilities of the full chain can be calculated and from these the volume fraction profile follows using equation 14. The scheme is started by realising:

$$G_i\left(z, 2_1^{\alpha\beta}\right) = G_i(z',1)G^{\alpha''}(z \mid z')G_i(z,2)$$
$$G_i\left(z, [N_i - 1]_2^{\alpha\beta}\right) = G_i(z, N_i - 1)G^{\beta''}(z \mid z')G_i(z', N_i)$$

[16]

The overall statistical weight to find a chain in the system (cf. equation 13) can now be calculated as: $G_i\left(N_{i1}\right) = \sum_\alpha \sum_z G_i\left(z, N_{i1}^\alpha\right)$.

The fraction of maximum bond density for bond σ in molecule i, $\varphi_{\sigma i}^{\alpha''}(z \mid z')$, is calculated by the summation of the volume fractions over all appropriate orientations of the segments on both ends of the bond. The total fraction of maximum bond density as used in equation 5 and 11 is then calculated by summation over the contributions of all bonds of all molecules:

$$\varphi^{\alpha''}(z \mid z') = \sum_i \sum_\sigma \varphi_{\sigma i}^{\alpha''}(z \mid z')$$
$$= \frac{1}{2}\sum_i \left\{ \begin{array}{l} \sum_{s=2}^{N_i-1}\sum_{\beta''}\left[\varphi_i\left(z, s_{12}^{\alpha\beta}\right) + \varphi_i\left(z', s_{12}^{\alpha'\beta'}\right) + \varphi_i\left(z, s_{12}^{\beta\alpha}\right) + \varphi_i\left(z', s_{12}^{\beta'\alpha'}\right)\right] \\ +\varphi_i\left(z, 1_2^\alpha\right) + \varphi_i\left(z', 1_2^{\alpha'}\right) + \varphi_i\left(z, N_{i1}^\alpha\right) + \varphi_i\left(z', N_{i1}^{\alpha'}\right) \end{array} \right\}$$

[17]

In this way every bond is counted half from one end, the segment with the lower ranking number, and half from the other end, the segment with the higher ranking number. End segments have only one bond connected to them and therefore only one half of the densities of the end segments add to the sum. The volume fraction of the end segments of molecule i in layer z with its bond in direction α, $\varphi_i\left(z, 1_2^\alpha\right)$ and $\varphi_i\left(z, N_{i1}^\alpha\right)$, are calculated through:

$$\varphi_i\left(z, 1_2^\alpha\right) = C_i\lambda^{\alpha\beta}G_i\left(z, 1_2^\alpha\right) = C_i\lambda^{\alpha\beta}G_i\left(z, 1^\alpha\right)G^{\alpha''}(z|z')\sum_{\beta\neq\alpha}\frac{1}{3}G_i\left(z', 2_2^{\alpha\beta}\right)$$
$$\varphi_i\left(z, N_{i1}^\alpha\right) = C_i\lambda^{\alpha\beta}G_i\left(z, N_{i1}^\alpha\right) = C_i\lambda^{\alpha\beta}G_i\left(z, N_i^\alpha\right)G^{\alpha''}(z|z')\sum_{\beta\neq\alpha}\frac{1}{3}G_i\left(z', [N_i - 1]_1^{\beta\alpha}\right)$$

[18]

Propagator Method for Flexible Branched Chains

The propagator method for branched flexible chains is slightly more involved than for linear flexible ones. The main and only difference is at the branch point. There, not two end segment weighting factors are connected to each other, but three or more, as defined by the chain architecture:

$$\varphi_i\left(z, s_{123...}^{\alpha\beta\gamma...}\right) = C_i \lambda^{\alpha\beta} \frac{\prod_{\sigma'} G_i\left(z, s_{\sigma'}^{\alpha\beta\gamma...}\right)}{G_i(z, s)^{N_{\sigma si}-1}} \tag{19}$$

The three dots (...) indicate the possibility that more than three bonds are present on the segment s. The bonds connected to segments s of molecule i are numbered from $\sigma' = 1, 2, ..., N_{\sigma si}$, where $N_{\sigma si}$ is the number of bonds on segment s of molecule i. Again, as mentioned above, a mean field approximation is applied for bonds parallel to the lattice layers (directions f and g) and, hence, chiral effects will not be reproduced.[*]

The end segment weighting factors in equation 19 are obtained again by equation 15. Only the probability for the specific local bond conformation $\lambda^{q_{\sigma i}}$, just near the node, can no longer be expressed in *gauche* and *trans* conformations. The end segment weighting factor for a segment s next to a branch point is calculated by an equation which, in a sense, is a mix between equations 15 and 19. In fact one should realise that the unnormalised volume fraction of the branch point (cf. equation 19) is needed (several chains are connected), but that one chain branch is not yet connected; and this branch is now to be propagated (cf. equation 15). In other words, the bond, σ, between the branch point s' and the segment s next to the branch point remains to be 'made'. For this, the free segment weighting factor of the segment s is multiplied by the anisotropic weighting factor for bond σ and the sum of the probabilities of finding the branch point, s', with all bonds (σ', σ'' etc.) but one (*i.e.* the one, σ, that is to be made) connected, weighted by the probability of the local bond conformation of the newly 'made' bond. Mathematically this is expressed as:

---

[*] We mention that it is, in principle, possible to account for an unequal occupancy of the two directions f and g. In the case of systems with molecules without asymmetric segments and with a lining-up tendency (in-plane phase transition) only symmetry breaking in the f or g direction [e.g. with a different initial guess for the anisotropic weighting factors $G^{f''}(z|z)$ and $G^{g''}(z|z)$] will lead to results different from equal populations of f and g directions.

$$G_i\left(z,s_2^{\alpha\beta}\right) = G(z,s)G^{\beta''}(z\mid z') \sum_{q_{\sigma i}^{\alpha''-\beta''-\cdots}} \lambda^{q_{\sigma i}^{\alpha''-\beta''-\cdots}} \frac{\prod\limits_{\sigma'\neq\sigma} G_i\left(z',s_{\sigma'}^{\beta'\cdots}\right)}{G_i\left(z',s'\right)^{N_{\sigma s'i}-2}} \qquad [20]$$

The sum over $q_{\sigma i}^{\alpha''-\beta''-\cdots}$ is over all local bond conformations with bond σ in molecule i as the central bond that have orientation β'' for bond σ and orientation α'' for the other bond on segment s, away from the branch point (bond σ° figure 3).

Branched molecules contain more that two chain ends. Each branch in the chain has an end-unit which, at some point in the scheme, is the starting point of the propagator scheme. These cases are obviously handled by equations 16.

The fraction of maximum bond density, $\varphi^{\alpha''}(z\mid z')$, has, compared to equation 17, extra terms for every segment that has an extra bond connected to it and also an extra sum over these extra bonds. For instance, for a system with molecules with some segments that posses three bonds equation 17 becomes:

$$\varphi^{\alpha''}(z\mid z') = \tfrac{1}{2}\sum_i \left\{ \begin{array}{l} \sum\limits_s \left[\varphi_i\left(z,s_1^\alpha\right) + \varphi_i\left(z',s_1^{\alpha'}\right)\right] + \\[2mm] \sum\limits_{s'}\sum\limits_{\beta''}\left[\varphi_i\left(z,s_{12}'^{\alpha\beta}\right) + \varphi_i\left(z',s_{12}'^{\beta'\alpha'}\right) + \varphi_i\left(z,s_{12}'^{\beta\alpha}\right) + \varphi_i\left(z',s_{12}'^{\beta'\alpha'}\right)\right] \\[2mm] + \sum\limits_{s''}\sum\limits_{\beta''}\sum\limits_{\gamma''}\left[\begin{array}{l}\varphi_i\left(z,s_{123}''^{\alpha\beta\gamma}\right) + \varphi_i\left(z,s_{123}''^{\beta\alpha\gamma}\right) + \varphi_i\left(z,s_{123}''^{\gamma\beta\alpha}\right) + \\[1mm] \varphi_i\left(z',s_{123}''^{\alpha'\beta'\gamma'}\right) + \varphi_i\left(z',s_{123}''^{\beta'\alpha'\gamma'}\right) + \varphi_i\left(z',s_{123}''^{\gamma\beta'\alpha'}\right)\end{array}\right] \end{array} \right\}. \qquad [21]$$

Here s denotes the end segments, with one bond, s' refers to the ordinary segments having two bonds and s'' indicates the segments with three bonds connected (the branch points). For systems that have molecules that contain branch points with more than 3 bonds connected to it, equation 21 has to be replaced by an equation with even more terms.

Propagator Method for Rigid Structures

The propagation scheme for linear and branched molecules was already (in a less general way) described before.[17] We now turn our attention to the extensions of the propagator scheme for molecules that contain rigid fragments.

Although the use of a lattice made the implementation of the theory relatively simple for linear and branched chains, problems arise when the bond lengths or the bond angles are not all uniform. In these cases segments will not automatically be situated at the centre of a lattice layer. In rigid structures this

problem presents itself. Since the segment potential field is, in essence, a step profile we choose to let the segment feel the potential field in the layer where its centre resides. This approach was also followed by Gruen, and Szleifer and Ben-Shaul[12-14] when they determine the local potential for a chain conformation. The same applies to end-segment weighting factors: the end segment is assumed to be in the layer closest to its actual position. The contribution of a segment to the volume fraction profile, on the other hand, is subdivided over the layers that it spans.*

Bond angles are not always parallel to the tetrahedral bonds in the lattice either. We chose a similar solution to this problem as for the segmental coordinates: for every conformation of the structure each bond that has an angle with the lattice plane larger than 45° is considered to be in the direction h, every bond, which angle is smaller that −45° is assumed to be in the direction e and all other bonds are equally divided between the directions f and g (isotropic approximation within the layer).

When incorporating rigid (ring) structures, not only the directions of the bonds connecting the segments that are part of the structure itself have to be defined, but also the directional information for the bonds of the substituent chain parts, linking these flexible chains to the ring, needs to be given. In this way we prevent direct backfolding of the flexible chain onto the rigid fragment. In a Markov

---

* We have distributed the segment volume fraction over two neighbouring layers when the segment position was not exactly on a lattice site. To calculate similarly the end segment weighting factor for a given segment s, on a position not at the layer centre, as a combination of the end segment weighting factor for the two neighbouring layers, has its problems. If we ignore for a moment chain stiffness aspects and the anisotropic field, the end segment weighting factor is the sum of the weighting factors of all conformations of the piece of chain ending with the segment s on a non-lattice site position. The weight of one conformation is the product of the Boltzmann factors of its constituent segments (equation 8). The Boltzmann factor is the exponential of the local segment potential field (equation 9). So the end segment weighting factor is a sum (over all conformations) of the product (over all segments) of exponentials of the segment potential fields. The end segment weighting factor of a segment not on a lattice layer should be the sum (over all conformations) of the product (over all segments) of exponentials of the *averaged* segment potential fields. To do this, the whole recursive scheme should be run for every off-lattice position of a segment in a rigid structure for every conformation. This would destroy the efficiency of the propagator scheme completely. Therefore we have used, as a first approximation, the end segment weighting factor for the segment as if it were located at the centre of the layer closest to the centre of the segment (z_r).

approximation the number of conformations of a flexible chain part is strongly dependent on N [$\propto (Z-1)^N$]. For rigid structures the number of conformations that we include is only linear in the number of segments and therefore we proceed by calculating every conformation of the ring explicitly. What is done for the rigid fragments resembles the calculation of the statistical weight of all possible local conformations of a set of three consecutive bonds in the linear chain case, because any three consecutive segments in the ring determine all the other coordinates of the ring units.

The various rigid structures in a molecule are denoted with the letter k = 1, 2, ... which each include N_{ki} segments. The local conformations of structure k in molecule i are denoted as: q_{ki}. To generate the full set of conformations of a rigid structure k the following procedure is followed (for full details see the appendix) for *each* segment s_k, member of the structure k:

> The given relative coordinates of the structure are translated in such a way that segment s_k is in the origin of an arbitrary continuous Euclid 3D space with a Cartesian coordinate system with unit vectors of length ℓ. Next, two independent orthogonal vectors that describe the orientation of the structure are connected to s_k. Once these two vectors are known, six well-defined orientations of the structure are generated by rotation around the origin (*i.e.* the position of segment s_k). The z coordinates in the continuous system of all segments in the structure, which need not be integers, are then projected into the lattice system such that segment s_k is exactly at the centre of a given layer z.

Since the segments are not always positioned at the centre of a lattice layer we use r as the non-integer z-coordinate, normalised on the lattice spacing ℓ of the centre of such a segment. The layer that is closest to the centre of the segment at position r is denoted as z_r.

To distribute the volume fraction of a segment over several layers the fraction of the segment volume of a given segment s in layer z is defined depending on the conformation, q_{ki}, of the structure k of which s is a member. This fraction is denoted as $f^{q_{ki}}(z, s^\alpha)$, where the superscript α selects only those conformations that have an outgoing bond on segment s in direction α (cf. figure 3). This fraction is calculated as if a segment had a cubic shape. So, if segment s in structure k in conformation q_{ki} has a position r, the fraction of the segment in the layer closest to its centre, z_r, is: $f^{q_{ki}}(z_r, s) = 1 - |r - z_r|$. The fraction of the volume of the segment in the next neighbouring layer is then $|r - z_r|$. Since the segments have the size of the lattice spacing they cannot span more than one layer and consequently $f^{q_{ki}}(z, s^\alpha)$ has only non-zero values for the above-mentioned two

neighbouring layers.

The sum of $f^{q_{ki}}(z, s^\alpha)$ over all conformations q_{ki} and all directions α gives the number of structure conformations relevant for the volume fraction of a segment s that is a member of the structure k at layer z, $N_{q_{ki}}$. The symbols z and s are dropped because this number is independent of the layer number z and the segment number s of structure k:

$$N_{q_{ki}} = \sum_\alpha \sum_{q_{ki}} f^{q_{ki}}(z, s^\alpha) = 6N_{ki} \qquad [22]$$

Below we will need a normalising factor for the sum of these conformations, $\lambda^{\alpha k}$. This factor is, in essence, part of the local bond probability for the bond on segment s, $\lambda^{q_{\sigma i}}$. As a first approximation we take the energy for rotation around the bond σ_0, connecting a flexible chain to the structure k, constant for all local conformations (no *gauche-trans* energies for σ_0). With this ansatz the normalisation factor is the inverse of the number of local conformations of structure k corrected for the *a priori* chance to find the outgoing bonds in direction α: $\lambda^{\alpha k} = Z/(N_{q_{ki}})$, where, as before, Z represents the number of different bond directions in the lattice.

Now, to calculate the volume fraction, $\varphi_i(z, s_{1k}^\alpha)$, of this segment s in structure k, we have to sum over all conformations of the structure and select those that have a fraction of segment s in layer z with the outgoing bond on segment s in direction α. The weight of each conformation is determined by the product of the end segment weighting factors, $G_i(z_r', s_1'^{\beta''})$, of the segments s' belonging to the structure and the anisotropy weighting factors $G^{\sigma'}(z' \mid z'')$ for all the bonds, σ', in the structure, where z' and z'' are determined by the position and the direction of the bond in the specific conformation. As mentioned above, if the bond σ' makes an angle with the lattice plane that is larger than 45° $G^{\sigma'}(z' \mid z'')$ becomes equal to $G^{h''}(z'\mid z'')$, if the angle is between −45° and 45° it becomes $G^{f''}(z'\mid z'')$ but if the angle is smaller than −45° $G^{e''}(z'\mid z'')$ is substituted. There is a special case if a bond σ' in orientation f'' or g'' starts in layer z', but ends another layer, z''. This can easily happen due to a finite angle of the bond with the lattice plane. In this case the anisotropy weighting factor for that bond is averaged over the two layers. For example for σ' in direction f'': $G^{\sigma'}(z' \mid z'') = \frac{1}{2} G^{f''}(z' \mid z') + \frac{1}{2} G^{f''}(z'' \mid z'')$.

All told, the anticipated equation reads:

$$\varphi_i(z, s_{1k}^\alpha) = C_i \sum_{q_{ki}} \left[\lambda^{\alpha k} f^{q_{ki}}(z, s^\alpha) \prod_{s' \in k} G_i(z_r', s_1'^{\beta''}) \prod_{\sigma' \in k} G^{\sigma'}(z' \mid z'') \right]_{q_{ki}} \qquad [23]$$

The subindex $1k$ in s_{1k}^{α} denotes that segment s has a chain end connected to the outgoing bond 1 in direction α and that structure k is connected to this segment as well. The subindex q_{ki} at the square brackets infers that all positions and directions of bonds and the coordinates of the segments within the brackets are determined by the conformations q_{ki}. Obviously, if on a unit in a structure no flexible constituent is attached it suffices to include the free segment weighting factor for this unit instead of the end segment weighting factor in equation 23.

The propagation step to compute the end segment distribution of a segment s member of a flexible chain part next to the rigid structure is analogous to that of the segment next to a branch point. It involves the calculation of the unnormalised volume fraction of the segment s′ in the rigid structure k, onto which the flexible chain will be connected, with the outgoing bond in the direction that the propagator will follow. Let s″ denote the other segments in the structure to which the flexible chain is not connected, then the propagator step can be written as:

$$G_i(z,s_2^{\alpha\beta}) = G_i(z,s)G^{\beta}(z \mid z') \cdot$$

$$\sum_{q_{ki}} \left[\lambda^{q_{\sigma i}} f_r^{q_{ki}}\left(z',s'^{\beta}\right) G_i(z_r',s') \prod_{(s''\neq s')\in k} G_i\left(z_r'',s_1''^{\gamma'}\right) \prod_{\sigma'\in k} G^{\sigma'}(z'' \mid z''') \right]_{q_{ki}} \quad [24]$$

In equation 24 z″ denotes the positions of the segments s″ depending on the conformation q_{ki} and σ' denotes the bonds in the fragment k. The factor $f_r^{q_{ki}}\left(z',s'^{\beta}\right)$ equals unity if $z' = z_r$ for segments s′ with outgoing bond β in structure k in conformations q_{ki} and zero otherwise.

In previous sections we have shown how to calculate $\varphi^{\alpha''}(z \mid z')$ for linear and branched semi-flexible chains (cf. equations 17 and 21). The same quantity has to be computed in the case that rigid structures are part of the molecules in the system. In equation 21 three terms are present, accounting for segments with one, two and three bonds, respectively. Segments in a rigid structure often have two or three bonds connected to it. Consequently they contribute to the corresponding terms in equation 21. If there are segments present in the rigid fragment that have more than three bonds, equation 21 has to be expanded with extra terms analogous to the case of branch points where four chain parts come together.

Numerical Solution Method

In the above we showed how, even for complex shaped molecules, the density distributions follow from the segment potentials and the bond weighting

factors. Both the segment potentials and the bond weighting factors can be derived from the density distribution. The fixed point of the equations is known as the self-consistent-field solution and is found numerically. The mirror-like lattice boundary conditions ensure through Gauß' law the electroneutrality of the system. For more details we refer to the literature.[19,30] Once the equilibrium profiles are known we can evaluate the partition function from which all mechanical and thermodynamic quantities follow.

The Modelling of Bilayer Membranes

Lattice Boundary Conditions

The lattice is composed of M layers. The appropriate lattice boundary conditions for the modelling of lipid membranes are, as mentioned above, mirror-like. Rigid structures can have relative positions that span more than one lattice layer and hence can sample coordinates $z' < 0$ and $z' > M + 1$, while having at least one of their units between the layers $1 \leq z'' \leq M$. The potential felt at these coordinates z' follow from the reflecting boundary conditions. These are realised by putting the field $u(1 - z) = u(z)$ and $u(M + z) = u(M + 1 - z)$ for all z. For linear and branched chains only potentials at layers $z = 0$ and $z = M + 1$ are required for the calculations.

Definition of the Molecules in the System

To model bilayer membranes, various types of molecules are introduced into the system. The basic system contains, besides lipids and water, also salt ions. These molecules self-associate into bilayer aggregates. To these bilayers foreign molecules, called additives, are added. For the lipid (and the additive) a canonical partition function is evaluated which means that the normalising constant C_i is calculated through equation 13. For water and ions the environment is considered open, hence the approach is grand canonical and C_i follows from equation 12.

Numerical Aspects

The numerical procedure is started by an initial guess of the potential fields in such a way that the centre of the membrane is initiated at the mirror at $z = \frac{1}{2}$. Effectively this fixes the membrane structure in space. From these potentials the segment density profiles are calculated. On their turn the segment potential profiles are recomputed from the density profiles and compared with the initial guesses. If the input and output potential profiles differ, or when the constraint of fixed density ($\sum_A \varphi_A(z) = 1$ for every z) is not obeyed, the input potentials are adjusted. This procedure is iteratively repeated until the solution is self-

consistent. Typically the precision of the resulting potentials is better than seven significant digits.

Membrane Equilibrium Condition

Membranes calculated in this way have in general a finite surface tension. The equilibrium conditions of a free-standing membrane can be deduced from the thermodynamics of small systems as pioneered by Hill[31] and applied by Hall and Pethica.[32] From this theory it follows that the membrane surface tension must be balanced by entropic contributions originating from translational and undulational degrees of freedom. Typically membranes are very large and thus their translational entropy is relatively small. Furthermore, biological membranes are rather stiff, so that the out-of-plane bending can, to a good approximation, be neglected.[33-35] It should therefore be concluded that the surface tension of lipid bilayers must vanish. In the calculation scheme this is realised by changing the amount of lipid per unit surface area (θ_{lipid}) iteratively until $\gamma = 0$.

The Partition Coefficient

The partition coefficient K_i is defined as the ratio between the amount of additive i per amount of lipid in the membrane and the same for the additive in the water phase:

$$K_i(id) = \frac{\left[\dfrac{\varphi_i}{\varphi_{lipid}}\right]_{membrane}}{\left[\dfrac{\varphi_i}{\varphi_{water}}\right]_{water}} \qquad [25]$$

where the index on φ indicates the species and the index on the square brackets the phase involved. The extension 'id' refers to the ideal definition of K_i to be distinguished from the pragmatic definition to be explained below. Since there are several ways to express the concentration of a substance, the partition coefficient can be defined in as many ways. Our measurements are set up in such a way that the partition coefficients are calculated as the quotient of the weight percent of additive in the bulk and that in the membrane phase. We assume that the specific densities of water and lipid are equal, which allows us to calculate the partition coefficient on the basis of volume fractions.

Experimentally, the partition coefficient is measured from the change in concentration of the additive in the water phase upon addition of the lipids. Thus, essentially the partition coefficient of an additive with respect to the partition coefficient of water is calculated. Note that in this way $K_i(exp)$ can assume a negative value if water partitions more favourably into the membrane than the

additive does. In this case one would experimentally measure a concentration *in*crease of the additive upon addition of the lipids. However, for most investigated additives $K_i(exp)$ remains positive, but, for example, $K_i(exp)$ is typically negative for small ionic species that do not complex with the head groups of the lipids.

A problem in calculating the partition coefficient from our numerical density profiles is to define the extent of the membrane phase. The membrane boundary is hard to define as there is no sharp interface between bulk water and the membrane. We define the volume of the membrane as the excess volume of lipids in the system, neglecting thereby the swelling of the membrane by water or by other species. This approach is also used in the experimental set-up. The amount of an additive in the membrane is defined as the excess amount of additives in the system plus the bulk concentration times the volume of the membrane phase. Defining the excess amount with respect to the bulk solution per surface area of the membrane as θ^{exc} we arrive at the following expression for $K_i(th)$:

$$K_i(th) = \frac{\left(\theta_i^{exc} + \theta_{lipid}^{exc} \cdot \varphi_i^b\right)\varphi_{water}^b}{\theta_{lipid}^{exc} \cdot \varphi_i^b} \qquad [26]$$

In the following we will drop the extension 'th' as it will be clear that we have used equation 26 to compute this value.

Parameters

The theory discussed above is implemented in a computer program called GOLIATH. The membrane, for which the results in this paper were generated, consists of DMPC molecules as shown in figure 4. This membrane is embedded in a solution of monomeric isotropic molecules mimicking water, wherein monovalent salt ions, referred to as Na^+ and Cl^- are present. The volume fraction of salt in all calculations was fixed to $\varphi_s = 0.002$, which is comparable to a concentration of about 50 mM.

A set of linear alcohols (from butanol up to octanol), several branched alcohols with seven carbon atoms, para alkyl-substituted phenols and a few linear alkyldiols were used to compare the theoretical predictions of the model with experimental results obtained by van Lent at Bayer AG, Leverkusen, Germany. For all the other additives only theoretical predictions are available. We analyse the behaviour of a set of isomers containing two charged groups, one segment with a positive charge, denoted as N^+, and one with a negative charge, denoted as S^-, positioned on a alkyl chain of 16 C units connected to a

dimyristoylphosphatidylcholine (DMPC)

1-heptanol

2-ethyl-1-pentanol

4-isopropylphenol

"additive 1"

"additive 2"

1,3,5,7-tetrahydroxynaftalene
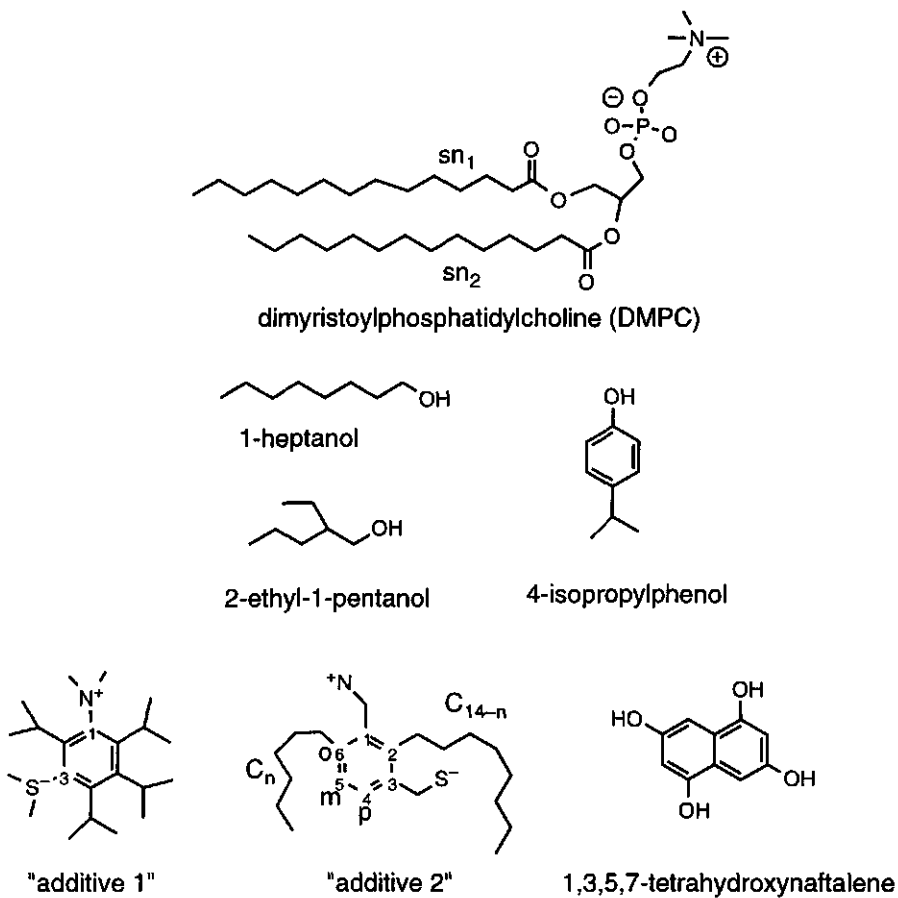
Figure 4. Some of the molecules considered in this study. DMPC makes up the lipid matrix of the membranes and the other molecules are additives.

benzene like ring with bond lengths equal to the lattice spacing ℓ (see figure 4 additive 1 and 2 for two examples). In addition, calculations are performed for tetrahydroxy naftalenes with the four hydroxyl groups substituted in various ways around the ring system (see also figure 4 for an example).

The system size was chosen large enough to prevent bilayer interaction (usually M = 40 layers). The lattice spacing, ℓ, was set to 0.3 nm. The energy difference between a *gauche* and a *trans* state (in a linear chain part) and between the *gauche-gauche* and the *trans-gauche* state (at a branch point) was set to 1 kT, irrespective of the segment types involved. Further segment properties were chosen as given in table 2. The relative dielectric constants of all components, except for the hydrocarbon (C), were taken as $\varepsilon_r = 80$, the value found for bulk water. For hydrocarbon the value $\varepsilon_r = 2$ was chosen,

Table 2. The parameters of the various segment types considered in this study.

		H_2O	C	O	S	PO	N	Na	Cl
ε_r		80	2	80	80	80	80	80	80
v		0.0	0.0	0.0	−1.0	−0.2	+1.0	+1.0	−1.0
χ	H_2O	0.0	1.6	0.0	−1.0	−1.0	−1.0	−1.0	−1.0
	C	1.6	0.0	1.6	2.6	2.6	2.6	2.6	2.6
	O	0.0	1.6	0.0	0.0	0.0	0.0	0.0	0.0
	S	−1.0	2.6	0.0	0.0	0.0	0.0	0.0	0.0
	PO	−1.0	2.6	0.0	0.0	0.0	0.0	0.0	0.0
	N	−1.0	2.6	0.0	0.0	0.0	0.0	0.0	0.0
	Na	−1.0	2.6	0.0	0.0	0.0	0.0	0.0	0.0
	Cl	−1.0	2.6	0.0	0.0	0.0	0.0	0.0	0.0

corresponding to the value found for bulk hydrocarbon fluids.

Regarding table 2, the contact energy between hydrocarbon and water, reflected in χ_{C,H_2O}, is the most critical parameter for membrane formation as it is the driving force for self-assembly. The value was chosen to be $\chi_{C,H_2O} = 1.6$, similar to that validated by earlier studies[17,19,20,23] and in accordance with other estimates found in the literature.[36] This value was found by comparing theoretical predictions of the critical micellar concentration (CMC) as a function of the surfactant tail length with experimental data.[18] We note that we did not introduce energetic differences between a C in a flexible chain and C in a ring. The χ-value for uncharged polar segments (O) with respect to hydrocarbon (C) was set equal to the water-hydrocarbon value. Charged components (N, Na, Cl, P, S and the O from the phosphate group) are assigned a favourable χ of −1 with water to mimic their tendency to be solvated by water and an unfavourable one with the hydrocarbons of +2.6 for the lack of solvation in hydrocarbon. The other interactions are not critical and their χ-values are kept zero for the sake of simplicity.

The phosphate group is modelled as being composed of five units. Since this group has a low intrinsic pK_a value of < 2.25 [37,38] it has a net negative charge of −1 at neutral pH. This charge is assumed to be equally distributed over all five segments. Thus, effectively we put a charge of −0.2 on each of these units.

Experimental Determination of the Partition Coefficient*

Materials

The additives (p.a.) were obtained from commercial sources and used as received. Lecithin was obtained from Lipoid KG.

Experimental Set-up

A known amount of additive (below the saturation concentration) is added to a (isotonic) buffer solution. The buffer solution contains 0.136 wt% potassium dihydrogenphosphate, 0.9 wt% sodium chloride and 0.68 wt% sodium hydroxide and is adjusted to pH = 7. From the additive solution 50 ml is filtrated through a 0.23 μm Millex-GS filter and added to a known amount of lecithin. This solution is equilibrated for 24 hours. The solutions are centrifuged for 90 minutes at 20,000 s^{-1} and 25 ^{0}C. Next, the samples were cooled with ice to 4 ^{0}C. At this temperature an additional centrifugation is carried out for 120 minutes and 20,000 s^{-1} to remove all the lipids from the solution. The concentration of the remaining additive in the supernatant has been determined by gas-chromatography or HPLC, dependent on the solute.

The amount of lipid was usually adjusted in such a way that the concentration of additive in the membrane was around 1 wt%.

The experimental partition coefficient is calculated by:

$$K(exp) = \frac{(c_0 - c_m)m_w}{c_0 m_L} \qquad [27]$$

where c_0 is the initial and c_m is the measured, final, concentration (in wt%) of additive in the supernatant. The parameters m_L and m_w describe the amounts in grams of lecithin and water, respectively. We note that, neglecting the density difference between water and lecithin, equation 27 coincides with the equation 26.

Results

In this section we will start by discussing the results for free standing liquid crystalline DMPC membranes. This information is of importance to interpret the behaviour of additives in the bilayers, which is the topic of the remainder of this section. The addition of three groups of relatively simple additives to these membranes will be analysed. For these additives the predicted partition coefficients are compared to experimental data. To illustrate the full strength of

---

* as conducted by B. van Lent and F. Ridder; Bayer AG; Leverkusen; Germany.

the theory, some theoretical results are presented for an extended group of isomeric, zwitterionic additives and some tetrahydroxy naftalenes. Not only the partition coefficient, but also the average positions of several segments within the membrane are probed and, from that, the orientations of the molecules are deduced. Positional and orientational information is used to interpret trends found in the partition coefficients for a series isomers.

Free Standing Liquid Crystalline DMPC Bilayers

The first lipid membranes that were investigated several years ago with a SCF analysis were rather primitive. The lipids were modelled as simple molecules with two long hydrophobic tails of 16 hydrocarbon segments and a hydrophilic head group of 5 structureless units. Isotropic, structureless monomers were used to model the water molecules.[17-19] The trends found for the tail region of the membrane are very similar to the results found in the modern calculations. The gel to liquid phase transition could be reproduced and details in the segment positions in the tail region have been predicted. The width of the distribution of tail segments increases the further the tail units are positioned away from the head group-tail boundary in the molecule. In line with this, it was found that the sn_1 tail is positioned a fraction of a nm deeper into the membrane core than the sn_2 tail (see figure 4). With respect to the head groups it was found that the maximum in their volume fraction profile was never higher than 0.3. This implied that even in the so-called head group region the most predominant segment-segment contact is the hydrocarbon-water one. We note that in all these calculations the membrane surface tension was kept to zero at all times, as should be the case for free standing bilayers.

In figure 5 we present state-of-the-art data of the structure of model membranes composed of DMPC molecules. The molecular structure of DMPC is more detailed, and the head group is bulkier as compared to the lipids considered earlier. Again, the total head group volume fraction profile never exceeds the value of 0.3 for equilibrium membranes and again the most frequent contacts in the head group region are the hydrocarbon-water ones. The head groups do not form a neatly packed layer shielding the hydrocarbon tails from the aqueous environment. Upon closer inspection, the head group is found lying predominantly flat on the membrane surface.[20,23] This result is in good correspondence with experiments[24] and other theories.[4,39,40] Generally, at moderate salt concentrations, the outer part of the head group, the choline moiety, has a wider distribution than the phosphate group which is closer to the head group-tail interface in the molecule. Moreover, it is found that, at high salt
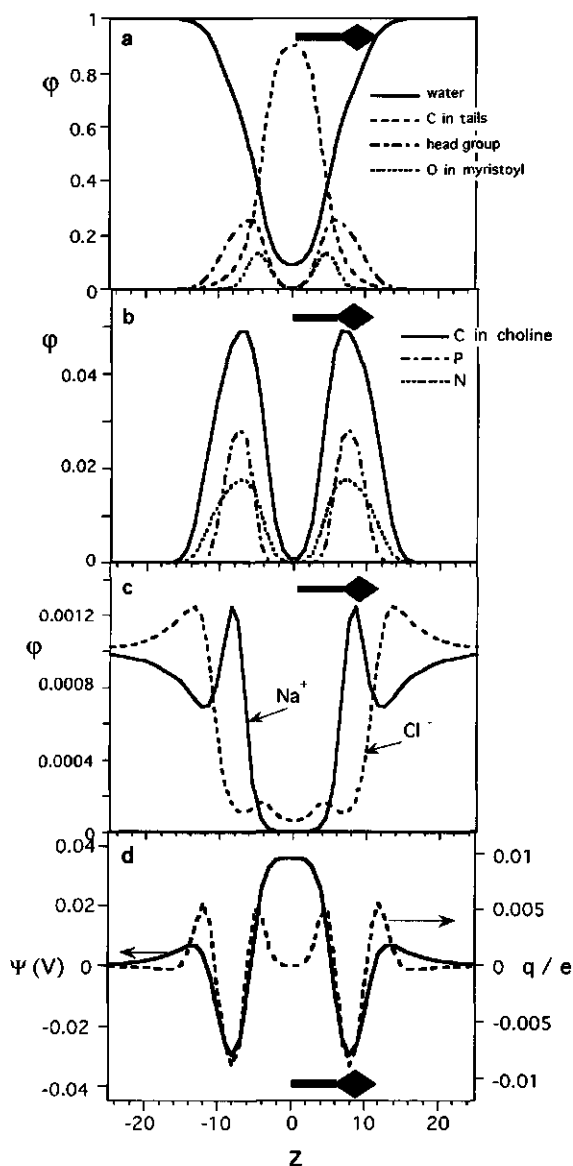
Figure 5. The volume fraction, φ, charge distribution, q, and electrostatic potential, Ψ, profiles through a cross section of an undoped free-standing liquid crystalline DMPC membrane. The director shown in every diagram is perpendicular to the membrane surface indicating the hydrophobic core with its tail and the head group area with its head. The volume fraction of salt solution in the bulk is 0.002, the relative dielectric constants, valences and χ-parameters are as in table 2. The centre of the membrane is at z = 0.
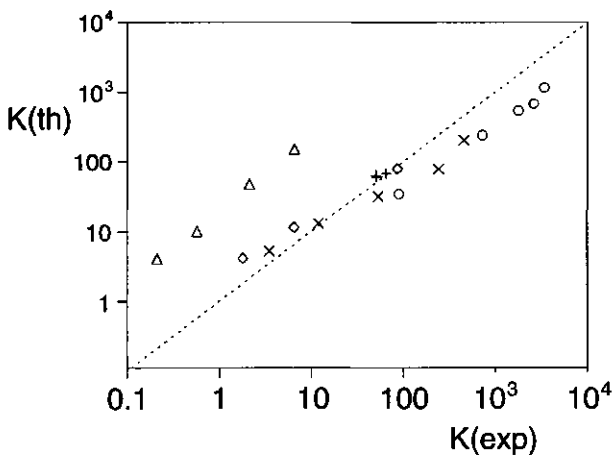
Figure 6. The comparison between the partition coefficient of our theory and the experiments, for several groups of alcohols. Crosses: linear 1-alkanols from low K-values to high: 1-butanol, 1-pentanol, 1-hexanol, 1-heptanol and 1-octanol. Plusses: branched alkanols with seven carbon atoms: 4-heptanol, 2,4-dimethyl-3-pentanol and 2-ethyl-1-pentanol; linear alkane diols are divided into two groups 1,2-alkanols shown as diamonds: 1,2-pentanediol, 1,2-hexanediol and 1,2-octanediol and 1,n-alcanediols shown as triangles: 1,5-pentanediol, 1,6-hexanediol, 1,7-heptanediol and 1,8-octanediol. The circles are several para-substituted phenols in order of increasing K value: phenol, 4-ethyl, 4-isopropyl, 4-propyl and 4-tert.butyl phenol. The additive concentration in the membrane was about 1.5 vol%. Salt concentration and other parameters were the same as in figure 5.

concentrations, the choline assumes a two-state distribution around the phosphate (not shown). This is interpreted in such a way that the head group has two preferred conformations, one with the choline closer to the hydrocarbon core of the membrane than the phosphate, and one with the choline closer to the water phase. This situation was also encountered in experiments.[24]

Due to the out of plane tilting of the head groups an electrostatic potential profile develops (see figure 5) with a negative value in the head group region on the position of the phosphate group and a positive value in the centre and on the outskirts of the membrane. Due to this profile, anions and cations distribute differently over the membrane phase. Both ions are expelled from the hydrophobic core due to the bad solvent quality of the hydrocarbon tails for ions, but anions are less expelled than cations. This can be part of the explanation for

the difference in permeability between anions and cations through DMPC membranes.

Partition Coefficients Of Alcohols

To compare our theory with experimental results the partition coefficients for linear and branched alcohols and those for phenols were computed according to equation 26 and measured according to the scheme explained in the experimental section, see equation 27. The results are shown in figure 6. There are two main features that are striking. The first is that nearly all points are on the diagonal, indicating that the theory predicts the correct value, and the second feature is the deviation of the 1,n-alkanediols from this diagonal (which indicates a problem).

The first observation is surprising since **no** parameter-fit of any kind was performed to match the experimental partition coefficients with the theoretical ones. Moreover, our parameter set is still quite crude. For instance, there is a known difference between CH_3 and CH_2 groups that is not accounted for in our approach. It can be concluded that apparently these differences are of minor importance in predicting the partition coefficients.

The systematic underestimation of the theoretical values for the 1,n-alkanediols as compared with the experimental ones is probably due to the fact that in the theory the molecules in homogeneous water solutions cannot develop any specific inter- or intramolecular interactions. This means that, for example, 1,2-pentanediol has the same activity as 1,5-pentanediol if these molecules have the same bulk concentration. In our model the chemical potentials of two isomers with the same bulk concentration within the same overall bulk composition are identical. This might not be the case in practice. There are probably specific interactions that causes one molecule to like the water phase better than the other one. An indication that this is playing a role is the difference in solubility between the two: 1,2-pentanediol has a solubility of 1.3 grams per litre, while the solubility for 1,5-pentanediol is 0.8 grams per litre. Therefore we conjecture that the predictive power of our model will increase when our theoretical predictions are combined with experimental data on *e.g.* octanol/water (O/W) partitioning. With information on O/W partitioning one can correct for activity effects of additives in the homogeneous water phase. See also the intermezzo above.

It appears that, for these relatively small molecules, the molecular architecture is not of main importance for the partitioning into the membranes as long as there are no specific intramolecular interactions in the water phase. Addition of a hydrophobic (hydrocarbon) segment or a hydrophilic (hydroxyl) segment has a considerable larger effect than branching or the incorporation of a para

substituted benzene ring. In a homologue series of molecules (*e.g.* n-alcohols) the addition of one C-segment increases the partition coefficient with a factor of approximately three. Clearly changing the architecture while keeping the overall composition constant, has only secondary effects on the membrane-water partition coefficient.

Comparing in figure 6 the theory with the experiments for the partition coefficient in some more detail, we notice that the theory underestimates K for the linear molecules more than for the branched ones. For instance, the plus signs in figure 6, representing branched alcohols with seven carbon atoms, are located on the diagonal, *i.e.* here the theory predicts the experimental K correctly, while the fourth cross (1-heptanol) is located below the diagonal indicating an under-estimation of K by the theory. Branched molecules have more CH_3 groups than linear ones. Apparently the experimental results suggest that CH_3 groups reduce the partition coefficient. This can be because their packing efficiency in the ordered tail region is less than optimal due to their larger volume compared to CH_2's. Another possible explanation for this effect is that $\chi_{CH_3\text{-water}} < \chi_{CH_2\text{-water}}$, *i.e.* that the CH_3 interaction with water is more favourable than the CH_2-water one. Most frequently, however, it is assumed that CH_3 groups are more hydrophobic. Neither the size of a CH_3 group nor the difference in solubility of CH_3 and CH_2 in water are accounted for in our theory. Therefore we do not see dramatic effects in our calculations for K on chain branching.

From figure 6 it can be observed that the benzene ring of phenols increases the partition coefficient, in contradistinction to branching. In first instance we would have expected that the effects of a ring on K would be the same as the introduction of branching, since it also introduces bonds that cannot line-up with the main director of the lipid tails. On the other hand, a ring introduces one extra bond which receives an extra weighting through the bond weighting factors $G^{\alpha''}(z|z')$. This extra bond most likely causes the relatively high affinity of rings for the membrane phase. Upon closer inspection we observe that both in the experiments and in our theory 4-isopropyl phenol partitioned to a greater extent in the membrane than the n-propylphenol. The opposite was observed by Davis *et al.* who measured the partitioning into gel state membranes.[41]

The volume fraction profiles of the additives of figure 6 do not contain many surprises. The carbon atoms pull several of the OH group of the alcohols into the centre of the membrane. However the density distribution of the OH still has a peak at the head group-tail boundary which is more pronounced for molecules with longer hydrophobic tail lengths. Here we do not show density profiles for these additives, instead we refer to previously published results on dodecanol
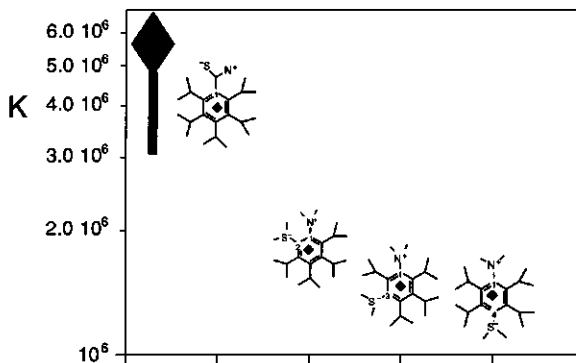
Figure 7. The partition coefficient of four, nearly symmetric, isomers of the class $C_{22}N^+S^-$ molecules, indicated by the diamond inside the structure, are presented. The director indicates the size and direction of the membrane (cf. figure5). The molecules as depicted represent schematically the average orientation of the additive in the membrane (see director) with the positive charge close to the phosphates in the head group region. The concentration of the additive in the membrane phase was about 0.1 vol%. Salt concentration and other parameters were as in figure 5.

which are typical.[42]

We have shown in our previous paper[42] that the sign of the charge on an additive can have large effects on its position in a DMPC membrane. This difference is due to the electrostatic potential profile across the membrane with a positive potential in the hydrophobic core and a negative one in the phosphate region followed by a positive one at the water side. In the following we turn our attention to zwitterionic additives.

Partition Coefficients, Orientations and Positions of Zwitterionic Isomers

Let us first discuss the most symmetric isomers of the $C_{22}N^+S^-$ molecules. In figure 7 the partition coefficient is shown, as well as the average orientation of the molecules in the membrane. The orientation of the membrane is represented by the director which was introduced in figure 5. All isomers have the positive charge on the rim of the hydrophobic core of the membrane close to the phosphate groups of the DMPC. Here the electrostatic potential is negative and the environment is relatively polar. When the two charges are spatially separated within the molecule, and thus when the local environment *in the molecule* is less

polar, the average position of the positive charge within the membrane is located relatively close to the centre of the membrane. The negative charge has less preference for a certain position in the membrane and is dragged into the membrane core if it is on the meta or para position on the ring with respect to the positive charge. This is not too surprising since the negative unit meets two forces: the membrane interior has a considerable positive electrostatic potential which attracts the negative charge whereas the hydrophobic nature of the core drives the negative charge to the water phase.

With the relative positions of the positive and the negative charges in the molecule we can explain the differences in partition coefficient between the four isomers. Note that this difference is as much as a factor 5, which is nearly equivalent to the effect that would be created by the addition of two carbon units (cf. figure 6). The fact that this difference is much larger than the differences in partition coefficient due to structural changes in the group of alcohols discussed above can have several causes. The first one is that the isomers of figure 7 are larger structural units than most flexible molecules shown in figure 6. Secondly, all molecules in figure 7 are zwitterions. These molecules feel the electrostatic potential profile which is strongly varying throughout the bilayer. The third reason is that in a rigid structure the variations in molecular architecture cannot easily be compensated. In flexible molecules rearrangements are possible and several compensation mechanisms can be envisaged. In rigid structures this is not possible and, especially in combination with the first point, substantial consequences of chain architecture for K should be expected. The deeper the negative charge is pulled to the hydrophobic core the lower the partition coefficient is.

To learn a bit more on the influence of the position of the positive and the negative charge in the molecule of this type of additives, we investigated the partitioning of the following subsets of the same type of isomers as considered in figure 7. The two charges are now on the one end of the hydrocarbon chain separated by two C segments. The ring is positioned in the hydrocarbon chain (para substituted) and its position is moved from close to the charges to the other end of the chain. Two different series are calculated: one with the positive charge and one with the negative charge at the end of the chain. In figure 8 the results are summarised. In this figure we also give the molecular structure of these isomers.

The difference in partition coefficient upon switching positions of the two charges within the molecule is striking. The cause of this difference can be found
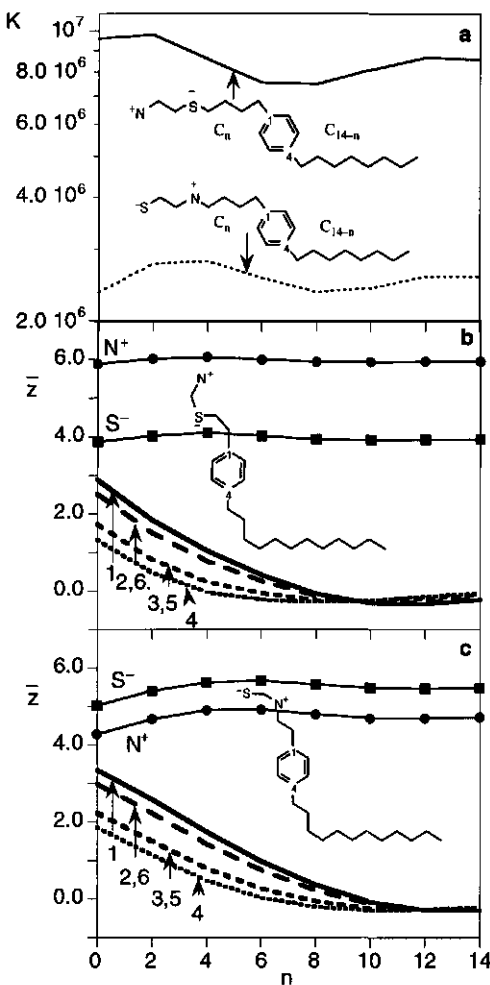
Figure 8. Diagram (a) shows the partition coefficient of two types of molecules (as indicated) which differ in the position of the two charges as a function of the position of the ring in the chain. Diagrams (b) and (c) give the average positions of the charged and the ring segments of a set of isomers as depicted. The position of the ring is moved from close to the charges (n = 0) to the end of the hydrocarbon chain (n = 14). The amount of additive, the salt concentration and all other parameters are the same as in figure 7.

by comparing figures 5 and 8. In figures 8b and c the average position $\bar{z}$ of the segments is plotted. These average positions are volume fraction-weighted average layers for the segment of type A involved and are calculated according to:

$$\bar{z}_A = \frac{\sum_{z=-H}^{H} z\varphi_A'(z)}{\sum_{z=-H}^{H} \varphi_A'(z)}, \qquad [28]$$

where H is the distance in layers between the two minima in the electrostatic potential profile due to the phosphates on both sides of the bilayer. H is typically about 20 layers and is a good measure for the (swollen) membrane thickness. By restricting the averaging in equation 28 from $-H$ to H we ensure that the whole membrane is taken into account and prevent that the bulk values do influence the average position too much. The volume fractions occurring in equation 28 are calculated from those conformations of the additive that had the positive segment restricted to one side (positive z values) of the membrane. The prime on φ therefore indicates that only a subset of all conformations is considered. If this restriction was not made, the average position would have been zero for all segments, since both sides of the symmetrical membrane contribute equally (see ref. 19 for details).

From the average positions shown for various units in the additive (cf. figure 8) it can be deduced that the partition coefficient is largely influenced by the position of the positive segment. This is at the same time the segment that has the largest gradient in the segment potential field at its average position in the membrane. The segment potential field can easily be deduced from figure 5c where the ions, being monomeric molecules, follow the segment potential essentially according to a Boltzmann factor. The positive ion, Na^+, has the largest gradient between layers 4 and 8. Consequently, the statistical weight of conformations of molecules with positively charged units in this region, is very sensitive to the actual position of these units. Hence, the partition coefficient of these molecules is strongly dependent on the average position of the positively charged segment.

We note that this reasoning can only apply when the amount of additive in the membrane is so small that it does not influence the overall segment potential profiles. Upon an increase of the additive concentration in the bilayers the charge profile and other segment profiles can change considerably and potentially influence the partition behaviour. These changes have then to be taken into account (see, e.g., ref. 42).

The consequence of changing the average positions of the ring segments in the membrane are shown figures 8b and 8c. A few noteworthy features can be observed. First of all, we recall that the ring is symmetrical with respect to the axis
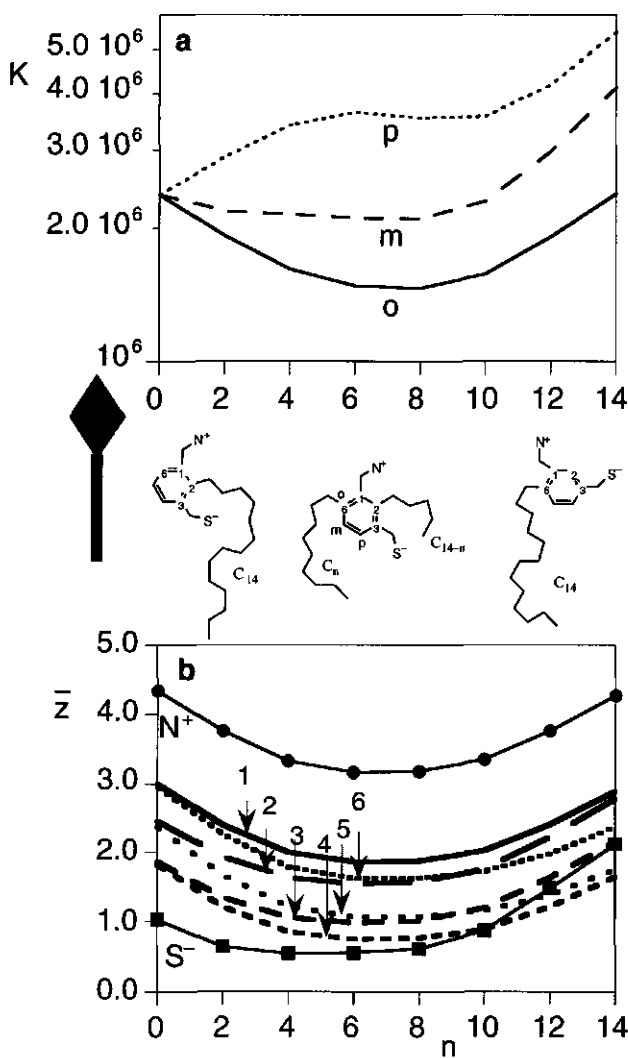
Figure 9. Diagram (a) shows the partition coefficient, K, for the ortho (o) meta (m) and para (p)-substituted alkyl chain (see text for details) as a function of the position of the ring in the alkyl chain. Diagram (b) shows the average position, $\overline{z}$, of the charged segments (N^+ and S^-) and the segments in the ring (1 to 6) of the ortho substituted ring as a function of the position of the ring in the alkyl chain. Parameters as in figure 7. The arrow indicates the director of the membrane (cf. figure 5) .

1-4. This symmetry is reflected in the fact that segments 2 and 6 and segments 3 and 5 have exactly the same average positions. We mention this as evidence for the correct implementation of the propagation method for these structures. Secondly, at small n, *i.e.* a long tail at the 4 position of the ring, the normal of the plane of the ring is parallel to the membrane surface. The difference in average positions (*i.e.* in the direction perpendicular to the membrane surface) of segments 2 and 3 is close to 1 layer, which is the length of the bond between them. Thirdly, the ring is pulled out more towards the water phase and the more so with its normal parallel to the membrane surface, when the positively charged unit is closer to it, *i.e.* not on the end of the chain (figure 8c) but rather around $n \approx 4$. Again two opposing forces are operative in determining the position of the ring: the positive charge is pulled electrostatically to the phosphate group whereas the apolar segments of the hydrocarbon tail prefer the membrane core and pull the ring to the centre. These forces cause the ring to orient itself perpendicular in the membrane. Fourth, when the ring is at the end of the hydrocarbon chain the average positions of the units in the ring become all zero. This does not necessarily mean that the ring is lying flat in the membrane centre. There are also conformations possible that pass the centre and then return. In fact this can be inferred from the $\bar{z}$ curve for ring-segment number 1 in figure 8b. The position of this unit drops below the ones for the other ring segments for $n > 9$. This can indicate two things: either the ring is for these molecules almost parallel to the membrane with a slight tilt, or several different conformations perpendicular to the membrane surface and their mirror images exist so that the averaged positions are zero. This last possibility is probably true.

The third subset of the same type of isomers as in figures 7 and 8 that was investigated was designed as follows (see figure 9). The positive and the negative unit are attached to the ring with one carbon segment as a spacer, on meta positions with respect to each other. This moiety was then moved along a chain of 14 carbon segments. One end of the chain ($14 - n$ segments long, with n between 0 and 14) is connected to the ring between the positive and the negative charge. The other end of the chain (n segments long) is connected to the ortho, meta or para position with respect to the positive charge. In figure 9 three pictorial examples of the ortho substituted chain are visualized. Their conformation represents (or at least mimics as well as possible) the theoretical prediction of the average conformation they assume in the membrane, cf. figure 9b. Note that the fat arrow is again the director of the membrane indicating with its tail the hydrophobic core and with its head the head-group region of the membrane.

At n = 0 the structures of all three (o, m and p) isomers are identical since in this case the o, m, or p chain is absent (see the left molecule in figure 9). For this molecule the orientation of the benzene ring is with the 1-6 bond almost parallel to the membrane surface. In this orientation the negative segment is forced towards the middle of the hydrophobic core of the membrane. The normal to the plane of the ring is almost parallel to the membrane surface. This can be concluded from the difference in average position between segments 1 and 3 in the ring which is almost 1.3 layers, while their distance within the ring is about 1.7 ℓ (ℓ is both the lattice spacing and the bond length in the ring). Upon increasing n, the number of carbon segments attached to the ortho position, the ring rotates around its normal and simultaneously the positive segment is drawn closer towards the membrane core. The occurrence of rotation can be inferred from the average positions of the ring segments: segments numbered 6 and 2 change z-positional order just like segment numbered 5 and 3 do.

The rotation of the ring can be explained through the tendency of hydrophobic parts of a molecule to accumulate close to the membrane centre. For small n, a hydrophobic tail is attached to the ring between the positive and negative charged units. As this ring tends not to lay flat on the membrane surface, it will pull at least one of the charges into the bilayer core. At n > 10 the ring segment number 2 has only a few carbon segments attached to it. Now both charges are located near the membrane surface. We mention that when the ring is about half-way in the chain, the average position of the positive charge is located closest towards the bilayer centre. Clearly the shape of the logarithm of the partition coefficient follows closely the average position of the positive segment. It first decreases upon increasing n and then for n > 10 it increases again to almost the same value as for n = 0.

The change in partition coefficient of the meta- and the para-substituted isomers upon changing n can be explained along similar lines. The difference with respect to the ortho case is that the chain with n segments is located further from the positive segment. Consequently, the hydrophobic segments are now moved from a chain close to the positive segment to a chain further away from it and therefore the surroundings of the positive charge within the molecule become more polar upon increasing n and its average position moves further away from the membrane core. This increases K for those molecules at large n.

Partition Coefficients, Orientations and Positions of Tetrahydroxy Naftalenes

All ring structures discussed up till now showed the tendency to orient themselves with the ring-normal parallel to the membrane surface. To find out if it

is possible to have rings oriented with the ring-normal perpendicular to the membrane surface, we have investigated the partitioning and orientation of some tetrahydroxy naftalenes. The orientation of the molecules is describe by the angle between two vectors in the molecule with the plane of the membrane. One vector is directed along the short axis of the molecule: from unit 4 to unit 1 and the other is parallel to the long axis of the molecule: from unit 7 to unit 2. The angle $[\angle(c1-c4)]$ is defined as the angle of the vector between the average positions of the units 4 and 1 and the plane of the membrane, and it is calculated through:

$$\cos \angle(C_1 - C_4) = \frac{\overline{z}_{C_1} - \overline{z}_{C_4}}{d(C_1 - C_4)} \qquad [29]$$

Here, C_1 and C_4 are the segments on position 1 and 4 in the structure respectively, and $d(C_1-C_4)$ is the distance between the positions in the ring normalised on the lattice spacing ℓ. The distance between, for instance, units 1 and 4 in a naphthalene structure is 2ℓ (we have chosen the bond lengths to be equal to the lattice spacing). The calculation of the average positions was performed by selecting only those conformations that had the hydroxyl group on the 1 or the 2 position on the ring to one side of the membrane.

We present three members of the tetrahydroxy naftalenes which differ with respect to the positions of the OH-groups over the rings. The first molecule that has been chosen has the OH's positioned two by two as far apart as possible: 2,3,6,7-tetrahydroxy naphthalene. In this case the molecule is, surprisingly, oriented spanning the membrane. Although the molecular dimensions are not really large enough to bring the hydroxyl groups in the head group area on both sides of the membrane, they are positioned close enough to the hydrocarbon-water interface so that they can make contact with the O segments of the myristoyl (of the DMPC) on both sides.

In the second molecule we consider the hydroxyls to be grouped to one side of the structure: 2,3,4,5-tetrahydroxy naphthalene. As compared with the previous example, the molecule rotated around the ring normal. The average position (cf. the pictorial of figure 10) of the hydroxyl groups is, on the average, closer to the centre of the head group region and, hence, the whole molecule moved more towards the water phase. The combined effect is that the partition coefficient is somewhat higher for this isomer as compared with 2,3,6,7-tetrahydroxy naphthalene.

For the third and last example considered, we have distributed the hydroxyl groups evenly over the molecule: 1,3,5,7-tetrahydroxy naphthalene (see figure
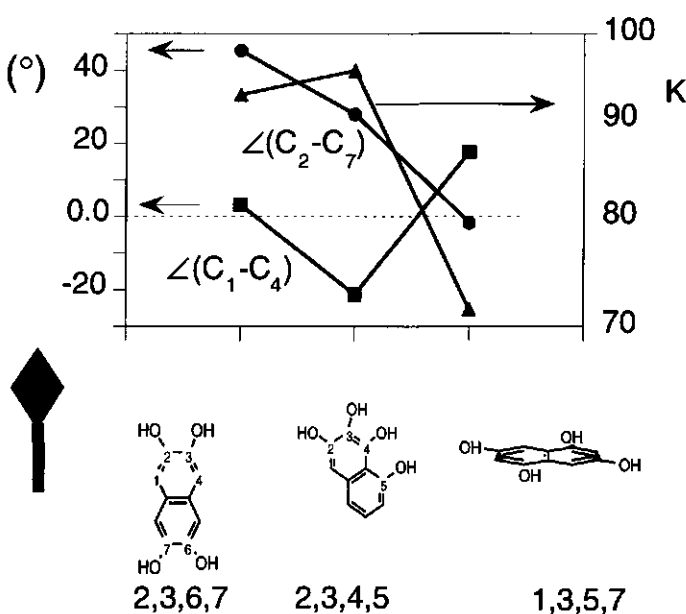
Figure 10. The partition coefficients and the average orientation of the rings of 2,3,6,7 tetrahydroxy naphthalene, 2,3,4,5-tetrahydroxy naphthalene and 1,3,5,7-tetrahydroxy naphthalene in a DMPC membrane. The average orientation is described by the two angles that the two molecular vectors make with the plane of the membrane. One vector pointing from unit 4 to 1 of the ring [$\angle(C_1-C_4)$] and the other pointing from unit 7 to 2 [$\angle(C_2-C_7)$] are given. The pictorials represent the approximate average orientation with respect to the membrane as indicated by the director (cf. figure 5). The conditions are the same as in figure 7.

10). Now the average orientation of the molecule is changed dramatically with respect to the previous two examples. The molecule now assumes an orientation with the plane of the rings almost parallel to the plane of the membrane. On average it is located just between the head group region and the hydrophobic core. Now, both the hydrocarbon segments and the hydroxyl groups have relatively more unfavourable contacts and the ring orientation is perpendicular to the direction of most molecules in the membrane. This all leads to a lower partition coefficient K than for the other two isomers mentioned above.

We note that, in spite of their considerable orientational changes, the differences in the partition coefficient between these molecules are still relatively small, in comparison with those of the zwitterionic isomers. Apparently, electrostatics dominate over non-electrostatic effects like the contact energies and the

anisotropic field. The segment potential profile of the hydrocarbon or hydroxyl groups is changing much more moderately than that of the charged segments. So the positions of these segment types have less influence of the partition coefficient. Electrostatics amplify the positional and orientational variability in these systems as with respect to K.

Further Discussion and Perspectives

With a limited and *a priori* parameter set it was shown to be possible to calculate with, an extended self-consistent-anisotropic-field theory, the partition coefficient of various alcohols to a surprisingly good match with experimental data. Although we did not account for all the molecular details yet, we have predicted noticeable differences in partition coefficients within a group of similar molecules (isomers). Therefore, these differences can not be assigned to aspects that were not yet included in the modelling. For instance, the difference between CH_2 and CH_3 groups for the partitioning of 4-isopropyl phenol and 4-n-propyl phenol is of minor importance since our prediction of this difference is essentially correct without incorporating any structural difference between these two groups of atoms. The conformational consequences of branching prevails over any chemical difference between the CH, CH_2 and CH_3 groups.

The theoretical results give specific detail on the cause of the difference in partition coefficient of related molecules. It is found that in the partitioning of zwitterionic isomers into DMPC bilayers the location of the positive charge in the membrane is of crucial importance for the magnitude of the partition coefficient. The actual position and orientation of rigid (benzene) rings can be influenced by the relative position and the nature of substituents. Of these, positive charges, positioned close to the ring in the molecule, have the stronger influence on the position and the orientation of the molecule in the membrane and on the partition coefficient. Negative charges exert their influence mainly on the partition coefficient but not so much on the orientation of mainly hydrophobic molecules. Their segment potential profile shows hardly any gradients between the positions of phosphate groups on both sides of the DMPC membrane, which is the region where these molecules accumulate. The segment potential profile for positive charges has a steep gradient on the edge of the hydrophobic core on the inside of the head group profile. Therefore, their position in this region does play a role.

Details concerning the positions and the orientations of the additives can give valuable information on the working mechanism of biologically active molecules like drugs or hormones. Information like this may help to design new molecules and to evolve existing ones to improve their performance.

In this chapter we considered extremely low amounts of additives in the membrane. In practical cases, however, a high loading is of obvious importance. Increasing the additive concentration in the bilayer can give rise to many interesting effects, which await further investigation. Such additive interaction can also be handled with the present approach.

Conclusions

We have demonstrated that it is possible to investigate the incorporation of complex foreign molecules in DMPC membranes with a detailed self-consistent-field model. With a limited and a priori parameter set we have successfully predicted the partition coefficient of a number of linear and branched alcohols. Our partition coefficient compares well with literature and own experimental data. The strength of our model is that predictions can be made for the partitioning of even more complex additives, such as molecules that contain rigid structures. We have studied a number of such molecules. We find that rigid structures serve as amplifiers in bringing about variation in partition coefficient in a series of isomers. Frequently the rigid rings orient mainly parallel to the tails in the lipid membrane. Only for specially designed additives we found the orientation of the ring to be parallel with the membrane surface. In general we have observed that positively charged units do not penetrate the hydrophobic region of the membrane as easily as negatively charged units do. This can be rationalised considering the electrostatic potential profile through the DMPC bilayer.

We have proven that it is possible to design isomeric molecules which have virtually the same partition coefficient in lipid bilayers but which differ greatly with respect to the position and orientation of the molecule in the membrane. The fact that these properties can be uncoupled is an interesting observation which in the future may help the design of new drugs.

Our model assumes that all molecules behave ideally in a homogeneous bulk phase. We therefore suggest that our calculations should be combined with experimental data for partitioning of additives in an octanol/water two-phase system or should be accompanied by, e.g., MD simulations of the molecule or a set of molecules in a homogeneous aqueous bulk phase.

Acknowledgements

Appendix

Generation and Definition of the Conformations q_{ki} of a Rigid Structure

In order to be able to sample all relevant conformations of an arbitrarily defined rigid structure, several considerations have to be taken into account.

First, to describe a conformation of such a structure, defined above in terms of the position of one segment and the directions of all the bonds (see theory section), only three parameters are needed: the position of one of the segments and the direction of two independent vectors chosen from the coordinates of the segments in the structure. It is necessary that these two vectors can be chosen independently of the way the coordinates of all the segments are presented with respect to each other.

It is also important that the full set of all possible conformations of a rigid structure is reduced similarly to that of flexible chains on a lattice: a finite set of conformations must be generated. The number of allowed conformations should be comparable to that which two connected segments in a flexible chain can have. In this way, the number of degrees of freedom of a rigid structure is the same as that of two segments connected by a bond which is, in essence, the smallest rigid structure. We chose here to use a simple cubic geometry to generate these conformations. In such a lattice it is logical to take six orientations per segment position. These orientations can be described simply by two independent vectors. We refer to those as $\bar{R}_{s_k}$ and $\bar{R}_{s_k\perp}$, the last one being perpendicular to the first one. The six conformations are defined as follows: conformation (1), with $\bar{R}_{s_k}$ in the z^+ direction, conformation (2), with $\bar{R}_{s_k\perp}$ in the z^+ direction, and conformation (3), with the outer product $\bar{R}_{s_k} \times \bar{R}_{s_k\perp}$ in the z^+ direction. The three other conformations are corresponding conformations parallel to the z^- direction. In figure 11 this procedure is visualised for a benzene-like molecule.

In the following we will first discuss how we determine the two determining vectors $\bar{R}_{s_k}$ and $\bar{R}_{s_k\perp}$ for and arbitrary rigid structure. The most descriptive vector for any (more or less flat) structure is the normal vector $\bar{N}_k$ of an average plane through the coordinates $\{\bar{r}_{s_k}\}$ of the segments that make up the structure. So, first this vector is calculated with the least square method according to Van Rootselaar.[43] To find the vector that describes the longest dimension of the structure, seen from the segment s_k, the position of which co-determines the conformation, first all coordinates $\{\bar{r}_{s_k}\}$ are translated over the vector of segment s_k ($\bar{r}_{s_k}$), $\Im \bar{r}_{s_k}$, so that segment s is in the origin:
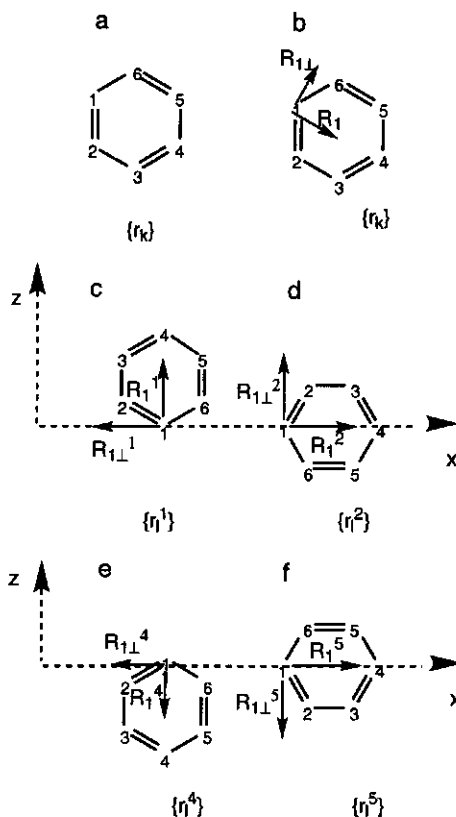
Figure 11. Part (a) shows the structure of a six-membered ring (e.g. benzene). Part (b) shows the molecule with the main vector attached to segment 1 (R_1) and its outer product with the normal of the pane of the molecule ($R_{1\perp}$). Part (c) to (f) show 4 of the 6 generated configurations with segment 1 as the segment in the origin. Only the conformations in the x-y plane are given. Configurations 3 and 6 are not shown since these would be represented by a line (all six segments lay in the x-y plane).

$$\left\{ \bar{r}_{s_k} \right\} \xrightarrow{\Im \bar{r}_{s_k}} \left\{ \bar{r}'_{s_k} \right\} \qquad\qquad [A1]$$

The normalised sum of all the positional vectors is the vector that describes the longest dimension of the structure seen from the segment, s:

$$\bar{R}'_{s_k} = \frac{\sum_{s'_k} \bar{r}_{s'_k}}{\left| \sum_{s'_k} \bar{r}_{s'_k} \right|} \qquad \text{[A2]}$$

where the sum over s'_k runs over all the segments in the structure. To find the second independent vector to describe the orientations orthogonal to this vector, simply the normalised outer product of this vector, $\bar{R}_{s_k}$, with the normal of the structure is taken:

$$\bar{R}'_{s_k\perp} = \frac{\bar{R}'_{s_k} \times \bar{N}_k}{\left| \bar{R}'_{s_k} \times \bar{N}_k \right|} \qquad \text{[A3]}$$

With these two vectors the orientation of the structure is determined uniquely with respect to segment s in the origin. To determine the six orientations in the simple cubic lattice the following procedure is followed.

The translated coordinates are rotated so that $\bar{R}^1_{s_k} \mathbin{/\!/} \bar{e}_z$ and $\bar{R}^1_{s_k\perp} \mathbin{/\!/} \bar{e}_x$. Where $\bar{e}_x$, $\bar{e}_y$ and $\bar{e}_z$ are the base vectors and $\Re \bar{e}_z, \angle\left(\bar{R}'_{s_k}, \bar{e}_x\right)$ is a rotation around vector $\bar{e}_z$) over the angle between $\bar{R}'_{s_k}$ and $\bar{e}_x$ ($\angle\left(\bar{R}'_{s_k}, \bar{e}_x\right)$):

$$\left\{ \bar{r}'_{s_k l}, \bar{R}'_{s_k}, \bar{R}'_{s_k\perp} \right\} \xrightarrow{\Re\bar{e}_z, \angle\left(\bar{R}'_{s_k}, \bar{e}_x\right), \Re\bar{e}_y, \angle\left(\bar{R}'_{s_k}, \bar{e}_z\right)} \left\{ \bar{r}^1_{s_k}, \bar{R}^1_{s_k}, \bar{R}^1_{s_k\perp} \right\} \qquad \text{[A4]}$$

The coordinates $\bar{r}^1_{s_k}$ obtained in this way are determining the first configuration. The second configuration is obtained by pivoting around the y axis so that $\bar{R}^2_{s_k} \mathbin{/\!/} \bar{e}_x$ and $\bar{R}^2_{s_k\perp} \mathbin{/\!/} \bar{e}_z$:

$$\left\{ \bar{r}^1_{s_k}, \bar{R}^1_{s_k}, \bar{R}^1_{s_k\perp} \right\} \xrightarrow{\Re\bar{e}_z, \angle\left(\bar{R}^1_{s_k\perp}, \bar{e}_x\right), \Re\bar{e}_y, \angle\left(\frac{\pi}{2}\right)} \left\{ \bar{r}^2_{s_k}, \bar{R}^2_k, \bar{R}^2_{k\perp} \right\} \qquad \text{[A5]}$$

The third configuration is generated by rotation around the x-axis over $\pi/2$:

$$\left\{ \bar{r}^2_{s_k}, \bar{R}^2_{s_k}, \bar{R}^2_{s_k\perp} \right\} \xrightarrow{\Re\bar{e}_x, \angle\left(\frac{\pi}{2}\right)} \left\{ \bar{r}^3_{s_k}, \bar{R}^3_{s_k}, \bar{R}^3_{s_k\perp} \right\} \qquad \text{[A6]}$$

The configurations 4 through 6 are found by rotation of the configurations 1 through 3 respectively around the x-axis over an angle π:

$$\left\{\bar{\zeta}_{s_k}^1, \bar{R}_{s_k}^1, \bar{R}_{s_k\perp}^1\right\} \xrightarrow{\Re\bar{e}_x, \angle(\pi)} \left\{\bar{\zeta}_{s_k}^4, \bar{R}_{s_k}^4, \bar{R}_{s_k\perp}^4\right\}$$

$$\left\{\bar{\zeta}_{s_k}^2, \bar{R}_{s_k}^2, \bar{R}_{s_k\perp}^2\right\} \xrightarrow{\Re\bar{e}_x, \angle(\pi)} \left\{\bar{\zeta}_{s_k}^5, \bar{R}_{s_k}^5, \bar{R}_{s_k\perp}^5\right\}. \qquad [A7]$$

$$\left\{\bar{\zeta}_{s_k}^3, \bar{R}_{s_k}^3, \bar{R}_{s_k\perp}^3\right\} \xrightarrow{\Re\bar{e}_x, \angle(\pi)} \left\{\bar{\zeta}_{s_k}^6, \bar{R}_{s_k}^6, \bar{R}_{s_k\perp}^6\right\}$$
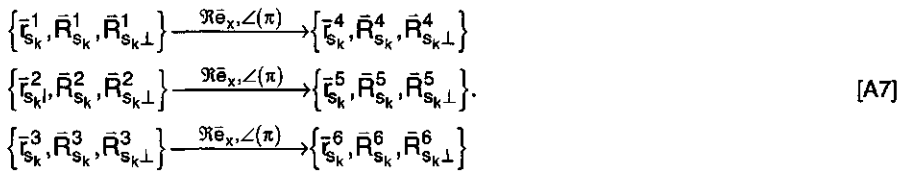
The procedure given by equations A1-A7 is done for each segment in the structure. In this way the number of generated conformations of a structure, $N_{q_{ki}} = 6N_{ki}M$, where N_{ki} is the number of units in structure k of molecule i. Every segment in the structure is the centre of six conformations per layer. So, the number of conformations with a segment s in layer z for rigid structure k, $q_{ki}(z,s)$, is six times the number of segments in the structure. For each conformation only the z coordinates of the members of the ring are relevant because the x-y information is typically averaged out in a mean field theory.

The Chemical Potential

The chemical potential as given by Leermakers *et al.*[19] and calculated as the derivative with respect to the number of molecules of type i in the system of the canonical partition function for the homogeneous phase reads:

$$\frac{\mu_i - \mu_i^*}{kT} = \ln\varphi_i^b - \frac{N_i}{2}\sum_A\sum_B\left(\varphi_{Ai}^* - \varphi_A^b\right)\chi_{AB}\left(\varphi_{Bi}^* - \varphi_B^b\right)$$
$$-\sum_{\alpha''}\left\{\left(N_i - N_i^{\alpha''b}\right)\ln\left(1-\varphi^{\alpha''b}\right) - \left(N_i - N_i^{\alpha''*}\right)\ln\left(1-\varphi_i^{\alpha''*}\right)\right\} \qquad [A8]$$

The last term in this equation can be rewritten by realising that, when a phase is homogeneous, the volume fraction of bonds in a certain direction α'', $\varphi^{\alpha''b}$ and $\varphi^{\alpha''*}$, are equal to the sum over all the bonds divided by the number of directions Z:

$$\varphi^{\alpha''b} = \frac{1}{Z}\sum_j\frac{N_{\sigma j}}{N_j}\varphi_j^b \quad \text{and} \quad \varphi^{\alpha''*} = \frac{N_{\sigma i}}{ZN_i}\varphi_i^*. \qquad [A9]$$

In this way the arguments of the logarithms are independent of α'' and can be taken through the summation. The sum over all direction of bonds of a molecule in the bulk, $N_i^{\alpha''b}$, is equal to all the bonds in the molecule, $N_{\sigma i}$. This also applies to $N_i^{\alpha''*}$. We now can execute the last summation of equation A8 leading to:

$$\sum_{\alpha''}\left\{\left(N_i - N_i^{\alpha''b}\right)\ln\left(1 - \varphi^{\alpha''b}\right) - \left(N_i - N_i^{\alpha''*}\right)\ln\left(1 - \varphi_i^{\alpha''*}\right)\right\} = \left[ZN_i - N_{\sigma i}\right]\ln\left[1 + \frac{N_{\sigma i} - N_i\sum_j\frac{N_{\sigma j}\varphi_j^b}{N_j}}{ZN_i - N_{\sigma i}}\right]$$

[A10]

which directly leads to the formula given in the main text for the chemical potentials:

$$\frac{\mu_i - \mu_i^\cdot}{kT} = \ln\varphi_i^b - \frac{N_i}{2}\sum_A\sum_B\left(\varphi_{Ai}^\cdot - \varphi_A^b\right)\chi_{AB}\left(\varphi_{Bi}^\cdot - \varphi_B^b\right) - \left[ZN_i - N_{\sigma i}\right]\ln\left[1 + \frac{N_{\sigma i} - N_i\sum_j\frac{N_{\sigma j}\varphi_j^b}{N_j}}{ZN_i - N_{\sigma i}}\right]$$

[6]

For systems that are composed of molecules without ring structures, so that it contains only linear and branched chains, the number of bonds, $N_{\sigma i}$, is $N_i - 1$. In this case equation 6 reduces to:

$$\frac{\mu_i - \mu_i^\cdot}{kT} = \ln\varphi_i^b - \frac{N_i}{2}\sum_A\sum_B\left(\varphi_{Ai}^\cdot - \varphi_A^b\right)\chi_{AB}\left(\varphi_{Bi}^\cdot - \varphi_B^b\right) - \left[(Z-1)N_i + 1\right]\ln\left(1 + \frac{-1 + N_i\sum_j\frac{\varphi_j^b}{N_j}}{(Z-1)N_i + 1}\right)$$

[A11]

Equation A11 has been published before.[42] For large Z the approximation $\ln(1+x) \approx x$ can be applied and equation A11 reduces to the usual Flory Huggins expression for μ_i:

$$\frac{\mu_i - \mu_i^\cdot}{kT} = \ln\varphi_i^b - \frac{N_i}{2}\sum_A\sum_B\left(\varphi_{Ai}^\cdot - \varphi_A^b\right)\chi_{AB}\left(\varphi_{Bi}^\cdot - \varphi_B^b\right) + 1 - N_i\sum_j\frac{\varphi_j^b}{N_j}.$$

[A12]

Literature

1.   Singer, J.S. and G.L. Nicholson, Science, 1972 **175** p. 720-731.
2.   Yeagle, P., ed. *The Structure of Biological Membranes.* 1992, CRC Press: Boca Raton.
3.   Van der Ploeg, P. and H.J.C. Berendsen, J. Chem. Phys., 1982 **76**(6) p. 3271-3276.
4.   Van der Ploeg, P. and H.J.C. Berendsen, Molecular Physics, 1983 **49**(1) p. 233-248.
5.   Berendsen, H.J.C., B. Egberts, S.-J. Marrink and P. Ahlström, in *Membrane Proteins: Structures, Interactions and Models,* Pullman, A., Editor. 1992, Kluwer Academic Publishers: Dordrecht p. 457-470.
6.   Egberts, E. and H.J.C. Berendsen, J. Chem. Phys., 1988 **89**(6) p. 3718-3732.
7.   Sperotto, M.M. and O.G. Mouritsen, Eur. Biophys. J., 1990 pre-print.
8.   Mouritsen, O.G., K. Jorgensen, J.H. Ipsen, M.J. Zuckermann and L. Cruzeiro-Hansson, Physica Scripta, 1990 **T33** p. 42-51.
9.   Ipsen, J.H., K. Jorgensen and O.G. Mouritsen, Biophys. J., 1990 **58** p. 1099-1107.
10.   Marqusee, J.A. and K.A. Dill, J. Chem. Phys., 1986 **85**(1) p. 434-444.
11.   Gruen, D.W.R., J. Phys. Chem., 1985 **89** p. 146.
12.   Gruen, D.W.R. and E.H.B. de Lacey, in *Surfactants in Solution,* Mittal, K.L. and Lindman, B., Editor. 1984, Plenum: New York p. 279-306.
13.   Szleifer, I., A. Ben-Shaul and W.M. Gelbart, J. Chem. Phys., 1985 **83**(7) p. 3612-3620.
14.   Ben-Shaul, A., I. Szleifer and W.M. Gelbart, J. Chem. Phys., 1985 **83**(7) p. 3597-3611.
15.   Gruen, D.W.R. and D.A. Haydon, Pure & Appl. Chem., 1980 **52** p. 1229-1240.
16.   Marčelja, S., Biochim. Biophys. Acta, 1974 **367** p. 165-176.
17.   Leermakers, F.A.M. and J.M.H.M. Scheutjens, J. Chem. Phys., 1988 **89** p. 3264-3274.
18.   Leermakers, F.A.M. and J.M.H.M. Scheutjens, J. Chem. Phys., 1989 **93** p. 7417-7426.
19.   Leermakers, F.A.M. and J.M.H.M. Scheutjens, J. Chem. Phys., 1988 **89** p. 6912-6924.
20.   Meijer, L.A., F.A.M. Leermakers and A. Nelson, Langmuir, 1994 **10** p. 1199-1206.
21.   Nelson, A., J. Chem Soc. Faraday Trans., 1993 **89** p. 2799-2805.

22. Nelson, A., J. Chem. Soc., Faraday Trans., 1993 **89** p. 3081-3090.
23. Meijer, L.A., F.A.M. Leermakers and J. Lyklema, Recl. Trav. Chim. Pays-Bas, 1994 **113** p. 167-175.
24. Hauser, H., I. Pasher, R.H. Pearson and Sundell, Biochim. Biophys. Acta, 1981 **650** p. 21-51.
25. Björling, M., *Polymers at Interfaces.* 1992, PhD thesis University of Lund, Sweden.
26. Barneveld, P.A., D.E. Hesselink, F.A.M. Leermakers, J. Lyklema and J.M.H.M. Scheutjens, Langmuir, 1994 **10** p. 1084-92.
27. Böhmer, M.R., O.A. Evers and J.M.H.M. Scheutjens, Macromolecules, 1990 **23** p. 2288-2301.
28. Di Marzio, E.A., J. Chem. Phys., 1977 **66** p. 1160.
29. Di Marzio, E.A., J. Chem. Phys., 1961 **35** p. 658.
30. Evers, O.A., J.M.H.M. Scheutjens and G.J. Fleer, Macromolecules, 1990 **23** p. 5221-5233.
31. Hill, T.L., *Thermodynamics of Small Systems.* Vol. 1 and 2. 1963, 1964, New York: Benjamin.
32. Hall, D.G. and B.A. Pethica, in *Nonionic Surfactants,* Schick, M.J., Editor. 1976, Marcel Dekker: New York p. 516-557.
33. De Gennes, P.-G. and C. Taupin, J. Phys. Chem., 1982 **86**(13) p. 2294-2304.
34. Rand, R.P. and V.A. Parsegian, in *The Structure of Biological Membranes,* Yeagle, P., Editor. 1992, CRC Press: Boca Raton p. 251-306.
35. Helfrich, W., Naturforsch., 1978 **33a** p. 305.
36. Tanford, C., *The Hydrophobic Effect: Formation of Micelles and Biological Membranes.* 1973, New York: John Wiley.
37. Tocanne, S.-F. and J. Teissié, Biochim. Biophys. Acta., 1990 **1031** p. 111-142.
38. Gutman, M. and E. Nachliel, Biochim. Biophys. Acta., 1990 **1015** p. 391-414.
39. Granfeldt, M.K. and S.J. Miklavic, J. Phys. Chem., 1991 **95** p. 6351-6360.
40. Stigter, D. and K.A. Dill, Langmuir, 1988 **4** p. 200-209.
41. Davis, S.S., M.J. James and N.H. Anderson, Faraday Discuss. Chem. Soc., 1986 **81** p. 1-15.
42. Meijer, L.A., F.A.M. Leermakers and J. Lyklema, Chapter 3, 1994 ibid.
43. Van Rootselaar, B., *Lineaire Algebra.* 1971, Groningen (NL): Wolters-Noordhoff N.V.

Chapter 5

Discussion and Outlook

At the final stages of this research project it is time to evaluate the present model. Despite of the promising results presented in this thesis there are several aspects of our theory that still need further attention.

We have modelled the self-assembly of lipids from an aqueous solution into bilayer membranes. These membranes float in a sea of salty water, and the nature of the membrane-water interface depend strongly on the properties of the water. Also the water-uptake is critially dependent on the watermodel used. In our theory the water molecules are modelled as isotropic monomers with isotropic interactions. This is a very crude model indeed. Improvements on this approach are possible along the lines pioneered by Besseling,[1,2] who developed a lattice gas model for water in which, in a quasi-chemical approximation, water molecules have orientation dependent interactions, of which the attractive ones are comparable to H-bonds. All other water-water contacts are slightly repulsive. In this model many known water properties are reproduced, e.g. the isobaric density maximum. This density maximum was related to the well-known hydrophobic effect which could be explained without the need of so-called iceberg structures around apolar solutes. The coupling of Besseling's water model to the modelling of lipid self-association is possible.

Another flaw in our theory is the neglection of the compressibility of the solution. All lattice sites are filled with a segment representing either an atom or a group of atoms. This implies that the pressure is not defined and consequently the volume is fixed. This limitation can be lifted by the introduction of a segment type that can be regarded as a vacancy into the theory. Besseling showed[3] that, in this way, the pressure can be calculated and, consequently, investigations of the pressure dependence of gel-liquid phase transition in membranes becomes within reach.

Preliminary work has been done by Uitdehaag to improve on both aforementioned problems.[4] He used a rather simple association model for water and introduced vacancies in the system. He applied this model to study the ion permeability of membranes. He predicted the variability of the ion permeability as a function of the amount of alcohol in the membrane. It was proved that, from a

homologue series of alcohols, butanol was the most effective in disturbing the membrane structure. This fact correlated with experimental data.

Another shortcoming in the present model is that the aspect ratio of a segment in a molecule is equal to unity. In many cases segments represent an atom group with a specific shape. The dimension of say a CH_2 group in the C-C bond direction is considerably less than that in the C-H direction. This problem can be dealt with by introducing lattice refinements along the lines as pioneered by Björling.[5] He allowed isotropic segments to exceed the lattice spacing. The extension of this scheme to asymmetrical shapes is a refinement that, in principle, can follow the same line of reasoning as used in chapter four of this thesis where we discuss rigid structures.

In calculations claiming biological relevance, pH-dependent charges should be included, especially when the pH of the system is close to the pK_A of the groups considered. This extension can easily be incorporated as shown by Israëls.[6] Along the same lines specific complexation interactions may be introduced which can give some insight in passive, carrier-mediated, transport mechanism through membranes.

An extension that has not yet been pioneered, but might be of some importance for the behaviour of molecules with large conjugated ring structures in electrostatic field gradients, is to include the polarisability of these molecules in the modelling. The effect of the polarisability of additives in a membrane is that the disability of a rigid structure to adjust its conformation is partly compensated by its ability to shift the charge distribution in the molecule. As an effect the free energy of the molecule in an electrostatic potential gradient will be reduced, which will cause the partition coefficient to increase.

The mean field character of the theory can give rise to considerable deviations from experiments. A typical example is the approximation that molecules feel a homogeneous segment potential $u^b = 0$ in the bulk. As a consequence, e.g., a polymer chain with length N will always behave ideal, irrespective of the solvent quality (the radius of gyration must scale as $\sqrt{N}$). This behaviour is typical for a Flory-Huggins-like theory. In this thesis we have examined subtle effects of additives in membrane systems. In particular we looked at the membrane-water partition coefficient of additives. This quantity is a measure for the free energy change involved with the transport of an additive from the water to the membrane phase. For this, not only the free energy of the molecules in the membrane, but also that in the homogeneous water phase needs to be known accurately. This last quantity is given by the chemical potentials. The expressions for the chemical potentials are those of the Flory-Huggins theory that depend one several quantities of which the concentrations

and interactions of all the components in the system are the most important. Unfortunately, these equations do not depend on the molecular architecture of the chains; isomers with different architecture have the same chemical potential. This problem can partly be relieved by studying the test molecule in an isotropic medium such as done recently by Van der Linden.[7] This reference state problem is most likely the cause of some noticeable deviation between predicted and calculated partition coefficient as discussed in chapter 4.

Finally, the theory as it is discussed in this thesis, can "only" probe equilibrium properties. However, most biological processes are (although close to equilibrium) not fully in equilibrium. Through off-equilibrium density functional theory Fraaije showed that it is possible to calculate dynamic properties in a mean field framework.[8] His results are promising and deserve more attention. It is possible to apply this method to the membrane system and study, e.g., the diffusion of ions through the lipid bilayer.

In the above we have shown that the present theory has still some shortcomings. Several of these flaws do not have a principle nature and can be removed. However, some problems, especially those related to the mean field character of the theory, are bound to stay. Nevertheless, we believe that the predictive power of the theory to model aspects of biomembranes will increase as more details are included.

1.   Besseling, N.A.M. and J. Lyklema, J. Phys. Chem., 1994 in press.
2.   Besseling, N.A.M. and J.M.H.M. Scheutjens, J. Phys. Chem., 1994 in press.
3.   Besseling, N.A.M., *Statistical Thermodynamics of Fluids with Orientation-Dependent Interactions. Applications to Water in Homogeneous and Heterogeneous Systems.* 1993, PhD thesis Wageningen Agricultural University.
4.   Uitdehaag, J., *Alkoholen en Alkanen in Membranen.* 1994, MSc thesis Wageningen Agricultural University.
5.   Björling, M., *Polymers at Interfaces.* 1992, PhD thesis University of Lund, Sweden.
6.   Israëls, R., F.A.M. Leermakers and G.J. Fleer, Macromolecules, 1994 **27** p. 3087-3093.
7.   Van der Linden, C.C., personal communications
8.   Fraaije, H., J. Chem. Phys., 1993 **99**(11) p. 9202-9212.

Summary

The aim of this study was to make accurate predictions on the interaction of biologically relevant molecules with lipid bilayer membranes. We emphasised on the partitioning of these molecules between the membrane phase, and the aqueous phase quantified by the partition coefficient. To make detailed predictions a theory had to be set up along the lines of the self-consistent-field theory developed by Scheutjens and Fleer and extended by Evers, Leermakers, Van Lent, Böhmer, Barneveld, Israëls, Wijmans, Van der Linden, and others for (chain) molecules in inhomogeneous systems.

As a first step towards this goal we have investigated bare membranes in chapter 1. A membrane of dimyristoylphosphatidylcholine (DMPC) has been used as a model for biological membranes, existing in plant and animals, in which this molecule is a major component. For comparison, membranes consisting of the anionic dimyristoylphosphatidylserine (DMPS) were also modelled. It was found that the zwitterionic phosphatidylcholine (PC) head group was laying on average flat on the membrane surface. This result is in line with experiments and in accordance with other theoretical calculations. At high salt concentrations however, two preferred conformations had to be distinguished, both about equally populated, one with the choline moiety closer to the water phase than the phosphate moiety and one the other way around. Due to the out of plane tilting of the head group, an electrostatic potential profile develops. The electrostatic potential is positive in the membrane centre and on the membrane surface, but negative in the middle of the head group region at the average position of the phosphate groups.

The ionic head groups of DMPS are found tilted towards the aqueous solution. Counterions interpenetrate the head group region and compensate the charge to a large extent even at low ionic strength. At high salt concentrations ions are depleted from the head group space but, due to asymmetric depletion of anions and cations, charge compensation is still achieved.

The variability of the PC head group orientation was investigated theoretically by attaching a hydrophilic chain to the choline moiety of DMPC. Varying the chain length had two effects: First, due to the interchain steric repulsion the head group area increased and therefore the dimension of the hydrophobic core decreased

which eventually destabilised the membranes. Second, the head group orientation changed non-monotonously. Short chains attached to the choline moiety 'drag' it towards the water phase, while longer chains attached to it do not affect the average orientation of the dipole, which is parallel to the membrane surface. This is caused by the fact that, for longer hydrophilic chains, the most bulky part of the head group is located further from the hydrophobic core in the centre of the polymeric coil. This relaxes the packing constraints at the position of the choline. Hence the phosphate moieties and the electrostatics forces, that favour a flat conformation, meet less opposition.

In the second chapter we concentrate on the interplay of the electrostatic potential profile across the membrane and the valence of the ions present in solution. From the calculations it can be concluded that the electrostatic interactions can explain the accumulation of charges in the head group area without introduction of specific chemical interactions between e.g. a divalent ion like calcium and the phosphate group.

An important issue in the modelling of non-interacting, free-standing membranes is the proof that the modelled bilayers are thermodynamically the most stable structures. From thermodynamic arguments, it can be shown that the surface tension of these layers should vanish. This is a necessary, but not sufficient condition. For isolated, free-standing bilayers to be stable, the membranes should be mutually repulsive. The interaction between bilayers is the topic of chapter 3. In this chapter a thermodynamic derivation is presented of the various ways the interaction curve can be calculated from the self-consistent-anisotropic-field (SCAF) theory. The results show that three force-distance regimes can be distinguished for a DMPC bilayer in a moderate salt concentration: two repulsive regimes, one of electrostatic and one of steric origin flank an attractive one that was shown to be of entropic origin. The entropic attraction is caused by an increase in the number of head group conformations. At large separation the head groups are oriented mostly parallel to the membrane surface. Upon closer approach of two bilayers the head group conformation is allowed to change. The head group can now cross the gap between the bilayers without an electrostatic penalty. As a function of the screening of the electrostatic interactions we observe various changes in the interaction curves. At high salt concentration both the electrostatic repulsion and the entropic attraction become negligible. At low salt concentration the entropic attraction increases whereas, at the same time,

the electrostatic repulsion vanishes. This last effect is caused by the perfect alignment of the head group parallel to the membrane surface so that virtually no charge separation occurs.

Stretching the membranes increases the entropic attraction but decreases the electrostatic repulsion. We did not incorporate undulations in our theory so the decrease of undulations was not the phenomenon that caused the stress-induced tendency to adhere. In our model stretched membranes have a larger head group area which relaxes the head group packing constraints. This allows these groups to assume a position more parallel to the bilayer surface, leading to a reduced electrostatic repulsion and a stronger entropic attraction.

Addition of non-ionic surfactants (dodecanol) to DMPC bilayers caused the membranes to grow thicker without changing the interaction curve. Ionic surfactants (e.g. dodecylammonium and dodecylsulphide) did not change the overall membrane thickness but made, due to a modification of the electrostatic interactions, the interaction profile completely repulsive. Cationic surfactants had a more pronounced effect than anionics. Cationics push the choline moieties outwards while the anionics pull these more inwards towards the membrane centre.

Finally in chapter 4 the SCAF theory for molecules containing rigid structures is given. The coupling of the segment potential $\{u(z)\}$ to the volume fraction profile $\{\varphi(z)\}$ is in principle accomplished according to the following simple, basic method. First, all conformations of the molecules are generated and then the statistical weights of these conformations in the potential field are added and normalised. For flexible molecules, that can assume very many conformations, an efficient technique exists that is just doing this in one single operation, it generate the conformations, calculate the statistical weight, and add the results to obtain the densities (the propagator method). For rigid structures, that can assume relatively few conformations, the basic methods is already effective. A hybrid scheme was developed for partly rigid molecules, where the basic method for the rigid parts was combined with the propagator method for the flexible parts.

Partition coefficients calculated for a number of linear and branched alcohols as well as for phenols were compared with measurements. Good quantitative comparison was found for these molecules. Trends known from literature, like the exponential dependence of the partition coefficient on the chain length in homologue series, were reproduced.

To illustrate the possibilities of the theory some results were presented of calculations on three groups of molecules having the same zwitterionic isomer ($C_{22N}{}^+S^-$, containing a benzene-like structure). The calculations showed that in DMPC membranes the partition coefficient can change by a factor of ten depending on the molecular architecture. The positional and orientational data revealed that negatively charged units partition much more readily into the membrane core than positively charged segments do. This can be rationalised by the electrostatic potential profile which, as told above, is positive both in the centre and on the outskirts of the membrane while being negative at the average position of the phosphate segments.

Calculations on a number of substituted tetrahydroxynaphthalenes showed that, with only small changes in the partition coefficient, large orientational and positional variations can be realised, changing from spanning the membrane for 2,3,6,7-tetrahydroxy naphthalene to parallel to the membrane surface positioned at the head group-hydrophobic core interface for 1,3,5,7-tetrahydroxy naphthalene. This kind of large orientational changes, while keeping the partition coefficient virtually constant, can be of great importance in the development and the improvement of new drugs, or in elucidating the working mechanism of existing ones.

Our model has provided a detailed insight into the nature of model lipid membranes and will hopefully advance the development of products and contribute to the optimisation and interpretation of experiments in which lipid bilayers play a role. At present reasonable (semi) quantitative agreement with many experimental results have already been achieved. There are however cases where the present theory does not yet give good enough predictions. For this it is good to know that the theory can be readily extended to incorporate more details in the calculations.

Samenvatting

Ieder levend wezen is opgebouwd uit cellen. Sommige levensvormen, zoals bacteriën, bestaan slechts uit één cel, terwijl andere, zoals mensen, uit zeer veel cellen bestaan. Al deze cellen zijn gescheiden van de rest van de wereld door een celmembraan. Zo'n membraan is een zeer dun, twee molecuullagen dik, vlies dat de cel volledig omringt. Ook binnenin een cel worden delen van de cel van de rest afgescheiden door membranen. Hierdoor kan de cel bepaalde processen scheiden en bijvoorbeeld verterende enzymen maken zonder zelf verteerd te worden, of in een kleine ruimte de omstandigheden gunstig maken voor specifieke reacties.

De moleculen waaruit een membraan bestaat zitten niet met chemische bindingen aan elkaar vast, maar worden bij elkaar gehouden door dezelfde krachten die verantwoordelijk zijn voor het ontmengen van olie en water. De lipidemoleculen, waar het membraan uit opgebouwd is, hebben een tweeslachtig, zogenaamd amfipolair karakter. Eén deel van zo'n molecuul, de kop, lost goed op in water, terwijl het andere deel, de staart(en), juist niet oplost in water maar wel in olie. In water associëren de lipidemoleculen zodanig dat de staarten van twee lagen lipiden naar elkaar toegricht zijn, zodat aan weerszijde de koppen zich gunstig met water kunnen omringen. De moleculen zitten, zoals gezegd, niet muurvast aan elkaar maar blijven beweeglijk en zodoende kunnen membranen gezien worden als zeer dunne, twee-dimensionale, laagjes vloeistof. Dit proefschrift gaat over zulke twee-dimensionale vloeistoffen.

Omdat membranen (lipide bilagen) een grensfunctie hebben doen ze ook aan grensbewaking. Dat wil zeggen dat ze passief en actief controleren welke moleculen er wel en welke er niet kunnen passeren. Geneesmiddelen moeten, om hun werk te kunnen doen, vaak één of meer membranen passeren. Omdat het meestal lichaamsvreemde stoffen zijn die normaal niet in het lichaam voorkomen, is er tijdens de evolutie voor deze stoffen geen actief transportmechanisme in het membraan ontwikkeld. Het passieve transport is dan het enig overgebleven alternatief. De interacties die deze moleculen hebben met de lipiden in het membraan zijn vanzelfsprekend belangrijk bij dit transport.

Geneesmiddelen moeten in het algemeen ergens in een cel hun werk doen. Aangenomen wordt dat er vaak één deel van het molecuul reageert met 'de

gevoelige plek' van de cel, meestal een eiwit, terwijl de rest van het molecuul ervoor moet zorgen dat het molecuul op de juiste plaats kan komen. Bijvoorbeeld, als 'de gevoelige plek' in een membraan zit dan moet het geneesmiddel wel het membraan in willen anders wordt de kans op een gunstige interactie wel erg klein. Aangezien zeer veel processen in de cel membraangebonden zijn, zijn er dus veel mogelijk 'gevoelige plekken' die zich in, of vlak bij, een membraan bevinden. Als je nu kan voorspellen hoe een molecuul er uit moet zien om op een bepaalde manier in of bij het membraan te gaan zitten is, het gemakkelijker om nieuwe geneesmiddelen te maken. De interacties van celvreemde moleculen met membranen is ook bij de orientatie van moleculen in het membraan van groot belang.

Het bestuderen en begrijpen van de interacties tussen lipidemembranen en additieven is het doel van het onderzoek dat heeft geleid tot deze dissertatie. Voor deze studie is een statistisch thermodynamische theorie gebruikt oorspronkelijk ontwikkeld door Scheutjens en Fleer voor flexibele polymeermoleculen aan grensvlakken, die later uitgebreid werd door onder anderen (in chronologische volgorde) Leermakers, Evers, Van Lent, Böhmer, Barneveld, Israëls, Wijmans en Van der Linden. Een principiële aanname in de theorie bestaat eruit dat het probleem van de vele moleculen die samen het te bestuderen systeem vormen, vereenvoudigd wordt tot één enkel molecuul in het potentiaalveld van alle anderen. Het veld, $\{u(z)\}$, bepaalt zo aan de ene kant de verdeling van de moleculen over de ruimte $\{\varphi(z)\}$ maar *wordt* aan de andere kant evenzo bepaald *door* diezelfde verdeling. We zeggen dat de oplossing is bereikt als het veld en de moleculaire verdeling consistent met elkaar zijn. Vandaar de naam zelf-consistente-veld theorie waaronder deze theorie in de litteratuur bekend staat. Deze theorie was door anderen al uitgebreid voor berekeningen aan zelf-associërende systemen. Ondergetekende heeft opnieuw een uitbreiding toegevoegd voor het in kaart brengen van de eigenschappen van starre molecuulstructuren (ringen) in inhomogene systemen. Als eerste toepassing van deze uitbreiding is gekozen voor de bestudering van deze moleculen in combinatie met lipidemembranen. Het onderzoek staat in dienst van de farmacologie. Vele geneesmiddelen bestaan namelijk deels uit starre, aromatische ringen.

In het volgende zullen kort de inhoud en de belangrijkste conclusies van de technische hoofdstukken de revue passeren.

In hoofdstuk één werd het kale membraan zonder additieven bestudeerd. Er werd gekozen voor een modelmembraan opgebouwd uit dimyristoylfosfatidyl-choline (DMPC) lipiden. Dit molecuul is gebruikt omdat het een frequent voorkomend lipidemolecuul is bij zowel planten als dieren. Het associërende gedrag van dit zwitterionogene lipide is vergeleken met dat van het negatief geladen dimyristoylfosfatidylserine (DMPS). De fosfatidylcholinekopgroep van het eerst genoemde lipide (DMPC) bleek gemiddeld evenwijdig aan het membraanoppervlak te liggen. De verdeling van de positieve choline-eindgroep is iets breder dan die van de negatieve fosfaatgroep. Doordat de verschillende ladingen een verschillende verdeling hebben, ontstaat er een elektrostatisch potentiaalprofiel over het membraan. Bij vrij hoge zoutconcentraties (1M of hoger) zijn er twee, ongeveer even waarschijnlijke, oriëntaties van de kopgroep gevonden: één met de cholinegroep dichter bij de waterfase dan de negatieve fosfaatgroep, en één waarbij de cholinegroep juist dichter bij het hydrofobe centrum van het membraan wordt gevonden.

Bij DMPS is de gemiddelde oriëntatie van de kopgroep nauwelijks afhankelijk van de zoutconcentratie. Het eind van de kopgroep steekt in de waterfase. De zoutionen dringen zich tussen de kopgroepen in en compenseren zo grotendeels de lading op de lipiden. Er adsorberen namelijk meer kationen dan anionen. Bij hoge zoutconcentraties is er een netto uitstoot van zoutionen in het kopgroepengebied. Echter doordat de anionen meer uitgestoten worden dan de kationen is ook hier sprake van ladingscompensatie.

Het gemak waarmee de oriëntatie van de PC-kopgroep kan worden veranderd is onderzocht door er een hydrofiele keten aan te koppelen. Bij het verlengen van de hydrofiele keten werden de volgende twee verschijnselen waargenomen. Ten eerste wordt het oppervlak per kopgroep groter naarmate de ketens langer worden. Hierdoor wordt het hydrofobe centrum van het membraan dunner totdat het membraan uiteindelijk niet meer stabiel is. Ten tweede verandert de oriëntatie van de kopgroep van evenwijdig aan het membraanoppervlak (zonder aangehechte hydrofiele keten), naar meer rechtop staand, met de cholinegroep aan de kant van de waterfase (voor korte ketens), tot weer vlakliggend op het membraanoppervlak (voor zeer lange ketens). De verklaring voor het rechtop gaan staan is dat de hydrofiele keten zich graag met het water omringt en dit optimaal kan doen door de cholinegroep mee te trekken in de richting van de waterfase. Langere ketens zijn, doordat het oppervlak per

kopgroep groter is, minder gestrekt, waardoor ze minder sterk aan de cholinegroep 'trekken'. De kopgroep gaat dan weer parallel aan het membraanoppervlak liggen.

In het tweede hoofdstuk werd de wisselwerking tussen de ionen in oplossing en het elektrostatische veld bij en in het membraan bestudeerd. Waarbij speciale aandacht werd besteed aan de invloed van de valentie van de ionen. De ophoping van positieve ionen rond de fosfaatgroep in de DMPC membranen kan verklaard worden zonder een specifieke interactie tussen kationen en de fosfaatgroep aan te nemen: de elektrostatische wisselwerkingen alleen zijn voldoende om een aanzienlijk verschil in adsorptie tussen één, twee en drie waardige ionen aan het membraan te bewerkstelligen.

De evenwichtsvoorwaarde voor vrijstaande membranen is dat deze structuur thermodynamisch de meest stabiele is. Hiervoor is het niet voldoende te constateren dat de oppervlaktespanning nihil is, maar moet ook de onderlinge wisselwerking tussen twee membranen repulsief zijn. Deze interactie is het onderwerp van hoofdstuk 3. Hier werd een thermodynamische analyse gegeven hoe, in het kader van de zelf-consistente-veld theorie, deze interactie onder verschillende omstandigheden uitgerekend moet worden. Het blijkt dat de interactiecurves verkregen via de methode waarbij de chemische potentialen constant blijven en die waarbij de oppervlaktespanning van het membraan constant gehouden wordt, nagenoeg hetzelfde zijn. Bij een gematigde zoutconcentratie (ongeveer 50 mM) werden drie verschillende regimes in de interactiecurve gevonden. Op grote afstand zijn de membranen repulsief doordat het diffuse deel van de dubbellaag daar overlapt. Op zeer korte afstand, waarbij de membranen zeer dicht bij elkaar gebracht zijn, werd er sterische repulsie waargenomen. Vlak voor de membranen elkaar fysiek raken werd een attractieve wisselwerking waargenomen. De attractie wordt veroorzaakt doordat de kopgroepen, als de membranen dicht genoeg genaderd zijn, de ruimte tussen de membranen kunnen overbruggen en met de cholinegroep van de ene kant tussen de fosfaatgroepen van de andere kant kunnen komen. Dit heeft geen energetische consequenties maar verhoogt wel het aantal realiseringsmogelijkheden en dus levert dit entropie op.

Bij hogere zoutconcentraties verdwijnt zowel de elektrostatische repulsie (afscherming door het zout) als de entropische attractie. Het verlies van de attractie vindt zijn oorzaak in het feit dat de kopgroepen niet meer in hun

realiseringsmogelijkheden beperkt worden door elektrostatische interacties. Bij verlaging van de zoutsterkte neemt ook de elektrostatische repulsie af. In dit geval worden de kopgroepen door de elektrostatische wisselwerkingen gedwongen om vrijwel perfect parallel aan het membraanoppervlak te gaan liggen. De negatieve lading van de fosfaatgroep compenseert dan de positieve lading van de cholinegroep en het potentiaalprofiel verdwijnt dan vrijwel geheel. De entropische attractie tussen de twee membranen wordt onder deze omstandigheden echter wel groter.

Als het membraanoppervlak zich sluit ontstaat er een soort ballonnetje, in goed Nederlands een vesikel genaamd. Het is mogelijk binnenin zo'n vesikel een overdruk te genereren waarbij het membraan onder spanning komt te staan. In hoofdstuk 3 hebben we ook gekeken naar de interactie tussen opgespannen membranen. In membranen onder spanning hebben de lipiden een relatief groot oppervlak per kopgroep. Daardoor zijn, vergeleken met spanningsvrije membranen, de pakkingsproblemen vooral in het kopgroepengebied kleiner en treedt er gemakkelijker ladingscompensatie op van de fosfaat- en cholinegroep. Hierdoor zal de kopgroep meer evenwijdig aan het membraanoppervlak gaan liggen. Wanneer men zich dit realiseert is het effect op de membraaninteractie te begrijpen: de elektrostatische repulsie neemt af terwijl de entropische attractie toeneemt met toenemende membraanspanning.

Het toevoegen van lineaire ongeladen amfipolaire moleculen (dodecanol) maakt de membranen dikker, maar verandert de interactiecurve verder niet. Geladen oppervlakte-actieve stoffen (ionogene surfactanten) maken de interactie-curve volledig repulsief. Doordat de kationogene surfactanten gemiddeld iets meer aan de buitenkant van het membraan gaan zitten begint hier de wisselwerking op grotere afstand dan bij de negatieve surfactanten.

In het vierde en laatste hoofdstuk werd de uitbreiding van de theorie voor starre moleculen uit de doeken gedaan. De koppeling van het potentiaalveld $\{u(z)\}$ aan de volumefractieverdeling $\{\varphi(z)\}$ gebeurt in principe volgens de volgende, simpele basismethode. Alle conformaties van de moleculen worden gegenereerd en vervolgens wordt het statistisch gewicht van iedere conformatie opgeteld en genormeerd. Voor flexibele ketens, die zeer veel conformaties kunnen aannemen, is een efficiënte methode bekend die dit genereren, statistisch wegen en optellen in één bewerking doet (de propagator-methode). Voor starre structuren, die relatief weinig conformaties aan kunnen nemen, is het doelmatiger om het

generen en het bepalen van het statistisch gewicht te scheiden zoals in de basismethode. Voor moleculen met zowel een flexibel als een star deel werd een hybride procedure ontwikkeld die voor het flexibele deel de propagatormethode, en voor het starre deel de basismethode kiest.

De verdelingscoëfficiënt voor verschillende groepen lineaire en vertakte alcoholen en fenolen werd berekend en vergeleken met gemeten waarden. De overeenkomst voor deze moleculen is beloftevol te noemen. Verder mag verder mag vermeld worden dat de in de literatuur bekende trends, zoals het exponentieel verloop van de verdelingscoëfficiënt met de ketenlengte in een homologe reeks, werden gereproduceerd.

Om de mogelijkheden van de theorie te illustreren zijn de oriëntaties, conformaties en verdelingscoëfficiënten van verschillende moleculen van hetzelfde isomeer ($C22N^+S^-$ met een benzeenachtige ring) in het lipidemembraan berekend. Het blijkt dat voor deze isomeren de verdelingscoëfficiënt, afhankelijk van de moleculaire architectuur, een factor 10 kan variëren. Het positief geladen segment van deze moleculen bleek veel minder geneigd te zijn om in het hydrofobe centrum van het membraan te gaan zitten dan de negatief geladen groep. Dit kan worden begrepen als men bedenkt dat de elektrostatische potentiaal in het centrum en aan de buitenkant van het membraan een positieve waarde heeft, terwijl rond de positie van de fosfaatgroep, centraal in het kopgroepengebied, een negatieve elektrostatische potentiaal heerst. Doordat de gradiënt van het gemiddeld veld voor positief geladen segmenten op de rand van het hydrofobe gedeelte van het membraan erg groot is, is de waarde van de verdelingscoëfficiënt erg gevoelig voor de gemiddelde positie van deze segmenten. Er werd een rechtstreekse correlatie waargenomen tussen de positie van het positieve segment en de verdelingscoëfficiënt voor deze groep van isomeren.

Berekeningen aan een aantal tetrahydroxynaftalenen lieten zien dat, met een nagenoeg gelijke verdelingscoëfficiënt, de oriëntatie van moleculen in het membraan aanzienlijk kan verschillen. Het 2,3,6,7-tetrahydroxynaftaleen-molecuul staat loodrecht op het membraanoppervlak in het centrum van het membraan terwijl het 1,3,5,7-tetrahydroxynaftaleen-molecuul evenwijdig aan het membraanoppervlak tussen het kopgroepengebied en het membraancentrum zit. Het feit dat de verdelingscoëfficiënt en de positie van het molecuul in het membraan nagenoeg onafhankelijk van elkaar in te stellen zijn is van bijzonder

belang voor het ophelderen van werkingsmechanismes van bestaande geneesmiddelen of bij het ontwikkelen en optimaliseren van nieuwe, biologisch actieve moleculen.

Resumerend mogen we stellen dat ons model de mogelijkheid biedt om een gedetailleerd inzicht te verkrijgen in de eigenschappen van lipidebilagen en hun interacties niet alleen met flexible maar ook met starre additieven. De theorie kan nu ingezet worden voor de ontwikkeling van nieuwe producten en zal zonder twijfel bijdragen leveren aan de interpretatie en optimalisatie van experimenten waarbij lipidebilagen een belangrijke structurele eenheid zijn. Een redelijke kwantitatieve overeenkomst met vele experimentele resultaten is reeds geboekt. Er zijn echter gevallen waar de theorie nog tekort schiet. Dan is het goed te weten dat de theorie nog niet uitontwikkeld is en relatief gemakkelijk kan worden uitgebreid om nog betere gedetailleerdere berekeningen en voorspellingen mogelijk te maken.

Curriculum Vitae

Lucas Alfons Meijer werd geboren op 18 november 1964 te Enschede. In 1983 behaalde hij het diploma gymnasium β aan het Jacobus College aldaar en begon vervolgens in september in Wageningen aan de studie Moleculaire Wetenschappen. Deze studie rondde hij in 1989 af met hoofdvakken in de fysische chemie, de moleculaire fysica en de wiskunde. Zijn stage periode bracht hij door bij de vakgroep fysische chemie aan de "Kungliga Tekniska Högskolan" in Stockholm, Zweden.

Het in dit proefschrift beschreven onderzoek werd uitgevoerd bij de vakgroep Fysische en Kolloïdchemie aan de Landbouwuniversiteit Wageningen in de jaren 1990 tot en met 1994.

Na- en D(r)ankwoord

Zoals menig ander ook al heeft opgemerkt (sla er maar een willekeurig proefschrift op na) had ook ik het werk waarvan dit proefschrift een neerslag vormt nooit alleen kunnen volbrengen. In min of meer willekeurige volgorde wil ik hier een aantal mensen bedanken zonder wie het zeker niet was gelukt, in ieder geval niet op deze manier. Ik hoop dat degenen die hier niet zijn genoemd zich niet tekort gedaan voelen. Hun bijdrage is veel belangrijker geweest, want hij was onopvallend.

In de eerste plaats is het Jan Scheutjens geweest die mij heeft geholpen om mijn afstudeerverslag op tijd af te krijgen zodat ik niet eerst in militaire dienst hoefde. Zijn zeer goede intuïtie en gedegen kennis hebben mij aan het begin van mijn onderzoek op de rails gezet. Na zijn vroegtijdige vertrek heeft Frans Leermakers het gapende gat zeer competent weten in te vullen. Ook mijn promotor Hans Lyklema was, hoewel hij een erg druk bezet man is, altijd bereid mee te denken als ik hem daarom vroeg. De onvermoeibaarheid van deze mensen is spreekwoordelijk (ik haal in dit verband slechts het gezegde "*die is zo onvermoeibaar als Scheutjes*" aan)*.

Verder zijn er vele anderen zonder wie alles anders, en vooral minder, geweest zou zijn.

Zo wil ik ook graag de mensen van de Bayer AG bedanken voor hun vertrouwen in Jan (en later ook in mij). Met name John Goossens en Boudewijn van Lent die niet alleen in woord maar ook in daad mij hebben bijgestaan. De resultaten daarvan zijn nu in hoofdstuk vier te vinden. Ik hoop dat ze met de theorie zoals die nu in goliath geïmplementeerd is uit de voeten kunnen.

Andrew Nelson heeft mij de eerste zet gegeven om iets op te schrijven. Het goede Engels in het tweede hoofdstuk is volledig van zijn hand. Door pogingen te ondernemen om met goliath te rekenen heeft hij, net als Yiannis Sdrannis en Arpad Vince, als α-tester zoveel bugs doen verwijderen dat het nu net werkt.

Verder hebben Joost Uitdehaag en Heleen Hollenberg met hun werk in het kader van een afstudeervak ook in belangrijke mate bijgedragen aan het begrip van de theorie in relatie tot de toepassingen.

---

* Barneveld, P.A., *The bending elasticity of surfactant monolayers and bilayers*. 1991, Thesis Wageningen.

Joost van Opheusden heeft mij de weg gewezen in de wiskunde literatuur waardoor ik de twee dimensionale lineaire ($\stackrel{?}{=}$ vlakke) regressie heb kunnen programmeren zonder welke ik mijn problemen niet zo algemeen had kunnen oplossen.

De 'bemensing' van het secretariaat was ook altijd erg vriendelijk en behulpzaam, of je nu om pennen, een praatje of een praatpaal kwam. Bert, Yvonne, Josie en Wil: dank.

De start van mijn AIO periode was een stuk slechter verlopen (of later begonnen als Gerrit van der Beek niet zo goed was geweest om mij en mijn gespalkte been zes weken lang naast hem in zijn auto te dulden en me dagelijks op en neer te brengen van de vakgroep naar huis en terug.

Naast al deze activiteiten op de vakgroep zou ik het, hoe geweldig wetenschap ook is, niet vol gehouden hebben als ik niet af en toe daar buiten ook wat kon doen. De "theorie groep" (.kelder $\approx$ Peter, Katinka, Klaas, Rafel, Chris, Martin (A. èn T.A.), Mats, Frans en natuurlijk Jan), waarvan eigenlijk niet iedereen theorie doet, is de oorzaak van de '(c)' in de titel van dit stukje. De vrijdagmiddag vergaderingen in Loburg, en discussies op verjaardagen en andere feesten over computers, netwerken of net-niet-werken dan wel de toepassingen van de thermodynamica op dagelijkse problemen zijn een grote inspiratiebron geweest.

Ook het sporten was een plezierige uitlaatklep zowel het volleybal met de kollosolex (Luuk, Henk, Theo, Anton, Janet, Luc, Peter en ook nog Rob) als het rugbiën bij de Rugbyclub Wageningen die mij de waarheid liet inzien van de veel geziene stelling "rugby is better than sex (sometimes)".

Last but not least is er natuurlijk Carla die mij, ondanks moeilijke periodes, toch altijd gesteund heeft.

Dank, zeker aan degenen die ik hier vergeten ben,

Cas.